

Adaptive and Distributed Beamforming for Cognitive Radio

Proefschrift

ter verkrijging van de graad van doctor
aan de Technische Universiteit Delft,
op gezag van de Rector Magnificus prof. ir. K.C.A.M. Luyben,
voorzitter van het College voor Promoties,
in het openbaar te verdedigen op dinsdag 15 oktober 2013 om 10.00 uur
door

Xiaohua LIAN

Master of Engineering aan de Nanjing University of Aeronautics and Astronautics,
P. R. China
geboren te Urumqi, P. R. China

Dit proefschrift is goedgekeurd door de promotor:
Prof. dr. ir. L. P. Lighart

Copromotor Dr. H. Nikookar

Samenstelling promotiecommissie:

Rector Magnificus,	voorzitter
Prof. dr. ir. L. P. Ligthart,	Technische Universiteit Delft, promotor
Dr. H. Nikookar,	Technische Universiteit Delft, copromotor
Prof. H. Steendam,	Universiteit Gent, België
Prof. E. Del Re,	Università di Firenze, Italië
Prof. dr. ir. E. R. Fledderus,	Technische Universiteit Eindhoven
Prof. dr. ir. W. C. van Etten	Universiteit Twente
Prof. ir. P. van Genderen	Technische Universiteit Delft
Prof. dr. ir. G. J. T. Leus,	Technische Universiteit Delft, reservelid

ISBN 978-94-6186-205-1

Printed by IJskamp Drukkers

Adaptive and Distributed Beamforming for Cognitive Radio
Thesis Delft University of Technology
Copyright © 2013 by Xiaohua Lian

All rights reserved. No parts of this publication may be reproduced or transmitted in any form or by any means, electronic or mechanical, including photocopy, recording, or any information storage and retrieval system, without permission on writing from the author.

Abstract

Cognitive Radio (CR) is an energy efficient technique that is capable of optimizing the premium radio resources, such as power and spectrum. In this thesis, we focus on exploiting spatial diversity for CR. We have adopted two spatial signal processing techniques, i.e., Adaptive Beamforming (ABF) and Distributed Beamforming (DB) for CR users and CR networks, respectively.

We have investigated and proposed a Bayesian ABF technique to CR Base Station (BS), which is able to direct CR BS main beams to CR users even when the Direction of Arrival (DOA) of each CR user is uncertain or completely unknown. Consequently by using this method, a CR BS at uplink (receiving) can adaptively enhance the signals of CR users by directing its main beams towards their wanted directions. We have also developed a Null Broadening (NB) technique for CR BS to be capable of generating spread nulls in the beampattern around directions of Primary Users (PUs), which guarantees radiated power reduction towards directions of PUs even considering scattering and multipath effects.

We have introduced a DB method to distributed CR networks, which are constituted of distributed CR nodes. Two multi beam generating methods have been presented for DB to generate more than one main beam towards Distant CR (DCR) users. Due to the limitation of the DB method, the main beam of the CR network will be extremely narrow considering the possible CR working frequency. Therefore we have proposed a Nodes Selection (NS) method to select proper CR nodes from the CR network to perform DB, and thus the beampattern has a wider main beam while maintaining the lower sidelobe levels towards PUs.

Contents

Abstract	I
Contents.....	III
Contents of Figures.....	VI
Contents of Tables.....	VIII
Chapter 1 Introduction	1
1.1 Research background	1
1.2 Research Motivations	3
1.3 Scope and Novelties of this thesis	4
1.4 Outlines of the thesis.....	5
Chapter 2 Adaptive Beamforming (ABF) Techniques for Cognitive Radio (CR)	7
2.1 Introduction of Cognitive Radio (CR).....	7
2.1.1 Concept of CR	7
2.1.2 Applications of CR.....	8
2.1.3 OFDM- A promising modulation scheme for CR	10
2.2 Beamforming techniques	11
2.2.1 Basic terminology and concepts of ABF	11
2.2.2 Adaptive beamformers for wireless communications	15
2.3 Applying Beamforming techniques to CR.....	16
2.3.1 Beamforming as an interference cancellation scheme for CR.....	16
2.3.2 Beamforming and CR functionality	18
2.3.3 Challenges of introducing beamforming to CR	19
2.4 Summary.....	22
Chapter 3 Uplink Adaptive Beamformers for CR	23
3.1 Introduction	23
3.2 Adaptive Bayesian uplink beamformers for CR.....	26
3.2.1 Adaptive Bayesian beamformer with MMSE criterion	26
3.2.2 Projection Method (PM).....	28
3.3 Adaptive uplink OFDM beamformers for CR.....	29
3.3.1 OFDM adaptive beamformer with iterative weights calculating	29
3.3.2 Computation complexity analysis	32
3.3.3 Adaptive OFDM beamformer with weights-masking.....	33
3.3.4 OFDM adaptive beamformer with weights-constraint	34

3.3.5 Adaptive OFDM Bayesian beamformer with constrained weights.....	36
3.4 Simulations and results	37
3.5 Summary.....	43
Chapter 4 Downlink Adaptive Beamformers with Broadened Nulls for the CR system	45
4.1 Introduction.....	45
4.2 A new Null Broadening (NB) method - VDA	47
4.2.2 VDA method	49
4.2.3 VDA with depth control.....	52
4.3 Simulation results and analysis	53
4.4 Summary.....	59
Chapter 5 Distributed Beamforming (DB) Techniques for CR	61
5.1 Introduction.....	61
5.2 DB of CR networks	63
5.2.1 Necessary assumptions	64
5.2.2 DB for CR networks.....	64
5.2.3 DB with multi main beams	67
5.3 Nodes Selection (NS) for CR networks with enlarged main beam.....	70
5.3.1 A NS method for CR networks.....	71
5.3.2 Simulation results of the NS method	74
5.4 Summary.....	77
Chapter 6 Adaptive and Distributed Beamforming Techniques for Intelligent WiMAX (I-WiMAX)	79
6.1 Introductions and background information.....	79
6.2 Concept of I-WiMAX	80
6.3 AOFRDM for I-WiMAX	82
6.4 A technique for I-WiMAX.....	84
6.5 DB for I-WiMAX	85
6.6 Application of I-WiMAX	87
6.7 Summary.....	89
Chapter 7 Conclusions and Recommendations.....	91
7.1 ABF techniques for CR	91
7.2 DB for CR networks.....	92
7.3 ABF and DB for I-WiMAX	94
7.4 Recommendations for future work.....	94
List of Abbreviations.....	97
List of Symbols.....	99
Appendix A.....	103

<i>Appendix B</i>	104
<i>Appendix C</i>	105
<i>Appendix D</i>	106
<i>Appendix E</i>	107
<i>References</i>	109
<i>Publications of the author</i>	115
<i>Summary</i>	117
<i>Samenvatting</i>	119
<i>Acknowledgement</i>	123
<i>Curriculum Vitae</i>	125

Contents of Figures

Figure 2.1 OFDM based CR transmitter at current timeslot t	11
Figure 2.2 Array antennas with beamforming.....	12
Figure 2.3 IC techniques at CR receivers and transmitters	17
Figure 2.4 The Cognition Cycle [1]	19
Figure 2.5 Coexistence of PUs and CR with exclusion regions.....	20
Figure 2.6a Coexistence of PUs and CR with ABF techniques	21
Figure 2.6b Coexistence of PUs and CR with DB techniques	21
Figure 3.1a Weights-masking technique for adaptive OFDM beamformer.....	25
(subcarriers $f_{16} - f_{31}$ and $f_{32} - f_{47}$ are deactivated)	25
Figure 3.1b Weights-constraint technique for adaptive OFDM beamformer	25
(constraints on subcarriers $f_{16} - f_{31}$ and $f_{32} - f_{47}$).....	25
Figure 3.2 System configuration of an adaptive OFDM beamformer.....	30
Figure 3.3 Learning procedure of an adaptive Bayesian beamformer	38
Figure 3.4 Adaptive Bayesian beamformer with Projection Method.....	38
Figure 3.5a Adaptive OFDM beamformer using the weights-masking method	39
Figure 3.5b Adaptive OFDM beamformer using the weights-constraint method.....	39
Figure 3.6 Beampattern of the adaptive OFDM Bayesian beamformer using the weights- constraint method and $N=10$ antenna elements	40
Figure 3.7 Beampattern of the adaptive OFDM Bayesian beamformer using the weights- constraint method and $N=20$ antenna elements	40
Figure 3.8a Frequency bands utilization of CR OFDM subcarriers and PUs	41
Figure 3.8b Adaptive OFDM beamformer using the weights-constraint method for two CR users.....	41
Figure 3.9 BER of Adaptive OFDM Bayesian beamformer with weights-masking and weights-constraint methods $M=64$	42
Figure 3.10 BER of the Adaptive OFDM Bayesian beamformer with weights-masking and weights-constraint methods $M=32$	43
Figure 4.1 Spatial channel observed at the PU with scattering from the CR BS	45
Figure 4.2 Von Mises pdf for the AOA of scattering components at the MS as function of θ around $\theta_p = 0$	46
Figure 4.3 Reconstructed covariance matrix of the VDA method for $V=1$	51
Figure 4.4 Reconstructed covariance matrix of the VDA method for $V=2$	51
Figure 4.5 NB technique for CR Beamforming with deeper and/or broader nulls	54
Figure 4.6 Beampattern of two NB methods: CMT and VDA.....	54
Figure 4.7a CDF of the power of the received CR signal by PU1	55
Figure 4.7b CDF of the power of the received CR signal by PU2	55
Figure 4.8 Beampattern of NB methods (CMT and VDA) with Poisson window.....	56
Figure 4.9 Beampattern of VDA with the Poisson window at different lengths.....	57
Figure 4.10 Beampattern of VDA with the Poisson window and cos window	57
Figure 4.11 Beampattern of VDA with the Poisson window at different α	58
Figure 5.1 CR networks with DCR and PUs.....	63
Figure 5.2 Distance between the k th node and an access point (A, ϕ)	65

Figure 5.3 Average beampattern of the DB method.....	66
Figure 5.4 Separation of CR nodes into a ring range and a circle range.....	67
Figure 5.5 Average Beampattern of DB with circle and ring ranges	69
Figure 5.6 Average beampatterns of DB methods with multi main beams.....	70
Figure 5.7 Converting locations of CR nodes into broadside and end-fire arrays	71
Figure 5.8 Beampattern of CR network, broadside array and end-fire array	72
Figure 5.9 NS for CR networks.....	73
Figure 5.10 NS for CR networks with two DCR users	73
Figure 5.11 Selected CR nodes in the CR networks $D = 15\lambda$ ($\phi_0 = 0^\circ$).....	74
Figure 5.12 Selected CR nodes in the CR networks $D = 35\lambda$ ($\phi_0 = 0^\circ$).....	74
Figure 5.13 Average beampattern of the selected CR nodes ($\phi_0 = 0^\circ$)	75
Figure 5.14 Selected CR nodes in the CR networks $D = 15\lambda$ ($\phi_1 = 0^\circ$ and $\phi_2 = 15^\circ$)	75
Figure 5.15 Average beampattern of the selected CR nodes for two DCR users	76
Figure 5.16 Average beampattern of the selected CR nodes with $\tilde{R} = 100, 200, 400$	76
Figure 6.1 I-WiMAX concept of maritime coastal/lake communications	80
Figure 6.2 Working flow chart of I-WiMAX	82
Figure 6.3 Adaptive modulation of I-WiMAX for green radio application	83
Figure 6.4 Power and subcarriers allocation of I-WiMAX for green radio application... Figure 6.5 NB technique for I-WiMAX (SS1 and SS2 share the same OFDM subcarriers)	84
.....	85
Figure 6.6 DB for I-WiMAX in long distance communications.....	85
Figure 6.7 DB for I-WiMAX in TDD scheme	86
Figure 6.8 DB for I-WiMAX in FDD scheme	86
Figure 6.9 Application of I-WiMAX for maritime coastal/lake environment communication	88
Figure 6.10 Emergency services provided by I-WiMAX	88

Contents of Tables

Table 3-1 Number of complex multiplications of the MMSE beamformer and the beamformer with iterative weights-calculation	33
Table 4-1 Normalized received power of CR signal by PUs	59

Chapter 1 Introduction

1.1 Research background

Many appealing applications of wireless communications have been emerging, such as mobile internet access, health care, medical monitoring and smart homes. With a remarkable growth in designing and manufacturing various sensors, including for health care, transportation, environment monitoring and so on, there has been an increasing demand of versatile wireless services. Another emerging trend of current wireless services is the demand of high data rate wideband services. Today the Universal Mobile Telecommunications System (UMTS) is one of the fastest solutions on the market that can operate in dispersive environments, but rapid progress of the telecommunications market has created a need for newer techniques that can accommodate data rates even higher than this, e.g., Long Term Evaluation (LTE), which is the standard of wireless communications for 4G. But for 5G or beyond, the preferable solution is to introduce a new wireless system as smart as possible to operate flexibly in a dynamic environment.

Thus there is a need to develop an energy efficient green technique that is capable of optimizing the premium radio resources, such as power and spectrum, while guaranteeing desirable Quality of Services (QoS). The new techniques should be designed to spatially, temporally and spectrally minimize the energy spent to transmit information to achieve high energy efficiency. Cognitive Radio (CR) is a promising solution meeting this requirement. CR has been initially introduced by Joseph Mitola [1], and he described how CR could enhance the flexibility of wireless services through a radio knowledge representation language. Though there are different existing definitions of CR, all of them deliver six keywords; they are: awareness, intelligence, learning, adaptation, reliability and efficiency. CR can be considered as a radio that is able to behave as a cognitive system, having at least the capabilities of observing, making decisions and adapting, i.e., the three main functions of the simplified cognitive cycle.

CR is able to utilize the unused spectrum efficiently in a dynamically changing environment. It provides three various solutions to accommodate this spectrum for use by unlicensed wireless devices without disrupting the communications of the Primary Users (PUs) of the spectrum. They “overlay”, “underlay” and “interwave” its signals with those of the PUs in such a way that the communications by PUs is as unaffected as possible [2]. The underlay approach protects PUs by enforcing a spectral mask on CR signals so that the interference generated by CR devices is below the acceptable noise power at the PUs. The overlay approach also allows concurrent PUs and CR transmissions, but the

enabling premises for the overlay system are that the secondary users can use part of their power for secondary communication and the remainder of the power to assist (relay) primary transmissions. Based on the idea of opportunistic communication [3], J. Mitola proposed the interwave approach. Being able to have dynamic access to the spectrum, CR must detect the existing temporary frequency voids, referred to as spectrum holes that are not in use by PUs, and then be technically able to autonomously resolve conflicts in spectrum access by avoiding interference with incumbent signals.

CR can achieve efficient radio resource management while providing high data rate and reliable wireless communication services via implementation cognitions in three domains. They are time, frequency and space domains. With detection and prediction of wireless channels, CR in time domain is able to reach the channel capacity via adopting the optimal waveforms. By detecting spectrum holes and making use of the temporally unoccupied spectrum bands, CR in frequency domain can have efficient utilization of the spectrum via employing the interwave spectrum access mode. In space domain, if CR is able to transmit signals to its users while ensuring those signals are unable to be received by PUs or at PUs the received power of CR signals is below the interference level of PUs, CR is able to adopt the underlay spectrum access mode of utilizing the spectrum. This helps CR to achieve the most efficient spectrum usage by totally sharing the whole spectrum with PUs.

CR capabilities may also be exploited in Wireless Sensor Networks (WSN), which are traditionally assumed to employ a fixed spectrum allocation and characterized by the communication and processing resource constraints of low-end sensor nodes[4]. Depending on the applications, WSN composed of sensor nodes equipped with CR may benefit from its potential advantages, such as dynamic spectrum access and adaptability for reducing power consumptions. The latter is the basic and primary requirement for green communications. The green CR radio is aiming at pursuing energy reduction to operate radio access networks via investigating and creating innovative methods or identifying proper radio architecture that enables such a power reduction.

In this thesis, we pay attention to how to overcome limits in the spectrum and to optimize usage of holes in the spectrum. CR can be the solution. The focus of the thesis is on the potentials and limitations in CR. By considering space domain, CR can achieve full spectrum reuse with PUs via distinguishing itself from PUs by different spatial directions. We study the techniques for spatial CR and thus limit the scope of this thesis to space domain. We study both transmission and reception techniques for CR networks by exploring spatial diversity. Two system models are discussed in detail. First we consider a CR Base Station (BS) equipped with array antennas, while CR users and PUs have no array antennas and they are located around the CR BS as in centralized networks. The second model that we discuss is a distributed CR network, which regards CR users in the network as CR nodes and a (sub-) set of these nodes forwards signals to

distant CR (DCR) users in the presence of distant PUs. Both of them adopt the underlay spectrum access mode to share the spectrum band with PUs.

1.2 Research Motivations

As we are exploiting spatial diversity in CR and CR networks, we limit our observations to spatial signal processing techniques, i.e., the beamforming technique. This technique has first been introduced into Radar and Sonar systems when the designed signal and interferences occupy the same temporal frequency band and thus temporal filtering cannot be applied to separate signals from interferences. It utilizes the spatial diversity taking into account that the desired and interfering signals usually originate from different directions. This therefore allows for an approach which spatially separates signals from interferences. This beamforming technique, as a spatial filtering technique, is nowadays also used in communication systems.

With the Adaptive beamforming (ABF) technique, a CR BS with array antenna can transmit less power towards directions of PUs by spatially directing nulls in the antenna pattern towards them. Furthermore, a CR BS with multiple antennas can be replaced by a CR network which contains geographically distributed CR users. In the CR network, each CR user with a single antenna can be regarded as a virtual antenna element of an array. Thus they can form a desired beampattern to direct main beams towards distant CR users while null patterns are created towards PUs. This refers to the Distributed Beamforming (DB) technique.

Uplink beamforming (receiving beamforming) is capable of suppressing co-channel interferences which are caused by PUs transmission. By employing beamforming techniques, a CR BS can adaptively enhance the signals of CR users by directing its main beams towards their directions. However, since the signals received at the CR BS, which are coming from CR users, have low Signal to Noise Ratio (SNR), we have to investigate a robust beamforming technique which is able to direct CR BS main beams to CR users even when the Direction of Arrival (DOA) of each CR user is uncertain or completely unknown.

Compared with uplink Beamforming, more challenges exist in downlink beamforming (transmit beamforming). Since the equipment of CR users and PUs have no array antenna, even with nulls in the CR BS antenna pattern towards PUs, the PUs may still receive CR signals due to scatter and multipath effects from CR BS signals. As a result, beamforming techniques have to be improved or modified to be able to guarantee radiated power reduction towards directions of PUs including considerations on scattering and multipath effects.

DB for CR networks is a green technique, because it arranges all CR nodes to forward cooperatively the CR signal to DCR users so that the communication range can be enlarged. However, the working frequency of the CR network has significant impact on the width of the main beam in the beampattern generated by CR networks.

Considering a possible working frequency band, e.g., the Ultra High Frequency (UHF) band, the width of the main beam will dramatically decrease, which is extremely narrow to be applicable. Thus a new DB method or a new structure of the CR network has to be presented for practical applications of CR networks. The new method should be able to enlarge the main beam in the pattern and should also be able to provide sufficiently low sidelobes as well.

1.3 Scope and Novelties of this thesis

In this thesis we only discuss cases of a single CR BS coexisting with PUs and a single CR network coexisting with PUs. Thus there will be no message exchanging considered among multiple CR base stations and multiple CR networks. The suggested ABF is only applied to a single CR BS with an array antenna, and the DB technique is only applied to a single CR network.

In correspondence to the motivations of the research, the following novelties and primary results are delivered in this thesis.

We propose an adaptive Orthogonal Frequency Division Multiplexing (OFDM) Bayesian beamformer for uplink beamforming. The beamformers at the CR BS are able to direct main beams towards DCR users while null patterns are formed towards PUs. In the presence of interference to the Bayesian beamformer, we present a Projection Method (PM) to avoid that the CR BS confuses DOA's of CR users with those of PUs. Furthermore, the weights of the OFDM beamformer are determined iteratively using a method which has been developed by us so that the computational complexity is reduced. Two spectrum access schemes of modifying the adaptive beamformer weights of OFDM signals have been set up and compared. One is the weights-masking technique, which is based on the interwave spectrum access mode and the other is the weights-constraint technique, which achieves the same full spectrum reuse as the underlay spectrum access mode (chapter 3).

By studying the spatial channel properties, a novel Null Broadening (NB) method, which is called Virtual Direction Adding (VDA) technique, has been worked out as a downlink beamforming technique for CR BS. The proposed method can form spread null patterns towards directions of PUs instead of only a point null pattern. The method allows for enhancing the signal power suppression around PUs (chapter 4).

We introduce the DB technique to the CR network, which is constituted of distributed CR nodes. The goal of the DB method is to forward the CR signal to the Distant CR (DCR) users, while causing no harmful interferences to coexisting PUs by limiting its transmission power towards PUs. This is the same as the ABF technique employed by CR BS. Two DB methods have been proposed by us to generate multi beams towards directions of DCR users. We group the CR nodes geographically into ring and circle ranges and CR nodes located in different ranges directing main beams to

different DC users. In the second method CR nodes randomly choose the DCR user to direct main beams (chapter 5, section 5.2).

To solve the problem of the extreme narrow main beam in the pattern when we introduce the DB method into CR networks, we propose a novel Nodes Selection (NS) method. The presented NS method is based on the differences in beam width of a broadside array and an end-fire array. We select those CR nodes, which are able to form a full size end-fire array and a reduced size broadside array. This NS method chooses those CR nodes, which are located in the “belt” area along the direction of the DCR user (chapter 5, section 5.3).

We also demonstrate an application of the proposed ABF and DB techniques by introducing them into a new maritime wireless communication system, i.e., Intelligent-Worldwide Interoperability for Microwave Access (I-WiMAX). I-WiMAX promises a large coverage range, high data rates, efficient spectrum usage, and reliable communications in sea/lake scenarios. It consists of Smart Radio (SR) concepts and mobile WiMAX. SR introduces two beamforming techniques, ABF and DB, for ultimate efficient spectrum utilization and large coverage (chapter 6).

1.4 Outlines of the thesis

The organization of this thesis is as follows.

Chapter 2 introduces several existing concepts of CR, revealing CR intelligence and the capability of adaptation, as well as CR applications. It will also explain the reason why OFDM is recommended as CR modulation technique. Then the beamforming technique will be introduced. We show the reasons, the possibilities and the challenges of introducing beamforming techniques to the CR systems.

Chapter 3 aims at designing a robust adaptive beamformer for the CR uplink to direct main beams towards CR users even when the DOA information of CR users are inaccurate or even unknown. An adaptive Bayesian beamformer will be discussed and a PM method will be presented to modify the Bayesian beamformer in the presence of interferences. An adaptive OFDM beamformer for the CR BS with iteratively weights calculation will be demonstrated. If some of the OFDM subcarriers are falling into the same spectrum band with PUs, two spectrum access modes are considered by presenting two weights modifying methods, i.e., weights-masking and weights-constraint.

Chapter 4 illustrates the necessity of generating spread null patterns towards directions of PUs. It shows that the NB method for CR BS downlink beamforming is highly required. A new NB method, VDA, is presented and its performance is investigated.

Chapter 5 introduces the DB technique to the CR network, which is constituted of distributed CR nodes. In this chapter, we also present two multi main beams generating methods: the geographical grouping method and the random initial phase choosing

method. To solve the unavoidable extremely narrow main beam in the pattern of the DB method, we propose the NS method to enlarge the width of the main beam in the pattern.

Chapter 6 demonstrates a new maritime wireless communication system, which is I-WiMAX. It employs two beamforming techniques, AB and DB, for ultimate efficient spectrum utilization and a large coverage. For downlink adaptive beamforming the NB method, which has been discussed in chapter 4, is introduced in I-WiMAX to alleviate the cochannel effects due to spectrum reusing. In case of a Subscriber Station (SS) is at far distance beyond the possible communication coverage range, a relay network formed by accessible SS is presented to transmit the signals further to distant SS by employing the DB technique proposed in chapter 5.

Chapter 7 summarizes all main results, draws overall conclusions, and gives some recommendations for future work.

Chapter 2 Adaptive Beamforming (ABF) Techniques for Cognitive Radio (CR)

2.1 Introduction of Cognitive Radio (CR)

Imagine an intelligent radio, which automatically detects and exploits the empty spectrum to offer unlicensed users high data transfer rate. The same radio requires that it remembers the communication environments where your calls should be delivered. These are the ideas motivating the development of CR, whose control processes leverage situational knowledge and intelligent processing to achieve goals related to the needs of the user, applications and networks.

In this introductory chapter, we first introduce several existing concepts of CR, revealing CR intelligence and the capabilities of adaptation. Next we show applications and examples of CR, as well as a recommended CR modulation technique.

2.1.1 Concept of CR

Though the concept of CR has been introduced, and the prototypes, applications and essential components of CR have been developed, the CR community has by far not agreed upon exactly what is and is not CR. However, some of the prominent offered definitions of CR are the following.

Joseph Mitola defines CR as “A radio that employs model-based reasoning to achieve a specific level of competence in radio-related domain.”[5]

Simon Haykin defines CR as “An intelligent wireless communication system that is aware of its surrounding environment (i.e., outside world), and uses the methodology of understanding-by-building to learn from the environment and adapt its internal states to statistical variations in the incoming RF stimuli by making corresponding changes in certain operating parameters (e.g., transmit-power, carrier-frequency, and modulation strategy) in real-time, with two primary objectives in mind:

- Highly reliable communications whenever and wherever needed;
- Efficient utilization of the radio spectrum.”[6]

Coming from a background where regulations focus on the operation of transmitters, the Federal Communication Commission (FCC) has defined CR as “A radio that can change its transmitter parameters based on interaction with the environment in which it operates.” [7]

While aiding the FCC in its efforts to define CR, IEEE USA offered the following definition [8]: “A radio frequency transmitter/receiver that is designed to intelligently detect whether a particular segment of the radio spectrum is currently in use, and to jump into (or out if necessary) the temporarily-unused spectrum very rapidly, without interfering with the transmissions of other authorized users.”

The broader IEEE tasked the IEEE 1900.1 group to design CR which has the following working definition: “A type of radio that can sense and autonomously reason about its environment and adapt accordingly. This radio could employ knowledge representation, automated reasoning and machine learning mechanisms in establishing, conducting, or terminating communication or networking functions with other radios. CR can be trained to dynamically and autonomously adjust its operating parameters.” [9]

Though there exists no universal agreed CR definition, the above definitions reveal some commonalities, such as adaptation and autonomous environment sensing abilities. In general, CR is capable of acquiring information about its operating environment. Additionally, it is capable of changing its waveform and applying information, which implies that CR has intelligent adaptations.

2.1.2 Applications of CR

There are many compelling and unique applications of CR due to its intelligent and unique characteristics. We only list a few of them which will be used as inspirational examples later in this thesis.

A. Improving spectrum utilization and efficiency

The growing demand on wireless communication systems to provide high data rates has triggered a huge demand on bandwidth that is expected to grow fast in the future. Spectrum licensing has been the traditional approach to ensure diverse wireless systems. However, after many years of spectrum assignment to meet the ever increasing demand, the frequency allocations show a heavily crowded spectrum with most frequency band already assigned to different licensed users for specific services [1]. However, research performed by various entities such as FCC indicates that the assumption of spectrum scarcity is far from real, because there is available spectrum since most of the allocated spectrum is underutilized [10].

Thus a natural question is to explore if there is room in the licensed spectrum band to accommodate unlicensed wireless devices without disrupting the communications of the PUs of the spectrum. CR provides three various solutions: “overlay”, “underlay” and “interwave” [2]. We will explain these three spectrum access schemes in the following.

The underlay approach allows concurrent primary and secondary transmissions in a manner as used in Ultra wideband (UWB) systems. Underlay systems protect PUs by enforcing a spectral mask on the secondary signals so that the interference generated by the secondary devices is below the acceptable noise floor of the spectrum used by the

PUs of the spectrum. The spectral mask constraints are compensated by access to a wide bandwidth over which the secondary signal can be spread and dispread in order to provide sufficient signal-to-noise (SNR) for secondary communications. However, the interference power constraints associated with underlay systems allow short-range communications only.

The overlay approach also allows concurrent primary and secondary transmissions. The premises for an overlay system are that the secondary users can use part of their power for secondary communication and the remainder of the power to assist (via relay) the primary transmissions. By careful choice of the power split, the increase in the PUs' SNR due to the assistance from secondary relaying is compensating for the decrease in the PUs' SNR due to interference caused by the remainder of the secondary transmit power that is used for secondary communication.

Based on the idea of opportunistic communication [3], J. Mitola proposed the interwave approach. Recent studies conducted by the FCC and industry show that a major part of the spectrum is not utilized most of the time. In other words, there exist temporary frequency voids, referred to as spectrum holes that are not in use by the licensed owners. These gaps change with time and geographic location, and can be used for communication by secondary users. Consequently, the utilization of the spectrum is improved by opportunistic frequency reuse over the spectrum holes. CR must be technically able to autonomously resolve conflicts over spectrum access by avoiding interference with incumbent signals.

B. Improve link reliability

Before the concept of CR has been proposed, many present adaptive radios are able to improve link reliability by adapting power transmission level, modulation or error correction [11]. However, as we mentioned before, CR is an intelligent radio, which can remember and learn from its past experiences. This goes even beyond simple adaptations. An example can be found in [11].

C. Less expensive radios

Though the complexity of the radio control process appears to increase the cost, the integration of the cognitive control process may significantly decrease the device cost when cognition is available. In fact these cognitive processes should be implemented in a software defined control process for which additional computations and thus costs are relatively insignificant, especially when compared to the cost of improving the performance of the analog components. Adding a couple of hundred software cycles per second is virtually costless; improving the performance of a Radio Frequency (RF) front end by 3 dB can be a very expensive [11]. Whether included in the transmitter or the receiver, CR may facilitate the use of lower cost analog components.

D. Distributed antenna arrays

When a group of subscribers is out of range of an access node and no other subscribers are positioned well enough to serve as relay nodes, a set of subscriber devices can collaborate with each other in such a way that their effective range can be dramatically increased and which is far enough to reach the access point. This illustrates the idea of a distributed communication scheme. It requires distributed subscribers to act like a radio system with distributed array antennas, and to collaborate with each other to forward signals to a distant access node.

For these distributed schemes, the collaborative transmission algorithm will be greatly simplified if each distributed node is aware of its own location and that of the distant access node, as well as the locations of the other nodes. The improvement of the node intelligence will be of significant aid for the algorithms. If we assume each collaborative node is a CR, this necessary information will be easily provided.

2.1.3 OFDM- A promising modulation scheme for CR

The multicarrier communication technique has been proposed as a promising candidate for the physical layer of CR systems because it can provide a flexible spectrum shape that fills the gaps in the available bandwidth without causing interference to the PUs [12]. This is commonly referred to as spectrum pooling [13]. Essentially the idea behind spectrum pooling is to access the spectrum holes in an “interwave” way, i.e., to merge available spectrum holes into a virtual band for the CR users.

OFDM, the most popular multicarrier technique, has been proposed as first candidate for the physical layer of a CR system [12]. Since the OFDM technique has an inherent capability to combat multipath fading and avoid inter symbol interference, it is especially suitable for wideband wireless communications. In spectrum pooling, CR needs to sense the spectrum, and this requires spectral analysis. Since Fast Fourier Transform (FFT) can be used for the spectral analysis, and at the same time it is also the demodulator of an OFDM signal, the OFDM multicarrier technique is a natural choice for CR transmission [14].

The time-domain OFDM signal $s(t)$ is given by

$$s(t) = g(t) \sum_{m=1}^M b_m e^{j2\pi f_m t}, \quad 0 \leq t \leq T_s \quad (2-1)$$

where $g(t)$ is the time-domain windowing function, b_m denotes the symbol to be transmitted at the m th sub-channel, and T_s denotes the OFDM symbol duration. Let $F_{CR} = \{f_m, 1 \leq m \leq M\}$ denote the total set of frequencies that may be used for CR transmission and $D_t \subseteq F_{CR}$ denotes the available set of frequencies at the current time slot t . The carriers located at the spectrum band of the PUs network are required to be

deactivated, as is shown in Figure 2.1. For instance two frequencies $f_1, f_2 \in D_t$ have been selected for the current time slot t .

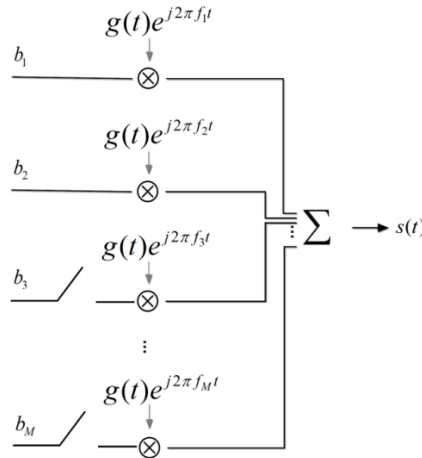


Figure 2.1 OFDM based CR transmitter at current timeslot t

2.2 Beamforming techniques

The term “beamforming” is derived from the fact that early spatial filters were designed to form pencil beams in order to receive a signal radiating from a specific location and attenuate signals from other locations [15].

Each system designed for receiving spatially propagating signals often encounters the presence of interference signals. If the designed signal and interferences occupy the same temporal frequency band, temporal filtering cannot be applied to separate wanted signals from interferences. However, the desired and interfering signals usually originate from different spatial locations. Then spatial separation can be explored to separate signals from interferences using a spatial filter. Therefore, the beamforming technique, as a spatial filtering technique, has been widely used and developed in Radar, Sonar and communication systems.

There are two beamforming technologies –ABF and DB. In this thesis we present, discuss and apply both of them for use in the CR system. In this section, we explain the ABF techniques. More details on DB can be found in chapter 5.

2.2.1 Basic terminology and concepts of ABF

ABF is a statistical technique for optimum beamforming. The output of adaptive beamformers is optimized to contain minimal contributions due to noise and interferences arriving from directions other than the desired signal direction. Next we explain several acknowledged adaptive beamformers with different criteria.

A. General system model of adaptive array antennas

An adaptive beamformer consists of multiple antennas, with complex weights $\mathbf{w} = [w_1 \ w_2 \ \cdots \ w_N]^T$ and an adder to add all of the processed signals. For a N -element

Uniform Linear Array (ULA) as shown in Figure 2.2, the received signal vector $\mathbf{x}(t)$ observed over time $t=1,2,\dots,N_t$ is multiplied by a complex weight vector \mathbf{w} . We assume that the number of time samples are N_t , i.e., there are N_t snapshots. The signals after weighting are then summed to form the beamformer output $y(t)$

$$y(t) = \sum_{n=1}^N w_n x_n(t) = \mathbf{w}^H \mathbf{x}(t) \quad (2-2)$$

where H denotes Hermitian transpose, and $\mathbf{x}(t) = [x_1(t) \ x_2(t) \ \cdots \ x_N(t)]^T$ are the received array signals at time t .

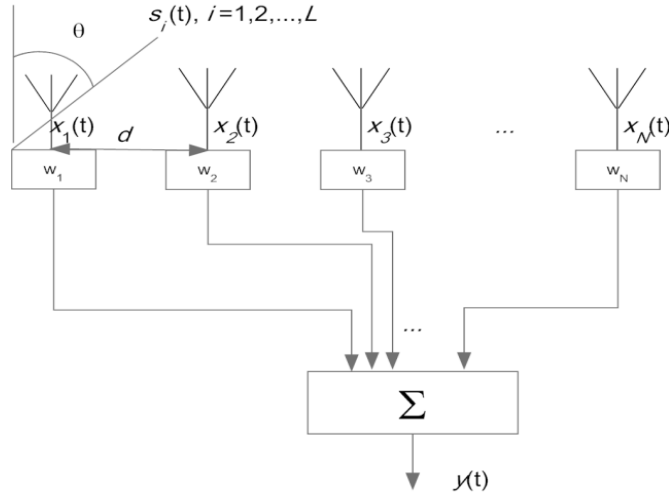


Figure 2.2 Array antennas with beamforming

For an N -element ULA in Figure 2.2, $\mathbf{x}(t)$ is obtained from:

$$\mathbf{x}(t) = \mathbf{A}^H \mathbf{s}(t) \quad (2-3)$$

where $\mathbf{s}(t) = [s_1(t) \ s_2(t) \ \cdots \ s_L(t)]^T$. $s_i(t)$, $i=1,2,\dots,L$ is the i th narrow band far-field signal impinging on the array antennas, coming from direction θ_i , as shown in Figure 2.2. In general, the incident signal $s(t)$ with time delay τ between receiving elements can be written as $s(t-\tau)$. If $s(t)$ is a narrow band signal, $s(t-\tau)$ can be simply approximated by a phase shift of $s(t)$, i.e., $s(t-\tau) \approx s(t)e^{j2\pi f\tau}$, where f is the central frequency of $s(t)$. Since we adopt the narrow band assumption, it is needed that over the relative bandwidth B and for limited sizes of the array aperture (i.e., the physical size of the antenna array measured in wavelengths) the condition should be satisfied that $B\tau \ll 1$, meaning that τ is much less than the inverse of the relative bandwidth [16]. The column of \mathbf{A} equals $\mathbf{a}(\theta_i)$, $i=1,2,\dots,L$, which represent the steering vectors of the impinging signals, i.e.,

$$\mathbf{A} = [\mathbf{a}(\theta_1) \ \mathbf{a}(\theta_2) \ \cdots \ \mathbf{a}(\theta_L)]^T \quad (2-4)$$

$$\mathbf{a}(\theta_i) = [1 \quad e^{-j\frac{2\pi d}{\lambda}\sin\theta_i} \quad \dots \quad e^{-j\frac{2\pi d}{\lambda}(N-1)\sin\theta_i}]^T \quad (2-5)$$

where d is the distance between successive adjacent array elements as shown in Figure 2.2, and λ is the wavelength of the impinging signal. In general, to apply ABF algorithms, the numerical dimension of the space spanned by $\mathbf{a}(\theta_i)$ should be less than N to be able to solve the matrix equations. In other words, the number of signals impinging on the array antenna is required to be less than the number of array elements, i.e., $L < N$.

If we define the autocorrelation matrix \mathbf{R}_x by

$$\mathbf{R}_x \triangleq \frac{1}{N_t} \sum_{t=1}^{N_t} \mathbf{x}(t)\mathbf{x}^H(t) \quad (2-6)$$

the output power is calculated from

$$P_y(\mathbf{w}) = E[y(t)] = \frac{1}{N} \sum_{t=1}^{N_t} \mathbf{w}^H \mathbf{x}(t) \mathbf{x}^H(t) \mathbf{w} = \mathbf{w}^H \mathbf{R}_x \mathbf{w} \quad (2-7)$$

B. Basic ABF algorithms

The ABF technique can be simply classified as either Direction Of Arrival (DOA)- based or as temporal-reference-based [17].

In DOA-based beamforming, the DOA estimation algorithm passes the DOA information to the beamformer. This is used to design a radiation pattern with the main beam directed towards the signal of interest and with nulls in the directions of the interferers. One example of a DOA-based beamformer is the Minimum Variance Distortionless Response (MVDR) beamformer [18], which designs the beamformer weights by minimizing the output power of the beamformer, combined with the constraint that the response of the beamformer should be unity in the direction of the signal of interest. This leads to the condition for the beamforming

$$\begin{cases} \arg \min_{\mathbf{w}} P_y(\mathbf{w}) \\ s.t. \mathbf{w}^H \mathbf{a}(\theta_1) = 1 \end{cases} \quad (2-8)$$

where θ_i is the DOA of the signal of interest provided by the DOA estimation. The minimization produces a beamformer with nulls in the directions of all the interfering signals, i.e., $s_l(t)$, $l \neq i$, $l = 1, 2, \dots, L$, and a maximum directed towards the desired signal $s_i(t)$. The MVDR beamformer computes the weights of each antenna element as

$$\mathbf{w}_{MVDR} = \frac{\mathbf{R}_x^{-1} \mathbf{a}(\theta_i)}{\mathbf{a}^H(\theta_i) \mathbf{R}_x^{-1} \mathbf{a}(\theta_i)} \quad (2-9)$$

The covariance matrix can be written as

$$\mathbf{R}_x = \sigma_i^2 \mathbf{a}(\theta_i) \mathbf{a}^H(\theta_i) + \mathbf{R}_N \quad (2-10)$$

where

$$\mathbf{R}_N = \sum_{l=1, l \neq i}^L \sigma_l^2 \mathbf{a}(\theta_l) \mathbf{a}^H(\theta_l) + \sigma_n^2 \mathbf{I}, \quad (2-11)$$

σ_l^2 is the power of the signal source $s_l(t)$ and σ_n^2 is the power of the noise. Due to $\mathbf{w}^H \mathbf{a}(\theta_i) = 1$, see equation (2-8), minimizing $\mathbf{w}^H \mathbf{R}_x \mathbf{w}$ is equal to minimizing $\mathbf{w}^H \mathbf{R}_N \mathbf{w}$. Thus the weights of the MVDR beamformer can also be given by

$$\mathbf{w}_{MVDR} = \frac{\mathbf{R}_N^{-1} \mathbf{a}(\theta_i)}{\mathbf{a}^H(\theta_i) \mathbf{R}_N^{-1} \mathbf{a}(\theta_i)} \quad (2-12)$$

The MVDR beamformer is also known as Capon's beamformer [18].

The temporal-reference-based beamformers use a known training sequence to adjust the weights, to form a radiation pattern with a maximum towards the signal of interest and to create nulls in the patterns towards the interfering signals. If $d(t)$ denotes the sequence of a reference or training symbol known a priori at the receiver at time t , an error $\varepsilon(t)$ is formed as the difference between the beamformer output $y(t)$ and $d(t)$. This error signal $\varepsilon(t)$ is used by the beamformer to adaptively adjust the complex weights \mathbf{w} , so that the Mean Square Error (MSE) is minimized, in other words

$$\begin{cases} y(t) = \mathbf{w}^H \mathbf{x}(t) \\ \arg \min_{\mathbf{w}} [|y(t) - d(t)|^2] \end{cases} \quad (2-13)$$

The choice of weights that minimize the MSE is such that the radiation pattern has a beam in the direction of the source that is transmitting the reference signal, and that there are nulls in the radiation pattern in the directions of the interferers. Once the beamformer has locked on to the reference signal, then the complex weights are maintained fixed, and transmission of the data packet begins. The complex weights of Minimum MSE (MMSE) are calculated by

$$\mathbf{w} = \mathbf{R}_x^{-1} \mathbf{r}_{xd} \quad (2-14)$$

where \mathbf{r}_{xd} is defined by

$$\mathbf{r}_{xd} \triangleq E[\mathbf{x}(t)d^*(t)] \quad (2-15)$$

where $*$ denotes complex conjugate.

C. Iterative ABF approaches

One iterative approach to realize the MMSE beamformer is based on the Least Mean Square (LMS) algorithm. This algorithm computes the $(n+1)$ th complex weights using [19]

$$\mathbf{w}(n+1) = \mathbf{w}(n) - 2\mu \mathbf{x}_n \varepsilon(n) \quad (2-16)$$

where μ denotes the step size, which is related to the rate of convergence. It also shows how fast the LMS algorithm reaches the steady state.

For a large eigenvalue spread of \mathbf{R}_x , the convergence of the LMS algorithm can be very slow. One alternative to the LMS algorithm is the exponentially weighted Recursive Least Squares (RLS) algorithm. The convergence of the RLS algorithm to find the statistically optimum weight is often faster than that obtained using the LMS algorithm. More details of the RLS method can be found also in [19].

2.2.2 Adaptive beamformers for wireless communications

Though ABF techniques are initially developed for military applications, it has been attracting a growing interest for use in commercial wireless communication systems. In general, ABF is regarded as a potential solution for bandwidth limitations. It is also called “Smart Antenna (SA)” when ABF techniques are employed by wireless communication systems which have array antennas. By exploiting the spatial dimension in signal processing, SA systems allow multiple mobile terminals to transmit co-channel signals, providing major benefits as described in the following [20].

A. Reduction of multipath fading effects

The effect of multipath fading in wireless systems can be reduced by using antenna diversity. Transmit diversity can be used to provide diversity benefits at a receiver having multiple transmit antennas only. With transmit diversity, multiple antennas transmit delayed versions of a signal, creating frequency-selective fading, which is equalized at the receiver to provide a diversity gain [21].

B. Increasing coverage

Multiple antennas capture more signal energy, which can be combined to improve the SNR. This array gain of SA systems makes it possible for the best station to cover wider areas than traditional single antenna systems. With increased cell coverage, the number of cells in a mobile cellular system can be decreased, which reduces the cost of infrastructure. Since the SNR is increased at the base station site, a proportionate reduction in the power transmitted from the mobile terminal to the base station is allowed, resulting in saving mobile devices’ battery life [22].

C. Increasing capacity

Since smart antenna systems exploit the spatial diversity of multiple mobile terminals, it is possible to separate co-channel signals and thus increase system capacity. SA suppresses interference through the uplink (signal from mobile terminal to base station) and downlink (signal from base station to mobile terminal) beamforming and resulting into focused beams towards the desired mobile terminal while steering nulls towards the others. It can thus significantly improve the Signal-to-Interference Ratio (SIR) which determines system capacity [23].

With all these advantages, adaptive SA systems are becoming an integral part of 3G, and beyond 3G wireless systems and also a promising technique for CR systems, which will be explained in the next section.

2.3 Applying Beamforming techniques to CR

In this section, we show the reason, the possibility, and challenges of introducing beamforming techniques into CR systems.

2.3.1 Beamforming as an interference cancellation scheme for CR

As mentioned in section 2.1, CR is envisioned to be capable of sensing and reasoning about the operating communication environment and thereby autonomously adjusting their transceiver parameters to exploit the underutilized radio resource in a dynamic way. Because of the spectrum sharing and opportunistic utilizing nature of CR, it inevitably operates in communication environments with intensive interferences. Therefore, interference management is essential to the coexistence of PUs and CR systems. It can be embedded into a CR system in various aspects of its design varying from network planning, radio resource management, Medium Access Control (MAC) to physical layer signal processing schemes. The latest is commonly known as Interference Cancelation (IC) techniques.

A few IC techniques have been studied in the context of CR networks [24]. The authors in [24] have presented an opportunistic IC scheme for CR receivers to adaptively cancel the PUs signals when they are unable to decode these signals. In [25], active spectrum shaping, transmit beamforming and transmit precoding techniques have been investigated for CR transmitters. Many other IC techniques can be found in [26]. They may use a filter based approach, transform-domain approach, cyclostationary based approach, higher-order statistics-based approach and spatial processing, also referred to as beamforming technique. Besides all the listed IC techniques, there are other types that may be also applicable to a CR system, such as non-linear signal processing using a neural network and analog signal processing.

The aim of introducing IC techniques at a CR receiver is to successfully operate under high levels of interference from PUs systems. A promising task in CR is to perform spectrum sensing and to identify the frequency bands of PUs. Based on the sensing results, the CR receiver can then choose to apply different spectrum access schemes as we have discussed in section 2.1, as well as apply corresponding IC techniques to obtain the optimized performance. Several major IC techniques at receiver and transmitter for CR are listed in Figure 2.3. They are the filter-based approach, transmit precoding, receive beamforming, cyclostationarity-based approach and higher order statistics-based approach. All these methods can be combined and implemented with each other.

- *filter-based approach*

The filter-based approach processes signals in time domain, and aims at separating the CR signals and interferences based on their power spectrum properties [25].

- *transform domain approaches*

Transform domain approaches, such as transmit precoding, first convert the received signal to the transformed domain, remove certain transform components, and then use the inverse transform to synthesize the CR signal. Transform domain approaches employ different time-frequency analysis tools (e.g. wavelet, short time Fourier transform, and chirplet) in order to provide a more powerful means for signal separation and classification [25].

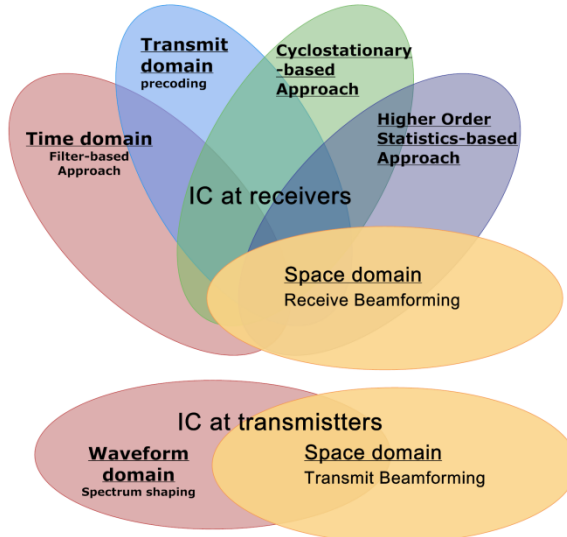


Figure 2.3 IC techniques at CR receivers and transmitters

- *cyclostationarity-based approach*

The Cyclostationarity-based approach has been proposed as a main approach in [3] for spectrum sensing in CR networks. It leverages the statistical properties of cyclostationary signals. It is a much more complete tool for signal analysis than those just relying on the power spectrum, since it provides more information on the carrier frequency, data rate and phase offset [25].

- *higher order statistics-based approach*

Incorporating higher order statistics (orders higher than two) into signal processing, the higher order statistics-based approach can provide additional distinction on the CR signals and interferences.

- *receiving beamforming technique*

In addition to signal and transform domain, the space domain can also be exploited in CR receivers to separate CR signals and interferences if they have different spatial signatures. In other words, when CR signals and interferences are coming from different directions, an array antenna can adaptively form different beam patterns to select the CR signals for receiving. This receiving beamforming technique requires that

each CR receiver is equipped with an array antenna to perform beamforming. The suppression gain of the receive beamforming technique is high, given a sufficient number of antenna elements, and the computational complexity is low [25].

CR transmission should be well managed to guarantee that PUs services are not harmfully interfered. It is therefore important for CR transmitters to adopt certain IC techniques to mitigate interferences that may disturb PUs receivers. Figure 2.3 also lists two typical transmitting IC techniques for CR.

- *spectrum shaping*

Spectrum shaping has been well investigated in UWB systems and in software defined radio. It generates proper waveforms for CR signals to minimize the power that may have leakage into the PUs bands.

- *transmit beamforming*

Similar to receiving beamforming, transmit beamforming can be applied to CR networks to mitigate interferences to PUs system by generating an emission beampattern with nulls towards PUs directions.

The aforementioned IC techniques can all be applied for CR networks at both receiving and transmission. Almost all IC techniques are proposed and discussed based on studies of CR transmission and reception in the signal domain, transform domain, frequency domain, waveform domain and space domain. Our work focuses on exploiting the space domain of CR networks by applying beamforming techniques for both CR receivers and transmitters. Next, we explain the feasibility of integrated beamforming techniques in CR systems as well as the challenges.

2.3.2 Beamforming and CR functionality

Mitola considers nine levels of increasing CR functionality as shown in Table 2.1 and ranging from software radio to complex self-aware radio [1]. In Table 2.1, we can see that adaptation is not new or beyond the functionalities of CR. At level 3 and level 4, the ABF technique can be integrated. If ABF is adopted by CR, at level 6, CR gains an additional learning capability of the spatial environment.

Table 2.1 Levels of CR functionality

Level	Capability	Comments
0	Pre-programmed	A software radio
1	Goal Driven	Choose Waveform According to Goal. Requires Environment Models
2	Context Awareness	Knowledge of What the Users is Trying to Do
3	Radio Aware	Knowledge of Radio and Network Components, Environment Models
4	Capable of Planning	Analyze Situation to Determine Goals (QoS, power). Follows Prescribed Plans
5	Conducts Negotiations	Settle on a Plan with Another Radio
6	Learns Environment	Autonomously Determines Structure of Environment
7	Adapts Plans	Generates New Goals
8	Adapts Protocols	Proposes and Negotiates New Protocols

Adaptation
ability of
beamforming

Mitola also introduces the cognitive cycle, as shown in Figure 2.4, as a “top-level control loop for CR” to demonstrate how CR could achieve these levels of functionality.

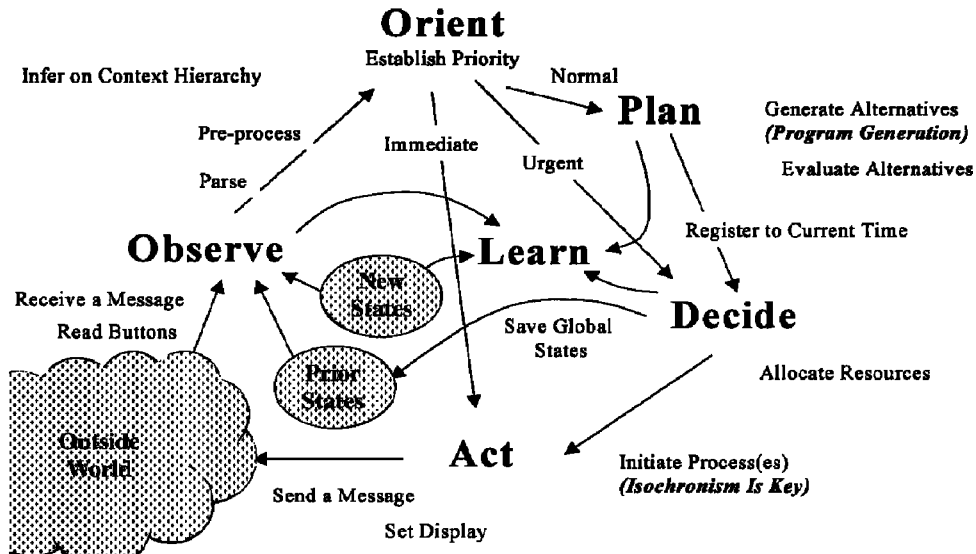


Figure 2.4 The Cognition Cycle [1]

In the cognition cycle, a radio receives information about its operating environment (outside world) through direct observation or signaling. This information is evaluated (Orient) to determine its importance. Based on the evaluation, the radio determines its alternatives (Plan) and choose alternatives (Decide) in a way that presumably would improve the result [1]. Assuming a waveform change is deemed necessary, the radio then improves the alternative (Act) by adjusting its resource and performing the appropriate signaling. These changes are then reflected in the interference profile presented by the CR in the outside world. As part of this process, the radio uses these observations and decisions to improve the operation of the radio (learn), perhaps by creating new modeling states, generating new alternatives, or creating new evaluations. Actually the implementation of beamforming can be obtained during the procedures of Observe, Decide and Act. No learning ability is involved in the beamforming procedure. However, when beamforming is integrated in the CR cognition cycle, the intelligence of CR can give smartness from beamforming by information sharing during processing steps of Orient and Plan. From this point of view, the beamforming technique also benefits from being part of CR due to its high level of intelligence.

2.3.3 Challenges of introducing beamforming to CR

The reason of introducing beamforming to CR is for IC management. The interferences of a CR system can be classified into two types: intra- and internetwork interferences [25]. Intranetwork interferences are also known as self-interference, which refers to interference caused within the CR network. It exists in every wireless communication system and there are plenty of techniques established to mitigate them effectively.

On the other hand, internetwork interference refers to the mutual interference between the PUs and CR networks. The problem of internetwork-interference management is twofold. First, CR transmitters need to carefully control their emissions to guarantee that the Quality of Service (QoS) of the PUs is not harmfully degraded by CR transmissions. Second, CR receivers should be able to effectively combat the interference from PUs to successfully decode CR signals and to provide useful QoS in CR networks. The problem of internetwork-interference management is extremely important for CR networks [25].

As a new metric to assess the interference in an underlay scheme, the interference temperature model has recently been proposed [6], which characterizes a worst-case interfering scenario in a particular frequency band and at a particular geographic location. In other words, it represents the maximum amount of interference that a receiver can tolerate. CR users are then allowed to use a frequency band as long as their transmissions do not violate the interference temperature limits. Several modified interference models have been proposed as more practical models for interference at primary receivers [27].

If CR intends to use the same spectrum band as PUs, the interference avoidance ability of CR transmitters has been considered by introducing the concept of an exclusion region [25]. As illustrated in Figure 2.5, an exclusion region is defined as a disk centered at a PU with a radius R . Any CR transmitter within the exclusion region is regarded as a harmful interferer and it is therefore forbidden to transmit.

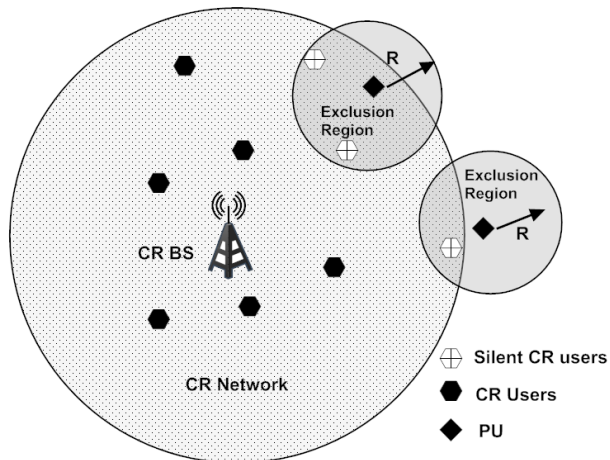


Figure 2.5 Coexistence of PUs and CR with exclusion regions

However, with a beamforming technique, the CR Base Station (BS) can transmit less power towards directions of PUs by spatially directing nulls towards them, as shown in Figure 2.6a. In Figure 2.6a, instead of being silent, CR users which are located within the exclusion region of PUs can be active. CR BS can still communicate with those CR users by employing beamforming techniques. The CR BS is thus required to be equipped with multiple antennas to perform beamforming, which applies weights on the antenna array to form the desirable beam.

Furthermore, the CR BS with multiple antennas in Figure 2.6a, can be replaced by CR networks which contain geographically distributed CR users, as shown in Figure 2.6b. In such CR networks, each CR user has a single antenna but is regarded as a virtual antenna element in an array. Thus they can form a desired beampattern to direct main beams towards distant CR users while nulls in the pattern are created towards PUs. This refers to a DB technique, which we will discuss and demonstrate for application in a CR network in chapters 5.

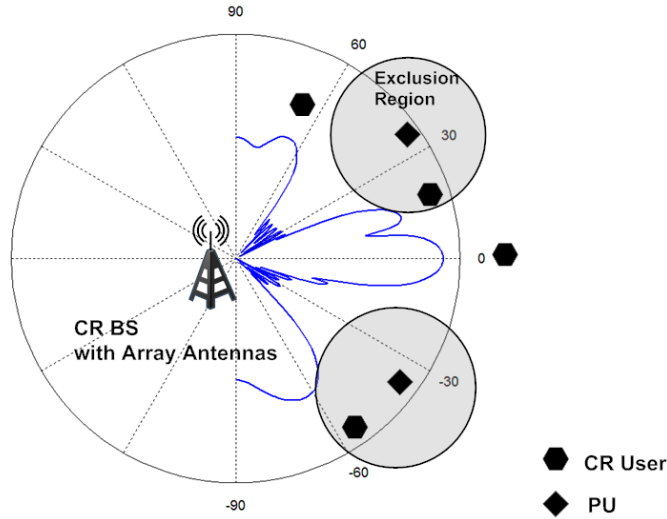


Figure 2.6a Coexistence of PUs and CR with ABF techniques

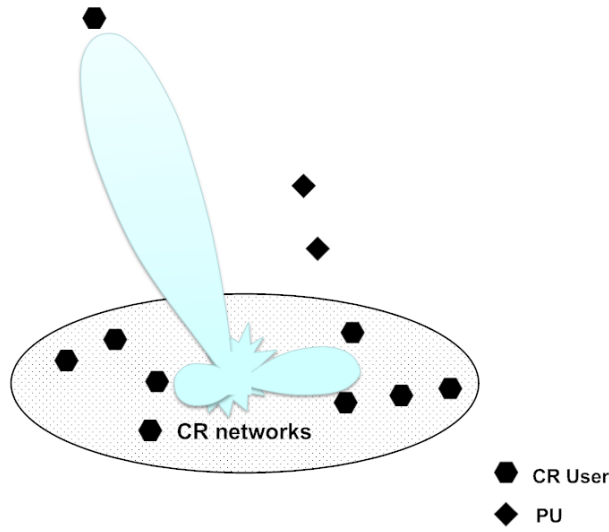


Figure 2.6b Coexistence of PUs and CR with DB techniques

Uplink beamforming (receiving beamforming), is clearly capable of suppressing co-channel interferences which are caused by PUs transmission. By employing beamforming techniques, the CR BS can adaptively enhance the signals of CR users by directing main beams towards their directions, even when the location information of CR users are imperfect. In chapter 3, we present robust adaptive beamformers for a CR system as examples of utilizing and realizing uplink beamforming techniques.

Most challenges exist in downlink beamforming (transmit beamforming). It can be applied to the CR BS for mitigating interferences to PUs by adaptively choosing weights on the transmit antenna elements to form an emission pattern with nulls towards directions of PUs. Implementation of a CR BS is more difficult and complicated in downlink beamforming than uplink beamforming. As can be seen in Figure 2.6a, CR users and PUs are not equipped with array antennas, and thus they have omnidirectional antennas instead. Therefore, even with nulls in the pattern towards PUs, the PUs may still receive CR signals due to scatter and multipath effects. As a result, we propose to spread nulls in a wider range around the direction of PU via employing a NB method, which will be discussed in detail in chapter 4.

Figure 2.6b illustrates that DB can be applied to CR networks to eliminate interference to PUs and to forward signals to distant CR users. The geographical distribution of the CR network leads to difficulties of generating a specific beampattern. However, DB provides an efficient and statistical way of directing main beams towards DCR users while nulls are made towards PUs. We will present a new DB method in chapter 5, as well as several schemes to select a smaller number of CR users in the network to become transmitters, in order to save the energy in the whole network.

2.4 Summary

CR is an intelligent radio system, which senses the communication environment and then adapts to it automatically. It improves the spectrum utilization and efficiency by providing underlay, overlay and interwave spectrum access schemes.

The beamformer can be regarded as a spatial filter, which enhances the signal coming from directions of interest while it attenuates other directions. It is capable of separating signals which are unable to be distinguished temporally or spectrally. Beamforming in general is achieved by forming a desired beampattern with main beam and nulls towards the required directions. There are two available beamforming techniques, ABF and DB for use in the CR system and CR networks. In this chapter, ABF is mainly discussed by introducing several adaptive beamformers as well as an iterative way of realizing it.

For CR, beamforming techniques are part of realizing cognition functionalities and can be integrated into its cognition cycle. Thus we propose the beamforming technique as an effective IC technique for the CR system. We propose that the CR BS is equipped with array antennas and thus it is able to flexibly direct the main beams towards CR own users while nulls are made towards PUs, when the CR system and PUs are coexisting with each other. Uplink beamforming is easier compared to downlink beamforming, because many available receiving beamforming techniques may be used. Downlink beamforming is a major challenge, which should be designed so that the power of the received signal at PUs due to CR BS transmission is lower than the required interference temperature.

Chapter 3 Uplink Adaptive Beamformers for CR

3.1 Introduction

As we have described in section 2.3, adaptive beamformers can be employed by a CR system as an efficient spectrum utilization technique due to its spatial filtering functionality. At uplink an adaptive beamformer at the CR BS can receive signals from CR users while mitigating signals from PUs, as shown in Figure 2.6a. In this figure, by utilizing the adaptive beamformer, the CR BS can direct main beams towards CR users while nulls in the pattern are made towards PUs. This spatial CR technique allows the CR system and PUs share the same spectrum band, because the CR system can at uplink distinguish the CR signals from PUs signals by exploiting the spatial diversity technique. As shown in Figure 2.6a, each CR user has an omnidirectional antenna pattern rather than a directional one. Thus CR users have to limit their transmission power in order to avoid interferences to each PU due to their transmissions. This is required because the interference power received at each PU should stay below its interference temperature, as we have discussed in chapter 2. It is noticed here that, at the CR BS it is difficult to estimate the accurate DOAs of CR users when the received signals from CR users have low SNR, and also suffer from multipath channel effects. As we know the performance of adaptive beamformers degrades substantially due to the imperfect knowledge on the array response, such as uncertainty of DOA, array calibrations and more [28-30]. Therefore, we need robust adaptive beamformers for the CR system to direct main beams towards CR users while DOA information of CR users are inaccurate or even unknown.

Investigations done to improve the robustness of adaptive beamformers [31-34] have resulted into the diagonal loading technique, the Linear Constrained Minimum Variance beamformer (LCMV), the eigenspace-based approach and the worst-case performance optimization, respectively. These methods can combat DOA uncertainties, but they are often conservative and only suitable in case of small DOA errors [35].

Different from the above mentioned methods we can use the Bayesian beamforming technique, which is able to estimate signals when the DOA is uncertain or completely unknown [36]. Applying a Bayesian model, the uncertain DOA is assumed to be a random variable with a prior distribution that describes the level of uncertainty. Thus the adaptive Bayesian beamformer can be considered as a combination of a conditional MVDR estimator and the data-driven posterior distribution function of DOA data. The Bayesian beamformer can be characterized by its adaptive learning ability via the

evolution of the posterior distribution for a wide range of SNR and data size, as has been explained in [35].

The adaptive Bayesian beamformer works perfectly in non-interference cases. However, when interference is present, or if its DOA is close to that of the desired signal, the adaptive Bayesian beamformer confuses these two directions and consequently fails to direct the null and main beam in the pattern towards the required directions. Beamforming technique allows CR BS to have access to the frequency band of PUs and reuse the same frequency band that used by PUs. Thus the CR BS receives PUs signals and immediately regards them as interferences. We then make use of a PM to solve the interference problem for the adaptive Bayesian beamformer. By projecting received signals on the orthogonal space of the steering matrix of interferences, we eliminate the presence of interferences in the approximation of the covariance matrix. The proposed method guarantees that the adaptive Bayesian beamformer is capable of directing main beams towards CR users even in case of low SNR and uncertainty of directions, while directing nulls towards directions of PUs even when DOAs of PUs are close to CR users.

Though the adaptive Bayesian beamformer presented in this thesis is only for narrowband systems, we can also apply it in the OFDM wideband system, which is regarded as the most proper modulation scheme candidate for CR, as we have discussed in paragraph 2.1.3.

ABF techniques in the context of wireless communications have already been applied to OFDM systems. In [37] a pre-FFT transform beamforming scheme to suppress the delayed signals of the desired user beyond the guard band has been described, while in [38] an adaptive OFDM beamformer has been proposed based on DOA estimation and maximum Signal to Interference plus Noise Ratio (SINR) criterion. In general, there are two kinds of adaptive OFDM beamformers at receiving side for an OFDM system, the pre-FFT [39] and the after FFT [40]. In this chapter, we adopt the adaptive OFDM beamformer at the receiving side with the after (post-) FFT structure, because it provides a more robust Bit Error Rate (BER) performance and always performs better than the pre-FFT beamformer [41].

To calculate the weights of downlink beamforming, the authors in [42, 43] have proposed a method to determine the downlink beamforming weights based on those of the uplink, which operates in different frequency bands. Based on this algorithm, we present here an iterative weights calculating method, which is less time consuming and has a smaller computational load; it will be discussed in paragraphs 3.3.1 and 3.3.2.

For the CR OFDM system, we consider both spectrum pooling and spectrum sharing techniques, and then present two methods to further modify the weights of adaptive OFDM beamformers for the CR system. If the adaptive OFDM beamformer utilizes spectrum pooling, which means that CR can access the spectrum in the “interwave” spectrum access scheme, then at uplink the CR BS forces the weights for those carriers which are in the same frequency bands with PUs, to become zeroes, as

shown in Figure 3.1a. This method masks some of the weights of the adaptive OFDM beamformer for OFDM subcarriers, and we call it “weights-masking technique”, which will be discussed further in paragraph 3.3.3.

Another efficient way of utilizing the spectrum is to require those weights to direct nulls to PUs in the space domain, in order to avoid PUs signals to be received by the CR BS from those directions. As a result, at uplink, the CR BS is capable of separating its own users from PUs. In this chapter, we present an adaptive OFDM beamformer for the CR BS based on a weights-constraint method described in paragraph 3.3.4. The weight-constraint method gives extra constraints on the weights of those OFDM subcarriers which are in the spectrum band with PUs, rather than simply giving them up. This method is visualized in Figure 3.1b.

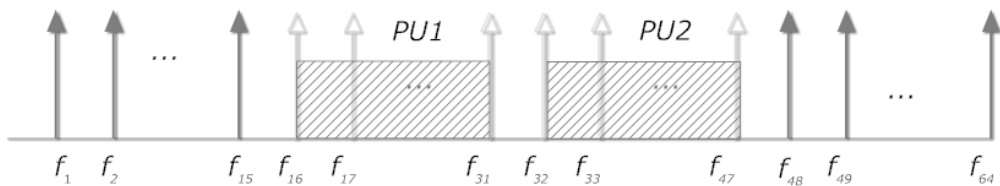


Figure 3.1a Weights-masking technique for adaptive OFDM beamformer
(subcarriers $f_{16} - f_{31}$ and $f_{32} - f_{47}$ are deactivated)

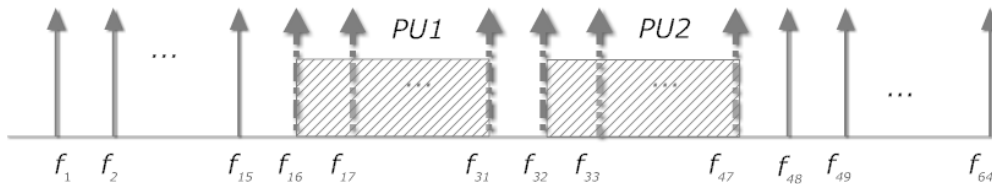


Figure 3.1b Weights-constraint technique for adaptive OFDM beamformer
(constraints on subcarriers $f_{16} - f_{31}$ and $f_{32} - f_{47}$)

If we replace in the adaptive receiving OFDM beamformer systems the MMSE beamformer after the FFT by the adaptive Bayesian beamformer, we can achieve an adaptive OFDM Bayesian beamformer, which will be discussed in detail in paragraph 3.3.5. The adaptive OFDM Bayesian beamformer adopts the weights-constraint method and thus is robust to CR users with low SNR and uncertainty in DOA estimations when they are coexisting with PUs.

For simplicity of derivation of all the results, we assume there is only one desired signal source per CR user, and per OFDM subcarrier. The case of more than one the desired signal sources can also be handled by our work. An example of more than one CR user is shown in section 3.4 on simulation and analysis.

3.2 Adaptive Bayesian uplink beamformers for CR

In this section, we propose a PM to ensure the CR BS to direct main beams towards CR users and nulls towards PUs via employing adaptive Bayesian beamformers. First we introduce the adaptive Bayesian beamforming technique and then we present our PM.

3.2.1 Adaptive Bayesian beamformer with MMSE criterion

We consider the model of a CR system coexisting with PUs in the same area and refer to Figure 2.5a. We adopt the array antenna model in Figure 2.2 for the CR BS by considering a CR BS that has a ULA containing N antenna elements. The total number of PUs are L , and their directions are $\theta_{PU1}, \theta_{PU2}, \dots, \theta_{PUL}$. \mathbf{A}_L denotes the steering matrix of the array in the directions of PUs and is defined by

$$\mathbf{A}_L \triangleq [\mathbf{a}(\theta_{PU1}) \quad \mathbf{a}(\theta_{PU2}) \quad \cdots \quad \mathbf{a}(\theta_{PUL})] \quad (3-1)$$

where $\mathbf{a}(\theta_{PUL}) = \begin{bmatrix} 1 & e^{-j\frac{2\pi d}{\lambda}\sin\theta_{PUL}} & \cdots & e^{-j\frac{2\pi d}{\lambda}(N-1)\sin\theta_{PUL}} \end{bmatrix}^T$, $l=1, 2, \dots, L$, d is the distance

between successive adjacent array elements and λ is the wavelength of the narrowband signals. If we assume there is only one CR user and $s_1(t)$ is its transmitted signal, the received signal at the array antenna of the CR BS in the presence of PUs can be described by

$$\mathbf{x}(t) = \mathbf{As}(t) + \mathbf{n}(t) \quad (3-2)$$

where

$$\mathbf{A} = [\mathbf{a}(\theta_1) \quad \mathbf{A}_L] \quad (3-3)$$

$$\mathbf{s}(t) = [s_1(t) \quad s_{PU1}(t) \quad s_{PU2}(t) \quad \cdots \quad s_{PUL}(t)]^T \quad (3-4)$$

θ_1 is the DOA of the CR user, $\mathbf{a}(\theta_1) = \begin{bmatrix} 1 & e^{-j\frac{2\pi d}{\lambda}\sin\theta_1} & \cdots & e^{-j\frac{2\pi d}{\lambda}(N-1)\sin\theta_1} \end{bmatrix}^T$ is the

direction vector of the CR user, and $s_{PUL}(t)$ ($l=1, 2, \dots, L$) are the transmitted signals of the l th PU. $\mathbf{n}(t)$ is Additive Gaussian White Noise (AWGN). The PUs signal sources and noise are considered to be statistically independent. The covariance matrix of the received signals in equation (2-6) can be written as

$$\mathbf{R}_x = E[\mathbf{x}(t)\mathbf{x}^H(t)] = \sigma_1^2 \mathbf{a}(\theta_1)\mathbf{a}^H(\theta_1) + \sum_{l=1}^L \bar{\sigma}_l^2 \mathbf{a}(\theta_{PUL})\mathbf{a}^H(\theta_{PUL}) + \sigma_n^2 \mathbf{I} \quad (3-5)$$

where σ_1^2 is the power of $s_1(t)$, $\bar{\sigma}_l^2$, $l=1, 2, \dots, L$ is the power of the l th signal and σ_n^2 is the variance of the noise. In order to know the communication environment, the DOA of the PUs, as well as other parameters of the communication environment are

estimated by the CR BS before starting its transmission. Therefore the CR BS has a prior information on $\theta_{PU1}, \theta_{PU2}, \dots, \theta_{PUL}$.

The MMSE beamformer minimizes the difference between the array output and the desired signal, as shown in equation (2-13). When the DOA of the desired signal is known, the solution of the MMSE beamformer is:

$$\mathbf{w}_{MMSE}(\theta_1) = \mathbf{R}_x^{-1} \mathbf{a}(\theta_1) \sigma_1^2 \quad (3-6)$$

When the DOA of $s_1(t)$ is unknown, it is assumed to be a random variable with a prior distribution function $p(\theta)$ defined on a set of Q points $\bar{\boldsymbol{\theta}} = \{\bar{\theta}_1, \bar{\theta}_2, \dots, \bar{\theta}_Q\}$. Let \mathbf{X} denote a collection of N_t array observations. The Bayesian MMSE beamformer becomes [36]:

$$\mathbf{w}_B = \sum_{i=1}^Q p(\bar{\theta}_i | \mathbf{X}) \mathbf{w}_{MMSE}(\bar{\theta}_i) = \sigma_1^2 \mathbf{R}_x^{-1} \sum_{i=1}^Q p(\bar{\theta}_i | \mathbf{X}) \mathbf{a}(\bar{\theta}_i) \quad (3-7)$$

where $p(\bar{\theta}_i | \mathbf{X})$ is the posterior distribution of $\bar{\theta}_i$. Given the observations, $p(\bar{\theta}_i | \mathbf{X})$ is determined and approximated in [36] by:

$$p(\bar{\theta}_i | \mathbf{X}) \approx a_x p(\bar{\theta}_i) \exp\left(-N_t \sigma_1^2 \mathbf{a}^H(\bar{\theta}_i) \hat{\mathbf{R}}_x^{-1} \mathbf{a}(\bar{\theta}_i)\right) \quad (3-8)$$

where $\hat{\mathbf{R}}_x$ is the estimation of \mathbf{R}_x , and a_x is a normalization factor that ensures the function integrates to one, i.e., $a_x = \left(\sum_{i=1}^Q p(\bar{\theta}_i | \mathbf{X}) \right)^{-1}$. When there are N_t snapshots used for calculating \mathbf{R}_x , we can write for $\hat{\mathbf{R}}_x$

$$\hat{\mathbf{R}}_x = \frac{1}{N_t} \sum_{t=1}^{N_t} \mathbf{x}(t) \mathbf{x}^H(t) \quad (3-9)$$

By replacing \mathbf{R}_x by $\hat{\mathbf{R}}_x$, the adaptive Bayesian beamformer can be realized by performing equations (3-8) and (3-7).

To achieve a relatively simple form of $p(\bar{\theta}_i | \mathbf{X})$, the authors in [36] have assumed that there is no interference signal impinging on the array antenna, which implies that

$$\mathbf{R}_x = \sigma_1^2 \mathbf{a}(\theta_1) \mathbf{a}^H(\theta_1) + \sigma_n^2 \mathbf{I} \quad (3-10)$$

When interferences are present (these interferences should be considered as signals transmitted by PUs) $p(\theta | \mathbf{X})$ is very difficult to be implemented, because \mathbf{R}_x is actually a function of the covariance matrix of interferences [44]. In addition, if the DOA of a PU is close to the DOA of the CR user, the adaptive Bayesian beamformer will probably include the DOA of the PU in the prior learning process, i.e., $\theta_{PUL} \in \bar{\boldsymbol{\theta}}, l = 1, 2, \dots, L$. Consequently, the adaptive Bayesian beamformer will confuse

these two directions due to the approximation of the posterior distribution function $p(\bar{\theta}_i | \mathbf{X})$. In order to guarantee that the approximation of $p(\bar{\theta}_i | \mathbf{X})$ is still valid in equation (3-8), we present the PM to eliminate the effects of the interference during Bayesian beamforming.

3.2.2 Projection Method (PM)

We define \mathbf{B} and \mathbf{B}_L by the following equations:

$$\mathbf{B} \triangleq \mathbf{I} - \mathbf{A}_L (\mathbf{A}_L^H \mathbf{A}_L)^{-1} \mathbf{A}_L^H \quad (3-11)$$

The eigenvectors $\mathbf{b}_1, \mathbf{b}_2, \dots, \mathbf{b}_{N-L}$ are corresponding to the non-zero eigenvalues of \mathbf{B} spanning the orthogonal complement space of \mathbf{A}_L , which has been defined in equation (3-1). With

$$\mathbf{B}_L \triangleq [\mathbf{b}_1 \ \mathbf{b}_2 \ \dots \ \mathbf{b}_{N-L}] \quad (3-12)$$

The condition $\mathbf{B}_L^H \mathbf{A}_L = \mathbf{0}$ is then satisfied, where $\mathbf{0}$ denotes a zero matrix. We define

$$\mathbf{z}(t) \triangleq \mathbf{B}_L^H \mathbf{x}(t) \quad (3-13)$$

Using $\mathbf{B}_L^H \mathbf{A}_L = \mathbf{0}$ and the result in equation (2-3), the covariance matrix of $\mathbf{z}(t)$ yields

$$\mathbf{R}_z = E[\mathbf{B}_L^H \mathbf{x}(t) \mathbf{x}^H(t) \mathbf{B}_L] = \sigma_1^2 \mathbf{a}_z(\theta_1) \mathbf{a}_z^H(\theta_1) + \sigma_n^2 \mathbf{B}_L^H \mathbf{B}_L \quad (3-14)$$

where $\mathbf{a}_z(\theta_1) = \mathbf{B}_L^H \mathbf{a}(\theta_1)$. When there are N_t snapshots available, the estimation of \mathbf{R}_z can be written as

$$\hat{\mathbf{R}}_z = \frac{1}{N_t} \sum_{t=1}^{N_t} \mathbf{z}(t) \mathbf{z}^H(t) \quad (3-15)$$

Using equation (2-13) and equation (3-6), the weights in the MMSE beamformer of $\mathbf{z}(t)$ satisfy the following two equations:

$$\mathbf{w}_{MMSE,z}(\theta_1) = \arg \min_{\mathbf{w}_{MMSE,z}} E \left[\left| \mathbf{w}_{MMSE,z}^H \mathbf{z}(t) - s_1(t) \right|^2 \right] \quad (3-16)$$

$$\mathbf{w}_{MMSE,z}(\theta_1) = \mathbf{R}_z^{-1} \mathbf{a}_z(\theta_1) \sigma_1^2 \quad (3-17)$$

We denote the weights of the adaptive Bayesian beamformer of $\mathbf{z}(t)$ as $\mathbf{w}_{B,z}$, which are calculated by

$$\mathbf{w}_{B,z} = \sum_{i=1}^Q p(\bar{\theta}_i | \mathbf{Z}) \mathbf{w}_{MMSE,z}(\bar{\theta}_i) = \sigma_1^2 \sum_{i=1}^Q p(\bar{\theta}_i | \mathbf{Z}) \mathbf{R}_z^{-1} \mathbf{a}_z(\bar{\theta}_i) \quad (3-18)$$

where \mathbf{Z} is a collection of observations of $\mathbf{z}(t)$

$$p(\bar{\theta}_i | \mathbf{Z}) \approx a_z p(\bar{\theta}_i) \exp \left(-N_t \sigma_1^2 \mathbf{a}_z^H(\bar{\theta}_i) \hat{\mathbf{R}}_z^{-1} \mathbf{a}_z(\bar{\theta}_i) \right) \quad (3-19)$$

and a_z is a normalization factor that ensures the function integrates to one, i.e.,

$$a_z = \left(\sum_{i=1}^Q p(\theta_i | \mathbf{Z}) \right).$$

We obtain the weights of the adaptive Bayesian beamformer of $\mathbf{x}(t)$ by

$$\mathbf{w}_{B,x} = \mathbf{B}_L \mathbf{w}_{B,z} \quad (3-20)$$

It is easy to verify that

$$\mathbf{w}_{B,x}^H \mathbf{A}_L = \mathbf{w}_{B,z}^H \mathbf{B}_L^H \mathbf{A}_L = \mathbf{0} \quad (3-21)$$

We define the array output signal $y(t)$, and the MSE error $\varepsilon(t)$ by

$$y(t) \triangleq \mathbf{w}_{B,x}^H \mathbf{x}(t) \quad (3-22)$$

and

$$\varepsilon(t) \triangleq E \left[\left| \mathbf{w}_{B,x}^H \mathbf{x}(t) - s_1(t) \right|^2 \right] \quad (3-23)$$

Using the result in equation (3-16), we can prove that the MSE error is the same as the adaptive Bayesian beamformer with input signal $\mathbf{z}(t)$

$$\varepsilon(t) = E \left[\left| \mathbf{w}_{B,x}^H \mathbf{x}(t) - s_1(t) \right|^2 \right] = E \left[\left| \mathbf{w}_{B,z}^H \mathbf{z}(t) - s_1(t) \right|^2 \right] \quad (3-24)$$

The basic steps of the PM are the following. We first calculate \mathbf{B}_L , and then replace $\mathbf{x}(t)$ by $\mathbf{z}(t)$. By assuming that the received signal at the array antenna is $\mathbf{z}(t)$, we then calculate $\mathbf{w}_{B,z}$, which is shown in equation (3-18). The final step is to project $\mathbf{w}_{B,z}$ to $\mathbf{B}_L \mathbf{w}_{B,z}$, expressed in equation (3-20).

During the Bayesian estimation procedure in equation (3-18) and (3-19), we eliminate the covariance matrix of interferences successfully because \mathbf{R}_z , which is defined in equation (3-14) contains no interference but only the desired signal $s_1(t)$ and the noise. Thus, we are allowed to use the approximation of $p(\bar{\theta}_i | \mathbf{X})$ given in literature [36].

3.3 Adaptive uplink OFDM beamformers for CR

3.3.1 OFDM adaptive beamformer with iterative weights calculating

Figure 3.2 gives the system configuration of the adaptive OFDM beamformer for CR. The MMSE beamformer is an “after FFT” for receiving and is called the post-FFT beamformer. Its basic idea is to regard OFDM signals as a combination of several narrowband signals, so that the weights of the receiving MMSE beamformer are decided after Multicarrier Modulator/Demodulator (FFT) blocks and thus for each OFDM subcarrier. We assume the radio channel is an AWGN channel.

As shown in Figure 3.2, if one set of weights \mathbf{w}_m for the m th OFDM subcarrier is computed, others will be deduced by mapping them into different frequency bands via transposition matrix \mathbf{T} , which is determined by two steering matrixes of different OFDM subcarriers. This transposition technique has been proposed for calculating the weights of downlink beamforming based on those of uplink in [42, 43], where both of the downlink and uplink operate in different frequency bands. We employ it in our work to determine the OFDM adaptive beamformer weights.

The array antenna in Figure 3.2 is assumed to be a ULA, containing N array elements, the distance between two consecutive element is $\lambda_0 / 2$, where

$$\lambda_0 = \frac{2c}{f_L + f_H} \quad (3-25)$$

and f_L, f_H are the lowest and highest frequencies of the OFDM signal, respectively. We assume that there are M OFDM subcarriers

$$f_m = f_L + (m-1) \frac{f_H - f_L}{M-1}, \quad m=1, 2, \dots, M \quad (3-26)$$

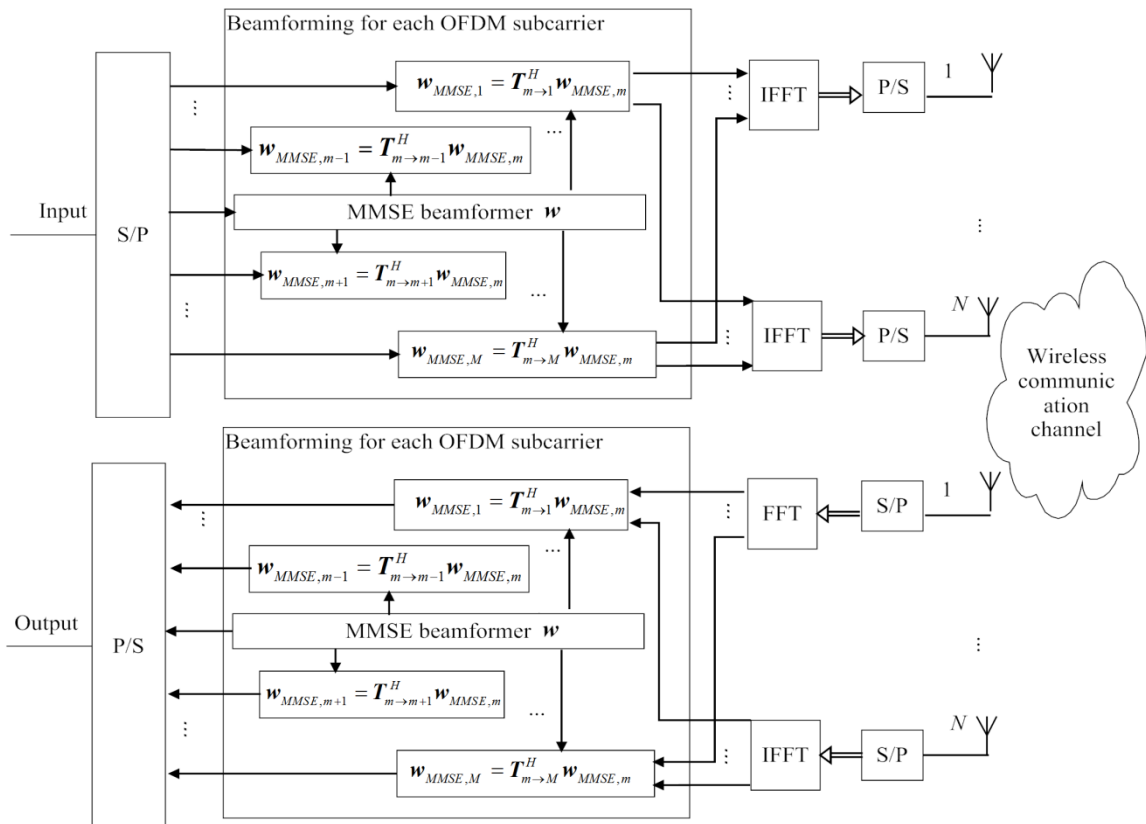


Figure 3.2 System configuration of an adaptive OFDM beamformer

The posterior FFT beamforming technique divides the OFDM signal into M different subcarriers, so that the beamforming technique for narrowband signal sources can be applied to each OFDM subcarrier. We consider the same model in section 3.2.1,

except that both the CR BS and CR users transmit OFDM signals. The received signal decomposed by the m th OFDM subcarrier is:

$$\mathbf{x}_m(t) = \mathbf{A}_m \mathbf{s}_m(t) + \mathbf{n}_m(t), \quad m=1,2,\dots,M \quad (3-27)$$

where \mathbf{A}_m is the steering matrix of the m th OFDM subcarrier,

$$\mathbf{A}_m \triangleq [\mathbf{a}_m \quad \mathbf{A}_{L,m}], \quad m=1,2,\dots,M \quad (3-28)$$

$$\mathbf{A}_{L,m} \triangleq [\mathbf{a}_m(\theta_{PU1}) \quad \mathbf{a}_m(\theta_{PU2}) \quad \cdots \quad \mathbf{a}_m(\theta_{PUL})], \quad m=1,2,\dots,M \quad (3-29)$$

$$\mathbf{a}_m(\theta_l) = \begin{bmatrix} 1 & e^{\frac{-j\pi f_m \lambda_0 \sin \theta_l}{c}} & \cdots & e^{\frac{-j(N-1)\pi f_m \lambda_0 \sin \theta_l}{c}} \end{bmatrix}^T, \quad m=1,2,\dots,M \quad (3-30)$$

$$\mathbf{a}_m(\theta_{PUL}) = \begin{bmatrix} 1 & e^{\frac{-j\pi f_m \lambda_0 \sin \theta_{PUL}}{c}} & \cdots & e^{\frac{-j(N-1)\pi f_m \lambda_0 \sin \theta_{PUL}}{c}} \end{bmatrix}^T, \quad m=1,2,\dots,M \quad (3-31)$$

$\mathbf{a}_m(\theta_{PUL})$ is the direction vector of the m th subcarrier for the l th PU signal, $\mathbf{a}_m(\theta_l)$ is the direction vector of the m th subcarrier for the CR user. $\mathbf{n}_m(t)$ in equation (3-27) is AWGN, and

$$\mathbf{s}_m(t) = [s_{1,m}(t) \quad s_{PU1,m}(t) \quad s_{PU2,m}(t) \quad \cdots \quad s_{PUL,m}(t)]^T \quad (3-32)$$

$s_{PUL,m}(t)$, $l=1,2,\dots,L$ is the decomposed part of the l th PU signal at m th frequency band and $s_{1,m}(t)$ is the decomposed part of the desired signal at m th OFDM frequency band.

We first discuss the MMSE beamformer for the OFDM system, which minimizes the difference between the array output and the desired signal, as shown in equation (2-13). Assuming that $s_{1,m}(t)$, $m=1,2,\dots,M$ is the desired signal, MMSE weights of the m th subcarrier $\mathbf{w}_{MMSE,m}$ satisfy the relation

$$\mathbf{w}_{MMSE,m} = \mathbf{R}_{x,m}^{-1} \mathbf{a}_m(\theta_l) \sigma_{1,m}^2 \quad (3-33)$$

where, $\mathbf{R}_{x,m}$ is the autocorrelation matrix of the received signal which have been demodulated on the m th subcarrier,

$$\mathbf{R}_{x,m} = E[\mathbf{x}_m(t) \mathbf{x}_m^H(t)] = \sigma_{1,m}^2 \mathbf{a}_m(\theta_l) \mathbf{a}_m^H(\theta_l) + \sum_{l=1}^L \sigma_{l,m}^2 \mathbf{a}_m(\theta_{PUL}) \mathbf{a}_m^H(\theta_{PUL}) + \sigma_{n,m}^2 \mathbf{I} \quad (3-34)$$

$\sigma_{1,m}^2$ is the power of $s_{1,m}(t)$ and $\sigma_{n,m}^2$ is the power of $\mathbf{n}_m(t)$.

We then present the adaptive OFDM beamformer with an iterative weights calculation method, which adopts the transposition matrix \mathbf{T} . We want to build a relationship between \mathbf{A}_m and \mathbf{A}_{m+i} . One simple way is to define a matrix which can map \mathbf{A}_{m+i} to \mathbf{A}_m by $\mathbf{T}_{m \rightarrow m+i} \mathbf{A}_{m+i} = \mathbf{A}_m$, $1 \leq m, m+i \leq M$. An obvious solution of calculating $\mathbf{T}_{m \rightarrow m+i}$ is to use equation (3-35).

$$\mathbf{T}_{m \rightarrow m+i} = \mathbf{A}_m (\mathbf{A}_{m+i})^+, \quad 1 \leq m, m+i \leq M \quad (3-35)$$

where $(\mathbf{A})^+$ is the pseudo-inverse of \mathbf{A} . In [42] the author has presented a similar way to define a transposition matrix for mapping the steering matrix from uplink at a frequency band to downlink at other frequency band. The same method has also been utilized in [43].

In order to explain the iterative weights calculation method, we assume that every PU utilizing the frequency bands $[f_1 \ f_M]$. If this is not satisfied, OFDM subcarriers may fall into different frequency bands of PUs. An example can be seen in Figure 3.1a and 3.1b. We will then adopt two different schemes: weights-masking and weights-constraint, which will be explained in detail in paragraphs 3.3.3 and 3.3.4.

Since the optimal weight $\mathbf{w}_{MMSE,m}$ of the MMSE beamformer also satisfies:

$$\begin{cases} \underset{\mathbf{w}_{MMSE,m}}{\text{argmax}} \|\mathbf{w}_{MMSE,m}^H \mathbf{a}_m(\theta_1)\| \\ s.t. \|\mathbf{w}_{MMSE,m}^H \mathbf{A}_{L,m}\| = \mathbf{C} \end{cases} \quad (3-36)$$

where \mathbf{C} is a $1 \times L$ constant vector, and each entry of \mathbf{C} is much smaller than $\|\mathbf{w}_{MMSE,m}^H \mathbf{a}_m(\theta_1)\|$, indicating the depth of nulls directed in the beampattern towards the interferences.

The weight for the $(m+i)$ th subcarrier $\mathbf{w}_{MMSE,m+i}$ can be obtained from:

$$\mathbf{w}_{MMSE,m+i} = \mathbf{T}_{m \rightarrow m+i}^H \mathbf{w}_{MMSE,m}, \quad 1 \leq m, m+i \leq M \quad (3-37)$$

Using the property

$$\mathbf{T}_{m \rightarrow m+i} \mathbf{a}_{m+i}(\theta_1) = \mathbf{a}_m(\theta_1) \quad (3-38)$$

$$\mathbf{T}_{m \rightarrow m+i} \mathbf{A}_{L,m+i} = \mathbf{A}_{L,m} \quad (3-39)$$

it is easy to verify that:

$$\begin{cases} \underset{\mathbf{w}_{MMSE,m+i}}{\text{arg max}} \|\mathbf{w}_{MMSE,m+i}^H \mathbf{a}_{m+i}(\theta_1)\| \Leftrightarrow \underset{\mathbf{w}_{MMSE,m}}{\text{arg max}} \|\mathbf{w}_{MMSE,m}^H \mathbf{T}_{m \rightarrow m+i} \mathbf{a}_{m+i}(\theta_1)\| \\ \Leftrightarrow \underset{\mathbf{w}_{MMSE,m}}{\text{arg max}} \|\mathbf{w}_{MMSE,m}^H \mathbf{a}_m(\theta_1)\| \\ \|\mathbf{w}_{MMSE,m+i}^H \mathbf{A}_{L,m+i}\| = \|\mathbf{w}_{MMSE,m}^H \mathbf{T}_{m \rightarrow m+i} \mathbf{A}_{L,m+i}\| = \|\mathbf{w}_{MMSE,m}^H \mathbf{A}_{L,m}\| = \mathbf{C} \end{cases} \quad (3-40)$$

3.3.2 Computation complexity analysis

The computation complexity is evaluated by counting the number of complex multiplications. We assume that the weight of the MMSE beamformer for the first OFDM subcarrier has been obtained. If we do not apply an iterative weights-calculating method, each weight of OFDM subcarriers can be computed independently by using equation (3-33). The complex multiplications of the estimation of the covariance matrix in equation (3-34) is of the order $O(N^2 \cdot N_t)$. The $O(\bullet)$ is an asymptotic notation,

which learns that the number of multiplications for each T_{MMSE} is of the order of $(N^3 + N^2) \cdot (M - 1)$. Repeating equation (3-33) for $(M - 1)$ times leads to a number of complex T_{MMSE} multiplications of the order of $O((N^3 + N^2 + N^2 \cdot N_t)(M - 1))$.

For the iterative weights calculating method, the weights in equation (3-37) can be further written as $\mathbf{w}_{MMSE,m+1} = \left[(\mathbf{A}_{m+1}(\theta))^+ \right]^H \mathbf{A}_m^H(\theta) \mathbf{w}_{MMSE,m}$. Due to the fact that $\mathbf{A}_m^H(\theta) \mathbf{w}_{MMSE,m}$ is repeated during each iteration, we can store it to avoid repetition of the calculations. To calculate $(\mathbf{A}_{m+1}(\theta))^+$, the number of complex multiplications becomes of the order $O((L+1)^3 + 2N(L+1)^2)$. The computational complexity of the iterative weights-calculating method is therefore $O((L+1)^3 + 2N(L+1)^2 + N(L+1)) \cdot (M-1)$.

Table 3-1 shows the results of $O(T_{MMSE})$ and $O(T_{iterative})$. We can see from table 3-1 that the adaptive OFDM beamformer with iterative weights-calculation has less complex multiplications than that of the MMSE beamformer. When we increase the number of array antennas, the computational load reduction of the iterative weights calculation method becomes even more significant.

Table 3-1 Number of complex multiplications of the MMSE beamformer and the beamformer with iterative weights-calculation

Simulation parameters	$O(T_{MMSE})$	$O(T_{iterative})$
$N=10 \quad L=5 \quad N_t=100 \quad M=64$	$O(7 \times 10^5)$	$O(0.6 \times 10^5)$
$N=20 \quad L=5 \quad N_t=100 \quad M=64$	$O(30 \times 10^5)$	$O(1 \times 10^5)$

3.3.3 Adaptive OFDM beamformer with weights-masking

When employing the spectrum masking technique, the OFDM ABF weights of those subcarriers in the OFDM system, which are in the frequency bands of PUs, need to be set to zero. This beamforming technique deactivates the weights for those OFDM subcarriers, as shown in Figure 3.1a.

We define:

$$\mathbf{w} \triangleq \begin{bmatrix} \mathbf{w}_{MMSE,1} & \mathbf{w}_{MMSE,2} & \cdots & \mathbf{w}_{MMSE,M} \end{bmatrix} \quad (3-41)$$

$$\mathbf{w}_{WM} \triangleq \begin{bmatrix} \mathbf{w}_{WM,1} & \mathbf{w}_{WM,2} & \cdots & \mathbf{w}_{WM,M} \end{bmatrix} \quad (3-42)$$

\mathbf{w} is an $N \times M$ matrix, where each column consists of the weights of the MMSE beamformer of the m th OFDM subcarrier, which is computed iteratively using the method presented in paragraph 3.3.1. \mathbf{w}_{WM} are the M weights of the weights-masking method.

The OFDM ABF with masking weights are:

$$\mathbf{w}_{WM,m} = \begin{cases} \mathbf{w}_{MMSE,m}, & f_m \notin f_{PU} \\ 0, & f_m \in f_{PU} \end{cases} \quad (3-43)$$

where f_{PU} is the frequency band occupied by all PUs, which are then forbidden for CR to be used. We define the following vector and matrix :

$$(\mathbf{M}_{PU})_{l,m} \triangleq \begin{cases} 1, & f_m \in f_{PUL} \\ 0, & \text{else} \end{cases}, \quad l=1,2,\dots,L; m=1,2,\dots,M \quad (3-44)$$

$$\mathbf{M}_{CR} \triangleq (\mathbf{1})_{N \times 1} \times \bigcap_{l=1}^L ((\mathbf{1})_{L \times M} - \mathbf{M}_{PU})_{l,1:M} \quad (3-45)$$

where $(\mathbf{A})_{m,n}$ denotes the (m, n) element in matrix \mathbf{A} , which is at the m th row and n th column. $(\mathbf{A})_{m,1:N}$ denotes the vector of the m th row of matrix \mathbf{A} . $(\mathbf{1})_{M \times N}$ denotes an

$M \times N$ matrix with all ones as its elements. $\bigcap_{l=1}^L \mathbf{a}_l$ means that

$\bigcap_{l=1}^L \mathbf{a}_l = \mathbf{a}_1 \odot \mathbf{a}_2 \odot \dots \odot \mathbf{a}_L$, where \odot is the Hadamard product, which is an element by

element multiplication of two vectors or in a matrix. Then we can write for the weights of the weights-masking method

$$\mathbf{w}_{WM} = \mathbf{w} \odot \mathbf{M}_{CR} \quad (3-46)$$

3.3.4 OFDM adaptive beamformer with weights-constraint

We assume that the l th PU utilizes the frequency bands f_{PUL} and that some of the OFDM subcarriers of the CR systems are allowed to access those frequency bands. For the m th OFDM subcarrier f_m , we assume that the total number of PUs, which utilizes this same frequency band f_m is l_m . Without losing generality, we assume that l_m is the biggest among l_1, l_2, \dots, l_M . If $f_m \in f_{PUL}$, we define the weights of the m th OFDM subcarriers of the MMSE beamformer by γ_m , which are designed to satisfy:

$$\gamma_m = \begin{cases} \arg \min_{\gamma_m} E \left[|\gamma_m^H \mathbf{x}_m(t) - s_{1,m}(t)|^2 \right] \\ \text{s. t. } \gamma_m^H \mathbf{A}_{l_m,m} = \mathbf{C}_{l_m} \end{cases} \quad (3-47)$$

where $\mathbf{A}_{l_m,m} \triangleq [\mathbf{a}_m(\theta_{PUL1}) \quad \mathbf{a}_m(\theta_{PUL2}) \quad \dots \quad \mathbf{a}_m(\theta_{PUL_{l_m}})]$. \mathbf{C}_{l_m} is a $1 \times l_m$ vector containing the constrained constants, which controls the depth of the nulls. Based on equation (3-28), we can further define \mathbf{A}_m by

$$\mathbf{A}_m \triangleq [\mathbf{a}_m(\theta_1) \quad \mathbf{A}_{l_m,m}], \quad m=1,2,\dots,M \quad (3-48)$$

The size of matrix \mathbf{A}_m is $N \times (l_m + 1)$. It now looks like that the transformation matrix $\mathbf{T}_{m \rightarrow m+i}$ defined in equation (3-35) may not be possible to be calculated, due to our assumption that $l_{m+i} \leq l_m$, $1 \leq m, m+i \leq M$. This problem can be overcome by making the modification defined as

$$\mathbf{Q}_{m+i} \triangleq \begin{pmatrix} (\mathbf{A}_{m+i})^+ \\ (\mathbf{0})_{(l_m - l_{m+i}) \times N} \end{pmatrix} \quad (3-49)$$

The size of the zero matrix “ $\mathbf{0}$ ” in \mathbf{Q}_{m+i} is $(l_m - l_{m+i}) \times N$. By constructing the matrix of \mathbf{Q}_{m+i} , we then define a new transposition matrix $\bar{\mathbf{T}}$ by

$$\bar{\mathbf{T}}_{m \rightarrow m+i} = \mathbf{A}_m \mathbf{Q}_{m+i}, \quad 1 \leq m, m+i \leq M \quad (3-50)$$

Now we can adopt equation (3-37) to calculate the weights iteratively

$$\boldsymbol{\gamma}_{m+i} = \bar{\mathbf{T}}_{m \rightarrow m+i}^H \boldsymbol{\gamma}_m \quad (3-51)$$

We can prove the following results

$$\left\{ \begin{array}{l} \arg \max_{\boldsymbol{\gamma}_{m+i}} \|\boldsymbol{\gamma}_{m+i}^H \mathbf{a}_{m+i}(\theta_1)\| \Leftrightarrow \arg \max_{\boldsymbol{\gamma}_m} \|\boldsymbol{\gamma}_m^H \bar{\mathbf{T}}_{m \rightarrow m+i} \mathbf{a}_{m+i}(\theta_1)\| \Leftrightarrow \arg \max_{\boldsymbol{\gamma}_m} \|\boldsymbol{\gamma}_m^H \mathbf{a}_m(\theta_1)\| \\ \boldsymbol{\gamma}_{m+i}^H \mathbf{A}_{l_{m+i}, m+i} = \boldsymbol{\gamma}_m^H \bar{\mathbf{T}}_{m \rightarrow m+i} \mathbf{A}_{l_{m+i}, m+i} = \boldsymbol{\gamma}_m^H \mathbf{A}_{l_m, m} \begin{pmatrix} (\mathbf{I})_{l_{m+i} \times l_{m+i}} \\ (\mathbf{0})_{(l_m - l_{m+i}) \times l_{m+i}} \end{pmatrix} = (\mathbf{C}_{l_m})_{1:l_{m+i}} \end{array} \right. \quad (3-52)$$

where $(\mathbf{C}_{l_m})_{1:l_{m+i}}$ denotes a vector consisting of the first l_{m+i} elements of the vector \mathbf{C}_{l_m} .

We define

$$(\mathbf{G})_{1:N, m} \triangleq \begin{cases} \boldsymbol{\gamma}_m, f_m \in f_{PU} \\ (\mathbf{0})_{N \times 1}, \text{ elsewhere} \end{cases}, \quad m = 1, 2, \dots, M \quad (3-53)$$

where $(\mathbf{A})_{1:N, m}$ denotes the m th column of matrix \mathbf{A} . Then we derive the weights of the weights-constraint method by

$$\mathbf{w}_{CW} = \mathbf{w} \odot \mathbf{M}_{CR} + \mathbf{G} \odot ((\mathbf{1})_{N \times M} - \mathbf{M}_{CR}) \quad (3-54)$$

The weights-constraint beamforming technique steps are summarized as follows:

1) Choose one of the OFDM subcarriers which is not in the same frequency bands occupied by PUs, e.g., $f_n, f_n \notin f_{PU}$;

2) Calculate the MMSE beamformer weights \mathbf{w} based on $\mathbf{w}_{MMSE, n}$ for all OFDM subcarriers using the weights iterative calculation method, as given by equation (3-37);

3) At the same time, compute the constrained weights for those OFDM subcarriers which are in the frequency band with PUs. First select the OFDM subcarrier, which is in the frequency band most used by PUs, e.g. f_m , and then calculate the

constrained weight γ_m for this OFDM subcarrier f_m . Using the weights iterative calculation method, derive the weights for other OFDM subcarriers based on γ_m , as shown in equation (3-51);

- 4) Use equation (3-54) to compute the final weights for all OFDM subcarriers.

3.3.5 Adaptive OFDM Bayesian beamformer with constrained weights

If we substitute for the “after FFT” MMSE beamformer in Figure 3.2 the adaptive Bayesian beamformer, we can achieve the adaptive OFDM Bayesian beamformer.

For the weights-masking method, no PM is needed because no signal receiving or transmitting by the adaptive Bayesian beamformer take place at those OFDM subcarriers, which are in the same spectrum band with PUs. However, when we introduce the weights-constraint method in the presence of PUs signals, the PM is suggested to be applied. Similar to the PM, the weights-constraint method also adds additional nulling directions in the pattern as can be seen in equation (3-47). Thus, the weights-constraint method is applicable to calculate the Bayesian weight of those OFDM subcarriers, which are in the same spectrum bands as used by PUs.

We define $\mathbf{w}_{B,m}$ as the Bayesian weights for the m th OFDM subcarrier, which is not in the same frequency band as utilized by PUs, $f_m \notin f_{PU}$, $m=1,2,\dots,M$. $\mathbf{w}_{B,m}$ can be obtained by using equation (3-7) which has been discussed in section 3.2 concerning the adaptive Bayesian beamforming technique for narrowband signal sources. If we define \mathbf{B}_m by

$$\mathbf{B}_m \triangleq \mathbf{I} - \mathbf{A}_{l_m,m} (\mathbf{A}_{l_m,m}^H \mathbf{A}_{l_m,m})^{-1} \mathbf{A}_{l_m,m}^H \quad (3-55)$$

the eigenvectors $\mathbf{b}_{m,1}, \mathbf{b}_{m,2}, \dots, \mathbf{b}_{m,N-l_m}$ which correspond to the non-zero eigenvalues of \mathbf{B}_m span the orthogonal complement space of $\mathbf{A}_{l_m,m}$. We define

$$\mathbf{B}_{m,L} \triangleq \begin{bmatrix} \mathbf{b}_{m,1} & \mathbf{b}_{m,2} & \cdots & \mathbf{b}_{m,N-l_m} \end{bmatrix} \quad (3-56)$$

$$\mathbf{z}_m(t) \triangleq \mathbf{B}_{m,L}^H \mathbf{x}_m(t) \quad (3-57)$$

$$\tilde{s}_{1,m}(t) \triangleq s_{1,m}(t) - \mathbf{C}_{l_m} (\mathbf{A}_{l_m,m}^H \mathbf{A}_{l_m,m})^{-1} \mathbf{A}_{l_m,m}^H \mathbf{x}_m(t), \quad (3-58)$$

and we assume that the received signal of the array antenna decomposed at the m th OFDM subcarrier is $\mathbf{z}_m(t)$ and consider $\tilde{s}_{1,m}(t)$ as the desired signal of the MMSE beamformer. The MMSE beamformer weights $\mathbf{w}_{z,m}$ should satisfy the following equation

$$\mathbf{w}_{z,m} = \arg \min_{\mathbf{w}_{z,m}} E \left[\left| \mathbf{w}_{z,m}^H \mathbf{z}_m(t) - \tilde{s}_{1,m}(t) \right|^2 \right] \quad (3-59)$$

The weight for the m th subcarrier can be obtained from:

$$\gamma_m = \mathbf{B}_{m,L} \mathbf{w}_{z,m} + \mathbf{A}_{l_m,m} (\mathbf{A}_{l_m,m}^H \mathbf{A}_{l_m,m})^{-1} \mathbf{C}_{l_m}^T \quad (3-60)$$

It is easy to verify that:

$$\left\{ \begin{array}{l} \arg \min_{\gamma_m} E \left[|\gamma_m^H \mathbf{x}_m(t) - s_{1,m}(t)| \right] \Leftrightarrow \arg \min_{\mathbf{w}_{z,m}} E \left[|\mathbf{w}_{z,m}^H \mathbf{z}_m(t) - \tilde{s}_{1,m}(t)| \right] \\ \gamma_m^H \mathbf{A}_{l_m,m} = \mathbf{w}_{z,m}^H \mathbf{B}_{m,L}^H \mathbf{A}_{l_m,m} + \mathbf{C}_{l_m} = \mathbf{C}_{l_m} \end{array} \right. \quad (3-61)$$

Thus we can achieve the adaptive Bayesian weights γ_m by equation (3-60). Substituting γ_m in equation (3-51), we then can obtain the constrained weights of all the OFDM subcarriers $\mathbf{w}_{B,CW}$ for the adaptive OFDM Bayesian beamformer.

3.4 Simulations and results

In the simulations we assume that the CR BS in Figure 2.6a and is equipped with a ULA. For narrowband signals, the distance between two successive array antenna elements equals half the wavelength ($d = \frac{\lambda}{2}$). For the OFDM signal, we assume that

$$d = \frac{\lambda_0}{2} = \frac{c}{f_L + f_H}, \text{ which is consistent with equation (3-25). We chose for } f_L = 300 \text{ MHz}$$

and $f_H = 320 \text{ MHz}$. Different numbers of OFDM subcarriers are simulated and compared. In addition, both Gaussian and Rayleigh channels in Figure 3.2 are taken into account. Figure 3.3-3.8 consider Binary Phase Shift Keying (BPSK) modulation, while Figure 3.9 and Figure 3.10 adopt Quadrature Phase Shift Keying (QPSK) modulation.

Figures 3.3 and 3.4 show the results of adaptive Bayesian beamformers with and without adopting the PM as proposed in paragraph 3.2.2. Figures 3.5a and 3.5b show the beampatterns of the adaptive OFDM beamformers based on MMSE beamformers and employing weights-masking and weights-constraint methods, which we have presented in paragraph 3.3.3 and 3.3.4, respectively. Figures 3.6 and 3.7 demonstrate the beampatterns of the adaptive OFDM Bayesian beamformer via adopting weights-constraint methods with different number of antenna elements. Figures 3.8a and 3.8b show the beampatterns of the adaptive OFDM Bayesian beamformer by employing weights-constraint methods with two CR users. Figures 3.9 and 3.10 consider the BER performance of the adaptive OFDM Bayesian beamformers in Gaussian and Rayleigh channels, respectively.

For understanding all results we return to Figure 3.3. This figure shows the learning performance of the Bayesian beamformer. We consider a ULA with 10 antenna elements ($N = 10$). We assume one CR user, which has a DOA of $\theta_1 = 4^\circ$, and its SNR is -15 dB . Meanwhile we assume there are two participating PUs coexisting with the CR system; their DOA's are $\theta_2 = -20^\circ$, $\theta_3 = 20^\circ$, and the SNR of both of them are 10 dB . The prior distribution function is chosen to be uniform over $[-10^\circ, 10^\circ]$. The number of the DOA candidates in equation (3-7) is assumed to be $Q = 21$. Thus the step

size of calculating the posterior distribution function in equation (3-8) is 1° . We consider the length of the learning sequence N_t is 100, which indicates that 100 snapshots of the received signal of the array antenna are utilized. We can see from Figure 3.3 that when the SNR of the CR signal is lower and the data size is shorter, the Bayesian beamformer focus on the prior information of the DOA. As a result, the Bayesian beamformer tends to cover the whole angle range of $[-10^\circ, 10^\circ]$ when N_t is small. When N_t is large, the Bayesian beamformer adapts to the data and points at the implicit estimated DOA, via the Bayesian mixture in equation (3-7).

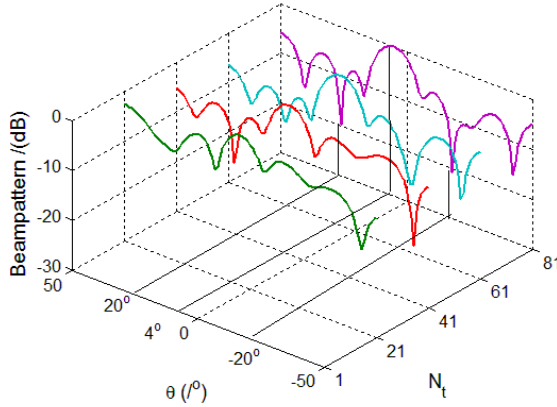


Figure 3.3 Learning procedure of an adaptive Bayesian beamformer

In Figure 3.4, we assume that the DOA of one participating PU is moving close to the CR user, i.e., $\theta_3=10^\circ$ instead of $\theta_3=20^\circ$. Other simulation assumptions remain the same with those in Figure 3.3. We can learn from Figure 3.4 that the adaptive Bayesian beamformer fails to direct the main beam towards the CR user, when θ_3 is included in the DOA candidates, which is defined over the interval of $[-10^\circ, 10^\circ]$. However the PM keeps the direction of the main beam towards the CR user. In addition, it also displays deeper nulls towards directions of PUs.

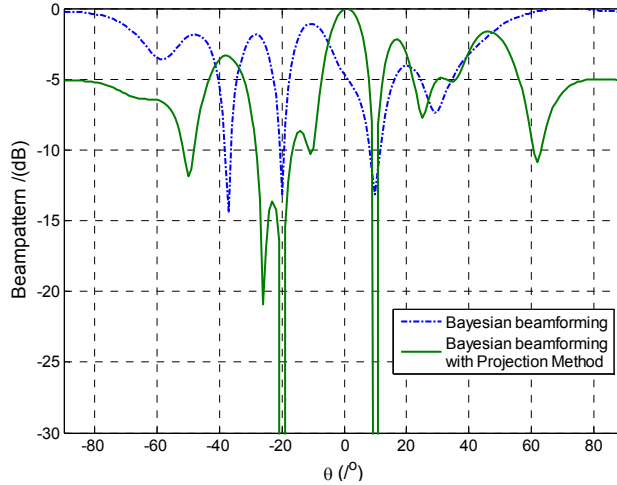


Figure 3.4 Adaptive Bayesian beamformer with Projection Method

Figure 3.5a and Figure 3.5b compare the beampattern of the adaptive OFDM beamformer based on the MMSE beamformer with weights-masking and weights-constraint methods. In Figure 3.5a and 3.5b, we adopt the same assumption of DOA and SNR of PUs and the CR user as for Figure 3.3. For the OFDM signal, we assume there are 64 OFDM subcarriers ($M = 64$). Each of the participants as PUs occupies 16 OFDM subcarriers of the CR BS, as is indicated in Figure 3.1a and 3.1b. As discussed in paragraph 3.3.3, weights-masking beamforming method gives up the OFDM subcarriers from f_{16} to f_{47} for use in PUs, i.e. only the first and last 16 subcarriers will be considered to be active for CR. Therefore, in Figure 3.5a the OFDM subcarriers from f_{16} to f_{47} are deactivated. As a result, the weights for those subcarriers are zeros, i.e. $\mathbf{w}_{MMSE,m} = 0$, $m = 16, 17, \dots, 47$, while with the weights-constraint beamforming method, CR can employ all the OFDM subcarriers. C_{l_m} in equation (3-47) is chosen to be $[10^{-3} \quad 10^{-3}]$.

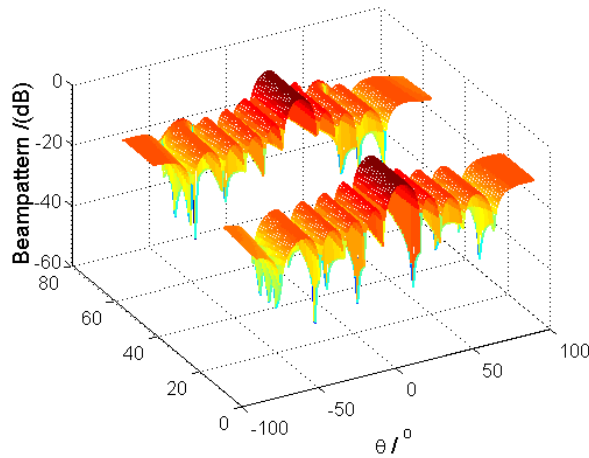


Figure 3.5a Adaptive OFDM beamformer using the weights-masking method

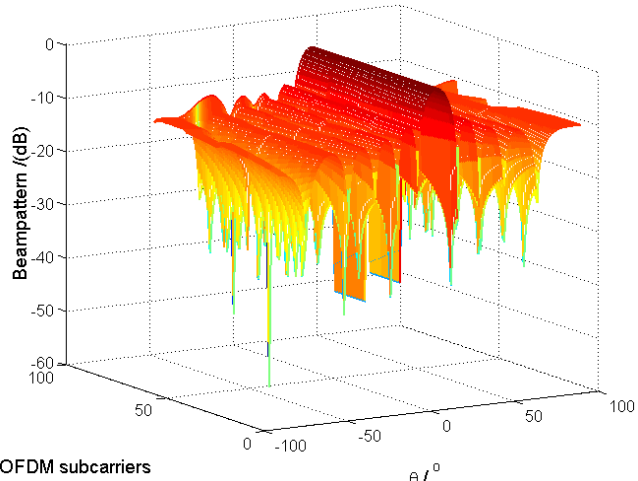


Figure 3.5b Adaptive OFDM beamformer using the weights-constraint method

Figure 3.5a and 3.5b both demonstrate that the adaptive OFDM beamformer can direct its main beam towards the CR user by iteratively calculating the weights of each OFDM subcarrier. In Figure 3.5b, the MMSE beamformer of the OFDM subcarriers f_{16} to f_{31} directs nulls towards the direction of -20° to the first PU, while the MMSE beamformer of the OFDM subcarriers f_{16} to f_{47} displays nulls towards the direction of 20° to the second PU.

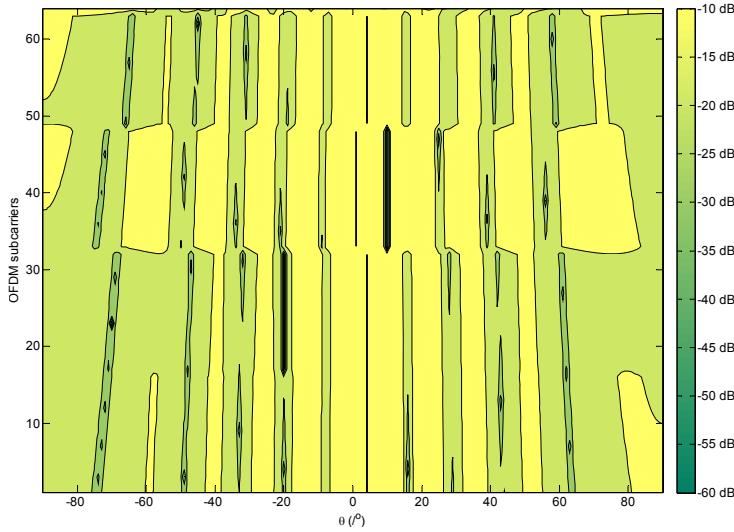


Figure 3.6 Beampattern of the adaptive OFDM Bayesian beamformer using the weights-constraint method and $N=10$ antenna elements

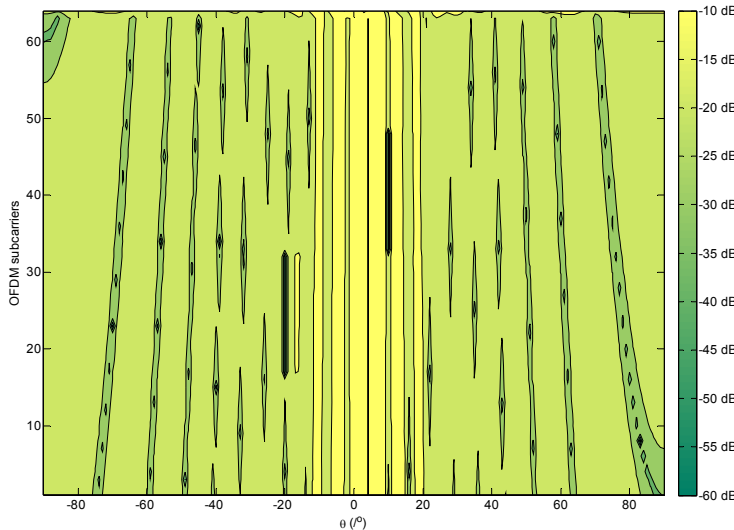


Figure 3.7 Beampattern of the adaptive OFDM Bayesian beamformer using the weights-constraint method and $N=20$ antenna elements

Figure 3.6 shows the contour figure of the beampattern of the adaptive OFDM Bayesian beamformer with the weights-constraint method when the DOA of the CR user is close to those of PUs. We consider the same simulation assumptions as in Figure 3.4 for each OFDM subcarriers. The allocation of OFDM subcarriers are the same as in

Figure 3.1b. We can see clearly two nulling areas. One is towards the direction of -20° performed by OFDM subcarriers f_{16} to f_{31} , and the other is towards the direction of 10° , performed by OFDM subcarriers f_{32} to f_{47} . The main beam shifts around -2° , due to the closeness of θ_1 and θ_3 .

Figure 3.7 considers the same simulation conditions as in Figure 3.6 but with more antenna elements. We assume $N = 20$. We know that with more antenna elements, the main beam of the adaptive beamformer becomes narrower and consequently we can achieve higher direction resolution. Figure 3.7 proves this result. It shows that when we employ more antenna elements of the array, the adaptive OFDM Bayesian beamformer can direct the main beams accurately towards the DOA of the CR user even when it is close to that of a participating PU.

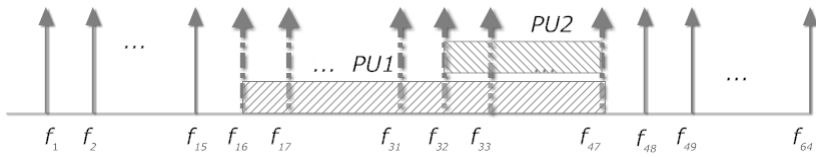


Figure 3.8a Frequency bands utilization of CR OFDM subcarriers and PUs

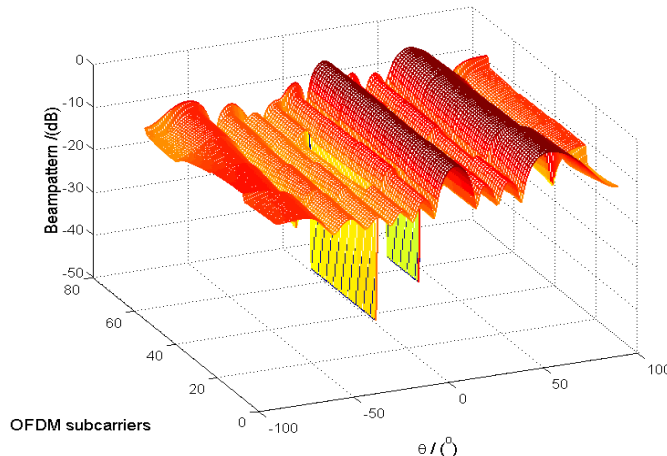


Figure 3.8b Adaptive OFDM beamformer using the weights-constraint method for two CR users

Next, we show the beampattern of the adaptive OFDM beamformer with different spectrum utilization of PUs and two CR users. In Figure 3.8a the first participating PU, which DOA is -20° , utilizes the frequency bands of OFDM subcarriers f_{16} to f_{47} .

We assume that there is another CR user, which has a DOA of 50° and its SNR is -10dB . The rest of the simulation assumptions are the same with those of Figure 3.5a and 3.5b. As shown in Figure 3.8b, the adaptive OFDM beamformer based on weights-constraint method can direct two main beams towards two CR users, respectively. Meanwhile the OFDM subcarriers f_{32} to f_{47} , which are in the same frequency bands

utilized by both participating PUs, are able to display both two additional nulls towards -20° and 20° , at the same time.

Figure 3.9 adopts the same simulation parameters with those in Figure 3.5a and 3.5b. It shows the BER performance of the adaptive Bayesian beamformer via employing weights-masking and weights-constraint methods in Gaussian and Rayleigh channels, respectively. A Rayleigh channel of two delay paths is here considered: the time delays are $0.1\mu s$ and $0.2\mu s$. The path loss of the two delay paths are considered as -10dB and -15dB , respectively. To cope with the multipath, we consider adopting Cyclic Prefix (CP) for the OFDM symbol, the length of which is decided to be one quarter of the length of an OFDM symbol. In Figure 3.9, the length of CP is $\frac{1}{4} \times 64 \times \frac{1}{20M} = 0.8 \mu s$. Since we mainly focus on the spatial performance of the adaptive OFDM beamformer, we do not pay attention to channel estimation and equalizer at the receivers. QPSK as a modulation technique is assumed. The power of every transmitted bit is E_b . The SNR (E_b / N_0) of the CR user changes from -10dB to 4dB . It can be seen from Figure 3.9 that the weights-masking method achieves lower BER due to the fact that it utilizes less number of OFDM subcarriers for transmission and reception. The BER performance of the Rayleigh channel is worse compared to the Gaussian channel.

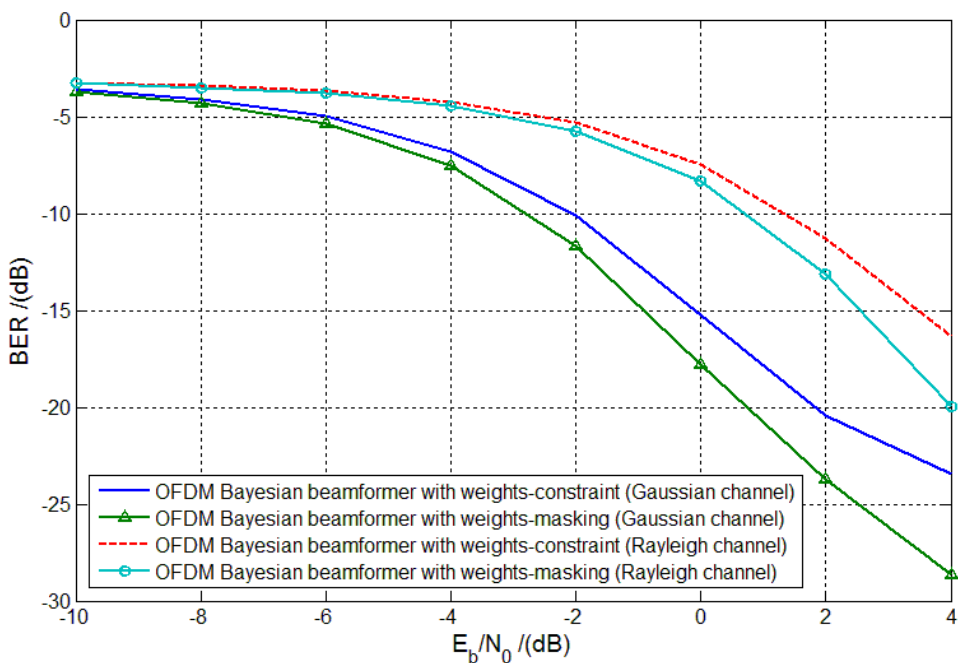


Figure 3.9 BER of Adaptive OFDM Bayesian beamformer with weights-masking and weights-constraint methods $M=64$

Figure 3.10 considers also the BER performance as in Figure 3.9 but with less number of OFDM subcarriers. We here consider $M = 32$, and thus the OFDM symbol duration is reduced to $32 \times \frac{1}{20M} = 1.6 \mu s$. Consequently the capability of coping with

multipath effects is decreased. Figure 3.10 shows that the BER performance with 32 OFDM subcarriers is in general slightly worse compared to the situation with 64 OFDM subcarriers.

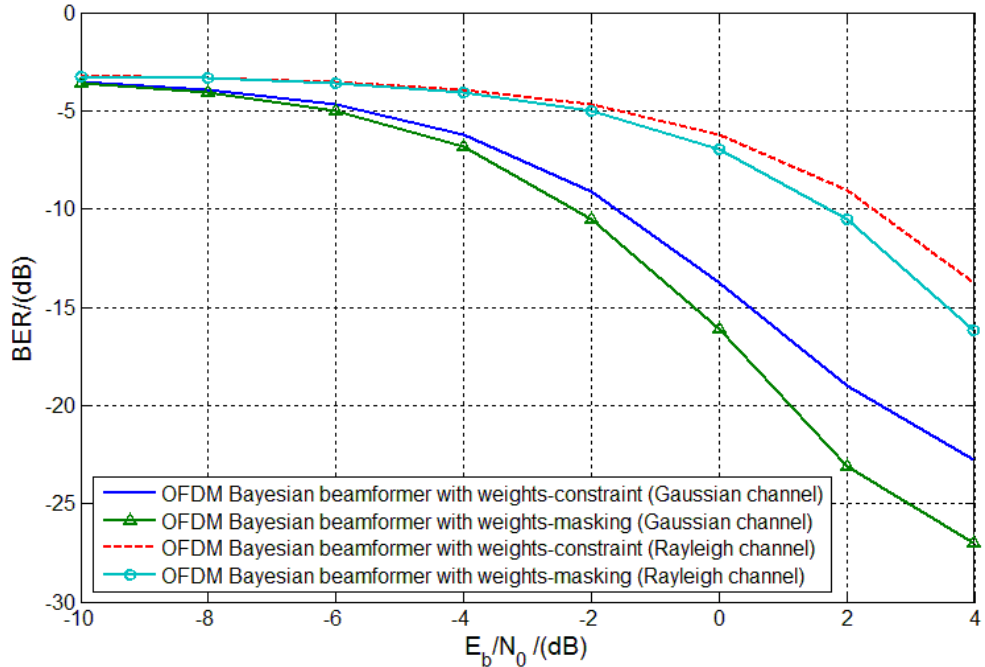


Figure 3.10 BER of the Adaptive OFDM Bayesian beamformer with weights-masking and weights-constraint methods $M=32$

The bit rates of the weights-masking method and weights-constraint method of Figure 3.9 are calculated by the following equations:

$$R_{WM} = \frac{32 \times \log_2 4}{64 \times \left(1 + \frac{1}{4}\right)} \times 20M = 16M \text{ (bit/s)} \quad (3-62)$$

$$R_{CW} = \frac{64 \times \log_2 4}{64 \times \left(1 + \frac{1}{4}\right)} \times 20M = 32M \text{ (bit/s)} \quad (3-63)$$

Equation (3-62) and (3-63) illustrate that the weights-constraint method can achieve a double transmit/receive rate compared with the weights-masking method.

3.5 Summary

We have presented two types of adaptive OFDM beamformers for the CR system at the up link to successfully receive signals from CR users while rejecting signals from PUs. They are the adaptive OFDM MMSE beamformer and adaptive Bayesian beamformer. The latter is suggested for the CR BS to perform beamforming when signals of CR users have low SNR and their DOAs are unknown or uncertain.

We proposed the PM to solve the problem of adjacent interferences coexisting with the desired signal sources for the adaptive Bayesian beamformers. When we apply the adaptive Bayesian beamforming technique with the PM for the OFDM beamformer, the CR BS can direct main beams towards the CR users accurately even when the DOA of the CR user is close to that of a participating PU. However, when the DOA of the CR user and that of a participating PU is too close to be separated, we suggest to increase the number of antenna elements of the array antenna to achieve better angular resolution.

We have calculated all the weights of adaptive OFDM beamformers for different OFDM subcarriers iteratively, which has less complex multiplication computations than the independent weights calculation for each OFDM subcarrier. Using the iterative weights calculation method, which we have adopted in this chapter, it will save computation time for weights calculation of the adaptive OFDM beamformer.

Based on different spectrum access schemes that CR adopts, we have proposed weights-masking and weights-constraint methods to modify the beamforming weights for those OFDM subcarriers which are in the same frequency band as PUs. The weights-masking method is adopted for the “interwave” spectrum access mode; it simply deactivates those OFDM subcarriers which are in the PUs frequency bands. The weights-constraint method benefits from higher spectrum efficiency by forcing the weights of those OFDM subcarriers to direct pattern nulls towards PUs. It is shown by simulations that the weights-masking method has a slightly better BER performance than that of the weights-constraint method. However, the latter can achieve a double bit rate for the CR OFDM system.

Chapter 4 Downlink Adaptive Beamformers with Broadened Nulls for the CR system

4.1 Introduction

At uplink, by introducing ABF techniques, the CR BS in Figure 2.6a can direct the main beams towards CR users while displaying nulls towards PUs. This ensures that the transmitted signals of CR users can be detected and then selected to be received by the CR BS via beamforming as discussed in chapter 3.

For downlink beamforming, the CR BS in Figure 2.6a should not disturb PUs, if it adopts the same spectrum bands with PUs. As we have discussed in chapter 2, the interferences to each PU caused by CR transmission should be kept below the interference temperature. By studying the properties of the spatial channel of PU, we discuss and propose a new IC technique for adaptive downlink beamformers which can be employed by the CR BS.

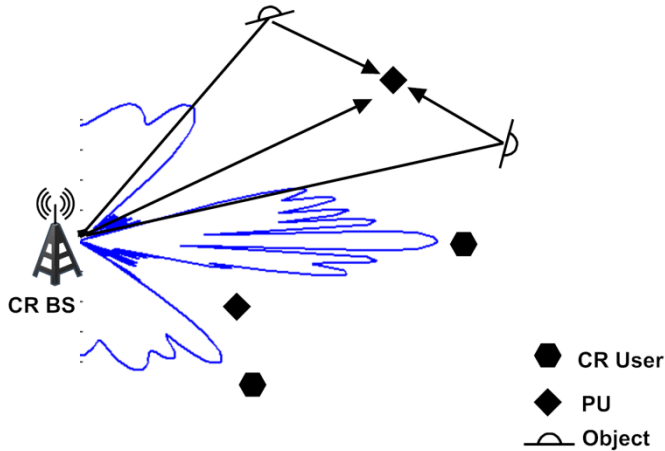


Figure 4.1 Spatial channel observed at the PU with scattering from the CR BS

As indicated in chapter 2, PUs are unable to receive signals transmitted by CR if we do not consider wave scattering or reflecting effects and assume that the CR BS points null patterns towards PUs' directions. However, a more practical case is shown in Figure 4.1. The objects around PUs are reflecting or scattering CR signals to PUs, which indicates that only putting pattern nulls towards the PUs by the CR BS is not enough to satisfy the interference criteria. Based on Figure 4.1, the study of the Angle of Arrival (AOA) of scattered or reflected waves is essential to describe the principle how the CR signal could be received by PUs.

The received signal and power spectra at the Mobile Station (MS) have been studied in [45-47]: it has been found out that they depend on the probability density function (pdf) of the AOA of the scattered wave. Clarke has considered a uniform AOA pdf over $[-\pi, \pi]$ [45]. However, it has been argued and experimentally demonstrated that the scattering encountered in many environments results into a non-uniform pdf for AOA at MS [46]. The authors in [47] have suggested a two-parameter Von Mises pdf as a flexible and generalized model for the pdf of AOA, which includes non-istropic scattering cases, and also the isotropic one as a special case. The pdf is given as [47],

$$p_{\Theta}(\theta) = \frac{e^{l_{\theta} \cos(\theta - \theta_p)}}{2\pi I_0(l_{\theta})}, \quad \theta \in [-\pi, \pi] \quad (4-1)$$

where $I_0(\bullet)$ is the zero-order modified Bessel function, θ_p accounts for the main direction of the AOA scatter components. Parameter $l_{\theta} \geq 0$ controls the width in the AOA of the scattering components. Figure 4.2 shows the $p_{\Theta}(\theta)$ for different l_{θ} and $\theta_p = 0$.

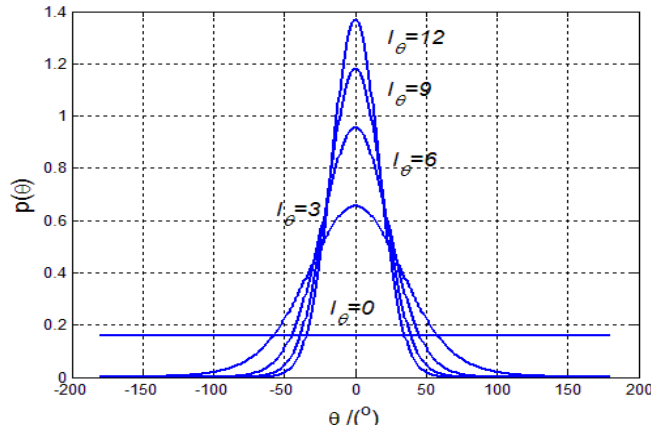


Figure 4.2 Von Mises pdf for the AOA of scattering components at the MS as function of θ around $\theta_p = 0$

In Figure 4.2, if the CR BS only directs a pattern null towards a specific participating PU, the signals transmitted by the CR BS towards adjacent directions may be reflected or scattered to this PU. Thus pattern nulls which can be generated by adaptive beamformers are not sufficient enough for energy depression, because the power around the nulling direction may also leak into the PU due to spatial scattering. We suggest that a certain range of spreading nulls should be generated around the direction of the PU. Therefore, we introduce the NB technique for the adaptive beamformer of the CR BS at downlink beamforming.

The NB technique has originally been developed as a robust array beamforming technique. It is also regarded as a beampattern synthesis method. Mailloux in [48] has presented a NB method as a simple modification of the covariance matrix of the received signal. In [49], a similar NB algorithm has been presented by applying a transform to the

same covariance matrix. Both methods are capable of providing notches at the locations of the interfering signals. In [50], these two NB algorithms have been defined as Covariance Matrix Taper (CMT) methods, and have been considered as effective robust ABF techniques, imparting robustness into the adaptive pattern by a judicious choice of the null placement and width. In [51, 52] it has been proved that NB is able to extract moving targets with a smaller number of snapshots to be derived from the covariance matrix in sonar applications. As for wireless communication, NB has been employed in a cellular communication system [53], and particularly an example has been given in Space Division Multiple Access (SDMA) systems for downlink beamforming. In [53], three different NB schemes have been compared. They are the Angular Spread (AS)-based approach, high order NB and multiple nulling. All of them have been shown to increase the SINR at the MS. What is more, they have also illustrated that NB for downlink beamforming is quite essential in the propagation environment in case AS is used. Recently in [54], a constrain optimization approach for NB has been proposed based on semi-definite programming. This NB method could also broaden the main beam for a desired detection and consequently it achieves a better coverage. Another iterative NB method has been discussed in [55] for suppressing side lobes in applications of array beampattern synthesis in case a low number of interference signals exist and high iteration speed is needed.

We present a new NB method in section 4.2, which is called Virtual Direction Adding (VDA). The new NB method gives us a closed-form relationship between the weights of the MVDR beamformer and those with broadened null patterns. Based on this result, we show that the weights of the adaptive OFDM beamformers using this NB technique can also be calculated iteratively by using the method that we have proposed in chapter 3. By filtering the weights of the NB beamformer, we also propose a method in section 4.2 that can achieve deeper depth in the broadened null patterns. We consider the window functions as our filters since their frequency responses successfully suppress side lobes. The depth of the broadened null patterns can be adjusted by choosing different window functions as filters or different parameters corresponding to the same window function.

In section 4.3, we demonstrate and compare the proposed VDA method with CMT, showing that the VDA method for the CR BS downlink beamforming is highly required and it decreases the interferences to PUs significantly. Both VDA and CMT methods are further discussed and shown to generate deeper nulls in the patterns using the filtering method.

4.2 A new Null Broadening (NB) method - VDA

In this section, we first introduce the CMT method which has been discussed in [50]. Then we will present our new NB method, VDA. Later we discuss how to control the depth of the null patterns in the NB method.

4.2.1 CMT method

We adopt the same model as introduced in paragraph 3.2.1. The uplink covariance matrix can be written by using equation (3-5),

$$\mathbf{R}_{uplink} = \mathbf{R}_x = \sigma_1^2 \mathbf{a}(\theta_1) \mathbf{a}^H(\theta_1) + \sum_{l=1}^L \sigma_l^2 \mathbf{a}(\theta_{PUL}) \mathbf{a}^H(\theta_{PUL}) + \sigma_n^2 \mathbf{I} \quad (4-2)$$

We then can estimate σ_n^2 , σ_l^2 and $\mathbf{a}(\theta_{PUL})$, $l=1,2,\dots,L$ by $\hat{\sigma}_n^2$, and $\hat{\sigma}_l^2$, $\hat{\mathbf{a}}(\theta_{PUL})$, $l=1,2,\dots,L$, which helps us to calculate the covariance matrix of the interference and noise for the downlink beamformer,

$$\mathbf{R}_N = \sum_{l=1}^L \hat{\sigma}_l^2 \hat{\mathbf{a}}(\theta_{PUL}) \hat{\mathbf{a}}^H(\theta_{PUL}) + \hat{\sigma}_n^2 \mathbf{I} \quad (4-3)$$

The CMT method has been proposed to be employed for the uplink mode [50]. However, when it is used for downlink beamforming, it needs to reconstruct the covariance matrix of the interference plus noise for downlink beamforming [54], which is shown in equation (4-3).

The weights of the MVDR beamformer at downlink are:

$$\mathbf{W}_{MVDR} = \frac{\mathbf{R}_N^{-1} \hat{\mathbf{a}}(\theta_1)}{\hat{\mathbf{a}}^H(\theta_1) \mathbf{R}_N^{-1} \hat{\mathbf{a}}(\theta_1)} \quad (4-4)$$

In order to produce a notch of width W in each interference direction, in the CMT method it is required to calculate \mathbf{R}_{CMT} by the Hadamard product of \mathbf{R}_N and \mathbf{T}_{NB} , i.e.,

$$\mathbf{R}_{CMT} = \mathbf{R}_N \odot \mathbf{T}_{NB} \quad (4-5)$$

where

$$(\mathbf{T}_{NB})_{m,n} = \text{sinc}[(m-n)W/2] \quad (4-6)$$

$(\mathbf{T}_{NB})_{m,n}$ represents the element of matrix \mathbf{T}_{NB} , which is located at the m th row and the n th column. $\text{sinc}(\bullet)$ is defined by $\text{sinc}(x) \triangleq \frac{\sin(\pi x)}{\pi x}$. W is the width between the outermost nulls in the beampattern, which has been defined in [48]. In [48], the author has assumed that if there is a signal coming from direction θ_j , by adding more signal sources around θ_j , the adaptive beamformer is able to generate spread nulls in the beampattern around θ_j . If the outermost signal source is at direction of θ_i , the following relationship between θ_j and θ_i has been defined by $d \sin \theta_i = d \sin \theta_j \pm W/2$, where d is the distance between successive adjacent array elements.

By using \mathbf{R}_{CMT} in equation (4-5) instead of \mathbf{R}_N , we can find the weights in the CMT method,

$$\mathbf{w}_{CMT} = \frac{\mathbf{R}_{CMT}^{-1} \hat{\mathbf{a}}(\theta_1)}{\hat{\mathbf{a}}^H(\theta_1) \mathbf{R}_{CMT}^{-1} \hat{\mathbf{a}}(\theta_1)}. \quad (4-7)$$

4.2.2 VDA method

By using the series expansion for the sinc function [56],

$$\text{sinc}(x) = \prod_{k=1}^{\infty} \left(1 - \frac{4}{3} \sin^2 \left(\frac{\pi x}{3^k} \right) \right) \quad (4-8)$$

the downlink covariance matrix \mathbf{R}_{VDA} of interference plus noise for the VDA method can be described by

$$(\mathbf{R}_{VDA}^V)_{m,n} \triangleq (\mathbf{R}_N)_{m,n} \prod_{k=1}^V \left(1 - \frac{4}{3} \sin^2 \left(\frac{\pi (m-n)W}{3^k} \right) \right) \quad (4-9)$$

If $V = \infty$, we can prove that

$$\mathbf{R}_{CMT} = \mathbf{R}_{VDA}^{\infty} \quad (4-10)$$

We can further rewrite equation (4-9) by converting \mathbf{R}_{VDA}^V into an iterative sequence

$$\mathbf{R}_{VDA}^V = \frac{1}{3} \mathbf{R}_{VDA}^{V-1} + \frac{2}{3} \mathbf{D}_{1,V} \mathbf{R}_{VDA}^{V-1} \mathbf{D}_{1,V} + \frac{2}{3} \mathbf{D}_{2,V} \mathbf{R}_{VDA}^{V-1} \mathbf{D}_{2,V}, \quad V \geq 1 \quad (4-11)$$

$$\mathbf{R}_{VDA}^0 = \mathbf{R}_N \quad (4-12)$$

where

$$\mathbf{D}_{m,k} = \begin{cases} \text{diag} \left(\left[\sin \left(\frac{\pi W}{3^k} \right) \quad \sin \left(2 \cdot \frac{\pi W}{3^k} \right) \quad \dots \quad \sin \left(N \cdot \frac{\pi W}{3^k} \right) \right]^T \right), & m=1 \\ \text{diag} \left(\left[\cos \left(\frac{\pi W}{3^k} \right) \quad \cos \left(2 \cdot \frac{\pi W}{3^k} \right) \quad \dots \quad \cos \left(N \cdot \frac{\pi W}{3^k} \right) \right]^T \right), & m=2 \end{cases} \quad (4-13)$$

and $\text{diag}(\mathbf{a})$ spans a diagonal matrix with each element of vector \mathbf{a} on the main diagonal. Equation (4-13) shows that the calculation of \mathbf{R}_{VDA}^V can be performed iteratively.

The proof of equation (4-11) is shown in Appendix A.

Equation (4-11) illustrates that the modification of the received signal of the V th iteration is to add two parts to that of the $(V-1)$ th. The first part is considered as one additional signal source, which has the following array vector $\mathbf{a}_{VDA1}^V(\theta_{PUL})$, where

$$\mathbf{a}_{VDA1}^V(\theta_{PUL}) = \left[\sin \left(\frac{\pi W}{3^V} \right) \quad \sin \left(\frac{2\pi W}{3^V} \right) e^{j \frac{2\pi}{\lambda} \sin(\theta_{PUL})} \quad \dots \quad \sin \left(\frac{N\pi W}{3^V} \right) e^{j \frac{2\pi(N-1)\sin(\theta_{PUL})}{\lambda}} \right]^T \quad (4-14)$$

The second part is considered as another additional signal source, which has the following array vector $\mathbf{a}_{VDA2}^V(\theta_{PUL})$, where

$$\mathbf{a}_{VDA2}^V(\theta_{PUL}) = \left[\cos\left(\frac{\pi W}{3^V}\right) \quad \cos\left(\frac{2\pi W}{3^V}\right) e^{j\frac{2\pi}{\lambda} \sin(\theta_{PUL})} \quad \dots \quad \cos\left(\frac{N\pi W}{3^V}\right) e^{j\frac{2\pi(N-1)\sin(\theta_{PUL})}{\lambda}} \right]^T \quad (4-15)$$

By adding the signals coming from the above two directions at each iteration, the VDA method displays a broadened pattern null around θ_{PUL} , $l=1,2,\dots,L$. The VDA method gives an implicit explanation of the modification of the covariance matrix of the downlink beamformer by demonstrating its iteration property. To achieve the wanted width W of the broadened pattern nulls by performing V times iterations, we define the starter width of the VDA method as W_0 , where

$$W_0 = \frac{W}{2^{V-1}} \quad (4-16)$$

Equation (4-10) shows that \mathbf{R}_{CMT} is an infinite expression for \mathbf{R}_{VDA} . \mathbf{R}_{VDA} approximates \mathbf{R}_{CMT} by only considering the first V items of the infinite sequence, which is shown by equation (4-9). Using the result in equation (4-8), the approximation is valid when

$$\max \left| 1 - \frac{4}{3} \sin^2 \left(\frac{\pi}{3^{V+1}} \frac{m-n}{2} W \right) \right| \approx 1 \quad (4-17)$$

or

$$\max \left| \frac{4}{3} \sin^2 \left(\frac{\pi}{3^{V+1}} \frac{m-n}{2} W \right) \right| \approx 0 \quad (4-18)$$

For example, we consider that the CR BS utilizes an array antenna with 10 array elements. If we choose $V = 2$ and $W = 0.2$, we need to satisfy the following equation in order to properly approximate \mathbf{R}_{CMT} by \mathbf{R}_{VDA}^2 ,

$$\max \left| \frac{4}{3} \sin^2 \left(\frac{\pi}{3^{V+1}} \frac{m-n}{2} W \right) \right| = \left| \frac{4}{3} \sin^2 \left(\frac{\pi}{3^{2+1}} \frac{9}{2} \cdot 0.2 \right) \right| = 0.015 \approx 0 \quad (4-19)$$

Since equation (4-18) is sufficiently valid, we can derive the iterative calculation of \mathbf{R}_{VDA}^2 by using equation (4-11) and (4-12). We derive

$$\mathbf{R}_{VDA}^1 = \frac{1}{3} \mathbf{R}_N + \frac{2}{3} \mathbf{D}_{1,1} \mathbf{R}_N \mathbf{D}_{1,1} + \frac{2}{3} \mathbf{D}_{2,1} \mathbf{R}_N \mathbf{D}_{2,1} \quad (4-20)$$

$$\mathbf{R}_{VDA}^2 = \frac{1}{3} \mathbf{R}_{VDA}^1 + \frac{2}{3} \mathbf{D}_{1,2} \mathbf{R}_{VDA}^1 \mathbf{D}_{1,2} + \frac{2}{3} \mathbf{D}_{2,2} \mathbf{R}_{VDA}^1 \mathbf{D}_{2,2} \quad (4-21)$$

The reconstructed covariance matrix of \mathbf{R}_{VDA}^1 in equation (4-20) is given in the scheme of Figure 4.3, while the covariance matrix of \mathbf{R}_{VDA}^2 in equation (4-21) is given in the scheme of Figure 4.4.

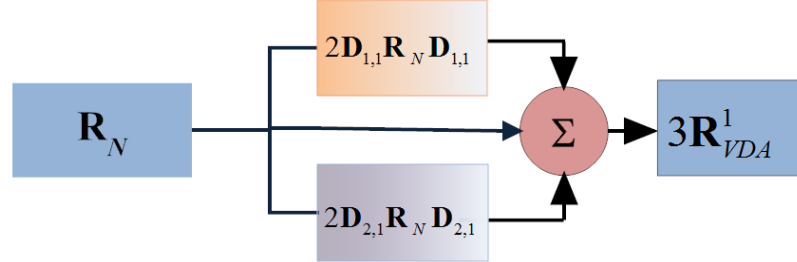


Figure 4.3 Reconstructed covariance matrix of the VDA method for $V=1$

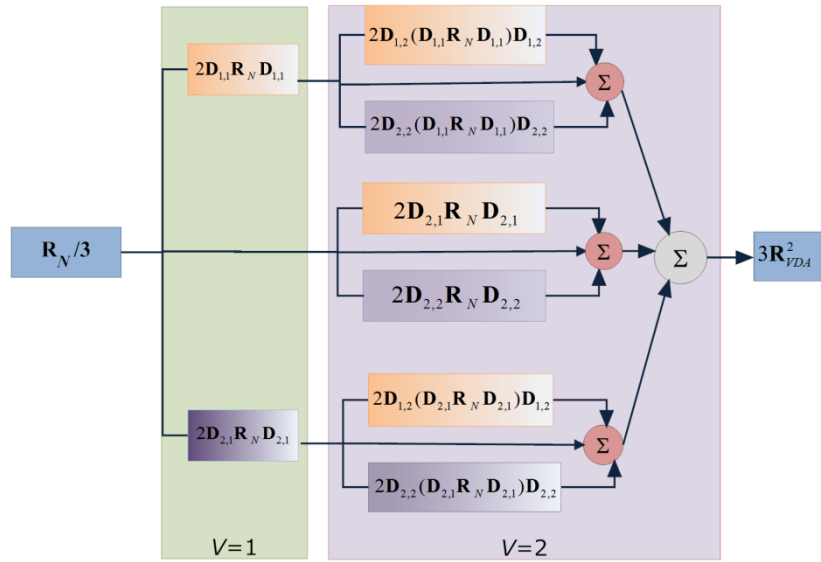


Figure 4.4 Reconstructed covariance matrix of the VDA method for $V=2$

If we adopt \mathbf{R}_{VDA}^V instead of \mathbf{R}_N in equation (4-4), we can compute the weights \mathbf{w}_{VDA} of the VDA method. We can derive

$$\mathbf{w}_{VDA}^{V+1} = \frac{\hat{\mathbf{a}}^H(\theta_1) (\mathbf{R}_{VDA}^V)^{-1} \hat{\mathbf{a}}(\theta_1)}{\hat{\mathbf{a}}^H(\theta_1) (\mathbf{R}_{VDA}^V + \tilde{\mathbf{R}}_{VDA}^{V+1})^{-1} \hat{\mathbf{a}}(\theta_1)} \left[\mathbf{I} + (\mathbf{R}_{VDA}^V)^{-1} \tilde{\mathbf{R}}_{VDA}^{V+1} \right]^{-1} \mathbf{w}_{VDA}^V \quad (4-22)$$

$$\mathbf{w}_{VDA}^0 = \mathbf{w}_{MVDR} \quad (4-23)$$

where

$$\tilde{\mathbf{R}}_{VDA}^{V+1} = 2\mathbf{D}_{1,V+1}\mathbf{R}_{VDA}^V\mathbf{D}_{1,V+1} + 2\mathbf{D}_{2,V+1}\mathbf{R}_{VDA}^V\mathbf{D}_{2,V+1} \quad (4-24)$$

The proof of equation (4-22) is shown in Appendix B.

Equation (4-22) shows that \mathbf{w}_{VDA}^{V+1} and $\left[(\mathbf{R}_{VDA}^V)^{-1} \tilde{\mathbf{R}}_{VDA}^{V+1} + \mathbf{I} \right]^{-1} \mathbf{w}_{VDA}^V$ only differ in scale.

Next we apply the VDA method to adaptive OFDM beamformers for CR as we have discussed in chapter 3. We consider the same model for the CR system as proposed

in section 3.3. We assume the weights of the V th iteration of the VDA method for the m th OFDM subcarrier are $\mathbf{w}_{VDA,m}^V$.

We further define

$$\mathbf{R}_{N,m} \triangleq \sum_{l=1}^L \hat{\sigma}_{l,m}^2 \hat{\mathbf{a}}_m(\theta_{PUL}) \hat{\mathbf{a}}_m^H(\theta_{PUL}) + \hat{\sigma}_{n,m}^2 \mathbf{I} \quad (4-25)$$

$$\mathbf{R}_{VDA,m}^V \triangleq \frac{1}{3} \mathbf{R}_{VDA,m}^{V-1} + \frac{2}{3} \mathbf{D}_{1,V} \mathbf{R}_{VDA,m}^{V-1} \mathbf{D}_{1,V} + \frac{2}{3} \mathbf{D}_{2,V} \mathbf{R}_{VDA,m}^{V-1} \mathbf{D}_{2,V} \quad (4-26)$$

$$\tilde{\mathbf{R}}_{VDA,m}^{V+1} \triangleq 2\mathbf{D}_{1,V+1} \mathbf{R}_{VDA,m}^V \mathbf{D}_{1,V+1} + 2\mathbf{D}_{2,V+1} \mathbf{R}_{VDA,m}^V \mathbf{D}_{2,V+1} \quad (4-27)$$

$$\mathbf{U}_m^V \triangleq \frac{\hat{\mathbf{a}}^H(\theta_1) (\mathbf{R}_{VDA}^V)^{-1} \hat{\mathbf{a}}(\theta_1)}{\hat{\mathbf{a}}^H(\theta_1) (\mathbf{R}_{VDA}^V + \tilde{\mathbf{R}}_{VDA}^{V+1})^{-1} \hat{\mathbf{a}}(\theta_1)} \left[\mathbf{I} + (\mathbf{R}_{VDA}^V)^{-1} \tilde{\mathbf{R}}_{VDA}^{V+1} \right]^{-1} \quad (4-28)$$

where $\hat{\sigma}_{l,m}$, $\hat{\mathbf{a}}_m(\theta_{PUL})$ and $\hat{\sigma}_{n,m}^2$ in equation (4-25) are estimations of $\bar{\sigma}_{l,m}$, $\mathbf{a}_m(\theta_{PUL})$ and $\sigma_{n,m}^2$, which have already been defined in equation (3-31) and (3-34).

The adaptive MMSE adaptive beamformer using the VDA method for all OFDM subcarriers can then be computed iteratively from:

$$\mathbf{w}_{VDA,m}^V = \left(\mathbf{T}_{VDA,m \rightarrow m+i}^V \right)^H \mathbf{w}_{VDA,m}^V \quad (4-29)$$

where

$$\mathbf{T}_{VDA,m \rightarrow m+i}^V \triangleq \left(\prod_{k=1}^{V-1} \mathbf{U}_{k,m}^H \right)^{-1} \mathbf{T}_{m \rightarrow m+i} \prod_{k=1}^{V-1} \mathbf{U}_{k,m+i}^H \quad (4-30)$$

and $\mathbf{T}_{m \rightarrow m+i}$ have been defined in equation (3-35).

The proof of equation (4-29) is shown in Appendix C.

4.2.3 VDA with depth control

So far we have shown how CR BS can generate broadened null patterns with defined width W . Next we will explain how to deepen these broadened nulls in the pattern.

The array beampattern $f(\theta)$ can be written as,

$$f(\theta) = \mathbf{w}_{MMSE}^H \mathbf{b}(\theta) \quad (4-31)$$

where $\mathbf{b}(\theta) = \begin{bmatrix} 1 & e^{-j\frac{2\pi}{\lambda}d\sin\theta} & \dots & e^{-j(N-1)\frac{2\pi}{\lambda}d\sin\theta} \end{bmatrix}^T$. The above equation shows that $f(\theta)$

can be regarded as the Discrete Fourier Transform (DFT) of \mathbf{w}_{MMSE} , with sampling at $2\pi d \sin \theta / \lambda$, i.e., $f(\theta) = \text{DFT}\{\mathbf{w}(n)\}$. We include the frequency response of the window functions, which suppresses the sidelobes of the signal in frequency domain. Thus, by filtering \mathbf{w}_{MMSE} by a window function, we can suppress the side lobes of $f(\theta)$, which

will result in deeper nulls. In order to investigate the impact of windows, we assume a window function $h(n)$, and $H(e^{j\omega}) = \text{DFT}\{h(n)\}$. The length of $h(n)$ is N_w . Then based on the property of DFT, we have

$$f(\theta)H(e^{j\omega}) = \text{DFT}\{w(n)*h(n)\} \quad (4-32)$$

Thus the new weight $\tilde{\mathbf{w}}$ is calculated from

$$\tilde{w}(n) = w(n)*h(n) \quad (4-33)$$

where $*$ denotes convolution. We can also write equation (4-33) in a matrix form as:

$$\tilde{\mathbf{w}} = \mathbf{H}_W \mathbf{w}_{MMSE} = \begin{pmatrix} (\mathbf{H}_1)_{N \times N} \\ (\mathbf{H}_2)_{(N_w-1) \times N} \end{pmatrix} \mathbf{w}_{MMSE} \quad (4-34)$$

where

$$(\mathbf{H}_W)_{i,j} = \begin{cases} h(i-j+1), & i \geq j; 1 \leq i \leq N + N_w - 1; 1 \leq j \leq N \\ 0, & i-j+1 > N_w; 1 \leq i \leq N + N_w - 1; 1 \leq j \leq N; i \leq j \end{cases} \quad (4-35)$$

If we define

$$\mathbf{H}_2 \triangleq \mathbf{P}\mathbf{H}_1 \quad (4-36)$$

$$\mathbf{Q} \triangleq [\mathbf{I} \quad \mathbf{P}^T]^T \quad (4-37)$$

we can rewrite equation (4-34) by

$$\tilde{\mathbf{w}} = \mathbf{Q}\mathbf{H}_1 \mathbf{w}_{MMSE} \quad (4-38)$$

Since the solution of the MMSE beamformer has the form $\mathbf{w}_{MMSE} = \sigma_1^2 \mathbf{R}_x^{-1} \mathbf{a}(\theta)$, we can calculate $\mathbf{H}_1 \mathbf{w}_{MMSE}$ by:

$$\mathbf{H}_1 \mathbf{w}_{MMSE} = \mathbf{H}_1 \sigma_1^2 \mathbf{R}_x^{-1} \mathbf{a}(\theta_1) = \sigma_1^2 \mathbf{R}_x^{-1} (\mathbf{R}_x \mathbf{H}_1 \mathbf{R}_x^{-1}) \mathbf{a}(\theta_1) \quad (4-39)$$

If we define $\Delta \triangleq \mathbf{R}_x \mathbf{H}_1 \mathbf{R}_x^{-1}$, equation (4-39) can be simplified by

$$\mathbf{H}_1 \mathbf{w}_{MMSE} = \sigma_1^2 \mathbf{R}_x^{-1} \Delta \mathbf{a}(\theta_1) \quad (4-40)$$

The above result illustrates that $\mathbf{H}_1 \mathbf{w}_{MMSE}$ can be considered as the outputs of the MVDR beamformer but with a modified angular direction $\Delta \mathbf{a}(\theta_1)$, instead of $\mathbf{a}(\theta_1)$.

The whole proposed method with depth depression in the NB beamformer is summarized in the scheme of Figure 4.5.

4.3 Simulation results and analysis

We consider the same ULA as in chapter 3, which has 10 array elements ($N = 10$ and $d = \frac{\lambda}{2}$). We assume that there are two participating PUs with DOA $\theta_2 = -20^\circ$, $\theta_3 = 20^\circ$ and SNR of both 10dB. We consider one CR user, which is located at $\theta_1 = 4^\circ$, and the SNR is 10dB. We adopt 500 snapshots. The width of the notch is set to

$W = 0.2$. We consider $V = 2$ steps for the iterative VDA as shown in Figure 4.4 and define $W_0 = \frac{W}{2} = 0.1$.

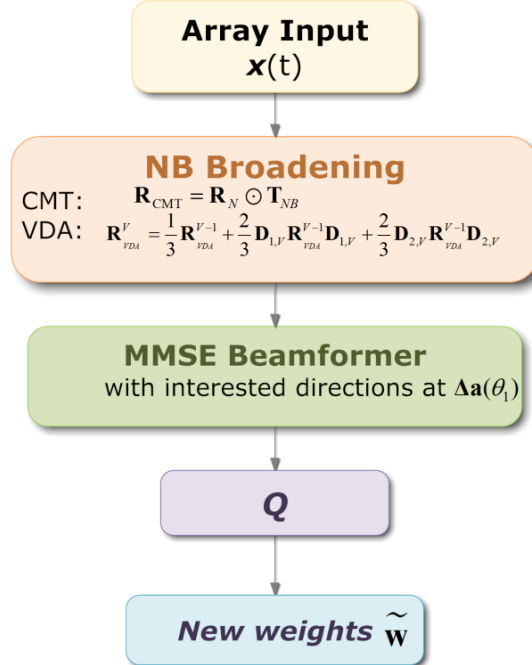


Figure 4.5 NB technique for CR Beamforming with deeper and/or broader nulls

Figure 4.6 shows the beampattern of both NB methods, i.e., CMT and VDA. Figure 4.6 learns that both methods can broaden nulls towards the directions of the two participating PUs with the same width $W=0.2$, while directing the main beam to the CR user. However, VDA can realize deeper nulls around the angular directions of the two participating PUs than CMT.

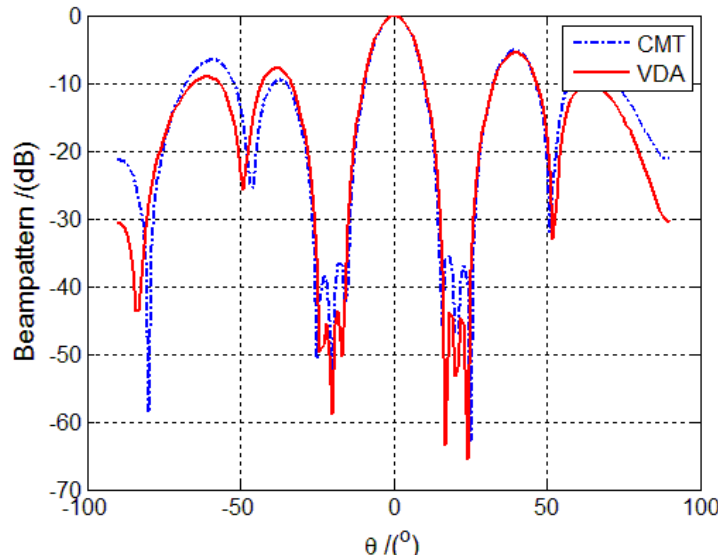


Figure 4.6 Beampattern of two NB methods: CMT and VDA

Figure 4.7a and Figure 4.7b show the Cumulative Distribution Functions (CDFs) of the power of the CR signal that is received by PU1 and PU2, respectively. The transmitted signal of the CR BS is regarded as interference to PUs. We define p_{PU1} and p_{PU2} as the normalized power of the CR signal received by PUs, which is defined by

$$p_{PUl} \triangleq \frac{p_{r,PUl}}{p_{t,CR}}, l = 1, 2, \dots, L \quad (4-41)$$

where $p_{r,PUl}$ is the power of the CR signal received by the l th PU, and $p_{t,CR}$ is the signal power transmitted by the CR BS towards the direction of the CR user. We assume the scatter components of the two participating PUs both follow a Von Mises pdf, which has been demonstrated in equation (4-1) and Figure 4.2, and we choose $l_\theta = 10$. We have performed simulations for 5000 times to achieve the CDF.

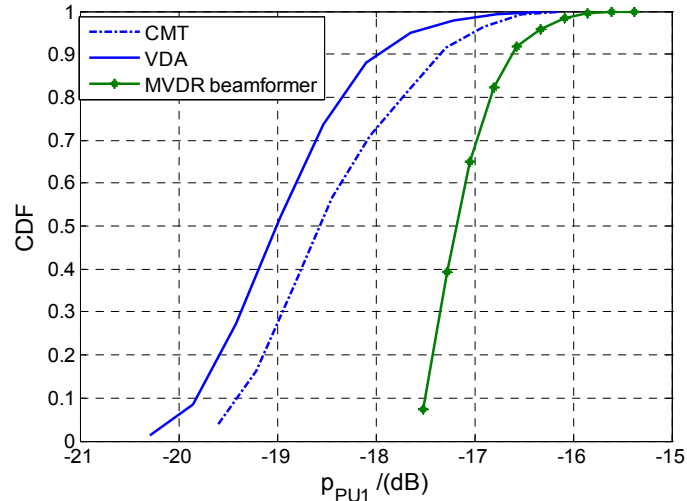


Figure 4.7a CDF of the power of the received CR signal by PU1

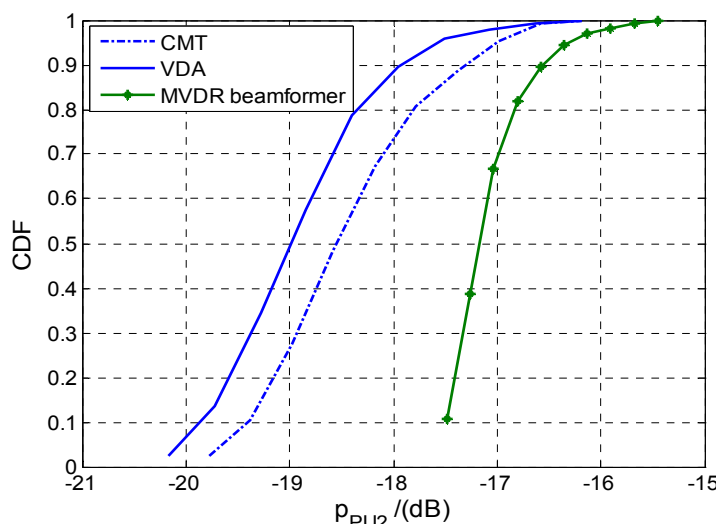


Figure 4.7b CDF of the power of the received CR signal by PU2

Figure 4.7a shows that CMT and VDA ensures that the most probable received interference power of PU1 due to CR transmissions is less than -16dB , while the MVDR beamformer without NB technique can only guarantee in around 97% of the cases. Figure 4.7b illustrates a similar performance. If we define the probability that the received CR signal power by PU is lower than the interference temperature P_0 ($P = \text{prob}\{P_{PU1} | P_{PU1} \leq P_0\}$), both Figures 3.7a and 3.7b show that the VDA method has the highest probability, i.e., $P_{VDA} \geq P_{CMT} \geq P_{MVDR}$.

Figures 4.8, 4.9 and 4.10 show the beampattern of the two NB methods, CMT and VDA, with filtering techniques. In Figure 4.8 and Figure 4.9 we consider a Poisson window as filter function, which is defined by

$$h_{poisson}(n) = \begin{cases} \exp(-2\alpha|n|/N_w), & 0 \leq |n| \leq N_w/2 \\ 0, & \text{elsewhere} \end{cases} \quad (4-42)$$

In Figure 4.10 we compare the beampattern of the VDA method with either a Poisson window or a cos window as filters. The cos window function equals

$$h_{cos}(n) = \begin{cases} \cos^\beta(\pi n / N_w), & 0 \leq |n| \leq N_w/2 \\ 0, & \text{elsewhere} \end{cases} \quad (4-43)$$

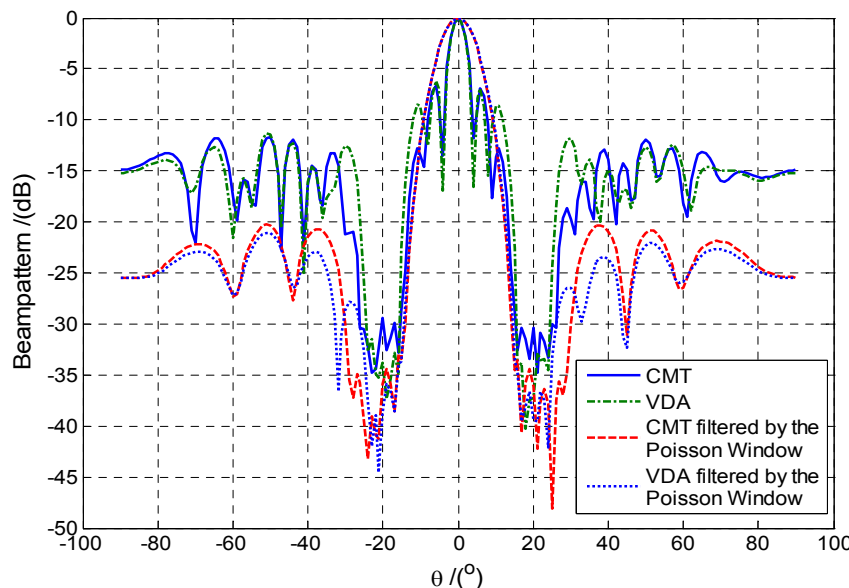


Figure 4.8 Beampattern of NB methods (CMT and VDA) with Poisson window

In Figures 4.8 and 4.9, α in equation (4-42) is chosen to be equal to $\alpha = 4$. The length of the Poisson window function in Figure 4.8 is chosen to be $N_w = 16$, and that in Figure 4.9 to be $N_w = 8$ and $N_w = 16$ for comparison. We consider a ULA with 32 array elements ($N = 32$). We calculate equation (4-18) and find out that in order to apply the VDA method to generate broaden null patterns with a width $W = 0.2$, V in equation (4-18) should satisfy the condition $V \geq 3$. Thus we define $V = 3$ for Figures

4.8, 4.9 and 4.10, and consequently $W_0 = \frac{W}{4}$. Other simulation conditions are the same as for Figure 4.6. It can be seen from Figure 4.8 that after employing the filtering technique to CMT and VDA methods, the depth of both the nulls at the directions of PUs are increased by about 5dB. Meanwhile, the shape of the main beam becomes wider.

Figure 4.9 shows the beampattern of the VDA method with a Poisson window at different lengths. We can conclude from Figure 4.9 that the longer the length of the window function is, the deeper the nulls will be. However, the main beam is also enlarged when the length of the window function increases.

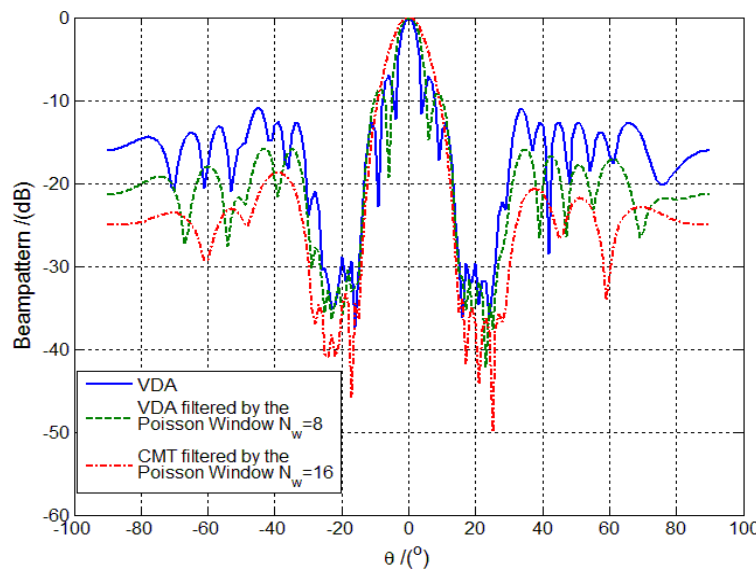


Figure 4.9 Beampattern of VDA with the Poisson window at different lengths

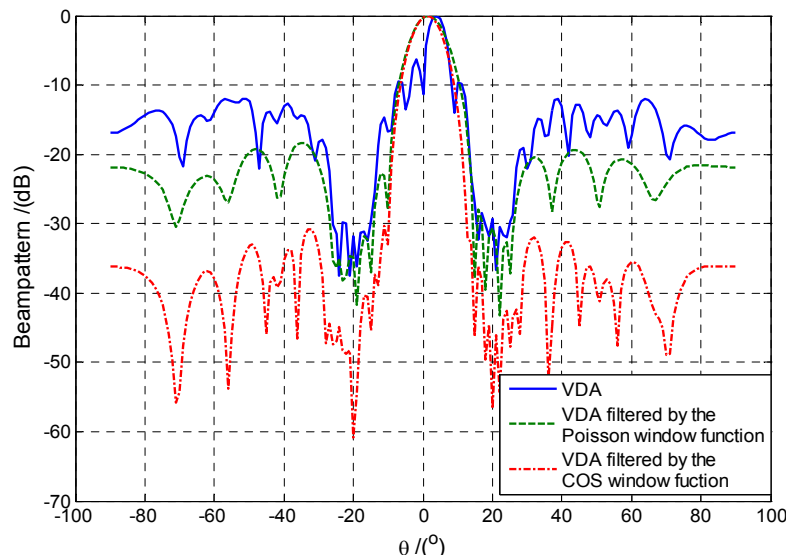


Figure 4.10 Beampattern of VDA with the Poisson window and cos window

Figure 4.10 compares the method for controlling the pattern using VDA by choosing different window functions as filters. We adopt both the Poisson window function and cos window function. β in equation (4-43) is set to 1.5. The other simulation conditions remain the same with those in Figure 4.8. Figure 4.10 shows clearly the abilities of deepening the pattern nulls using both window functions. It also shows that the cos window function decreases the depth of the nulls more than the Poisson window function, due to the fact that the cos window function has better side lobe suppression capability, while both of them have the same width for the main beam.

Figure 4.11 shows the possibility of adjusting the depth of the nulls by selecting the Poisson window function as filters with different α , while $N_w=16$. As demonstrated in Figure 4.11, when α increases, the main beam is broadened, but with less ability of suppressing the nulls depths.

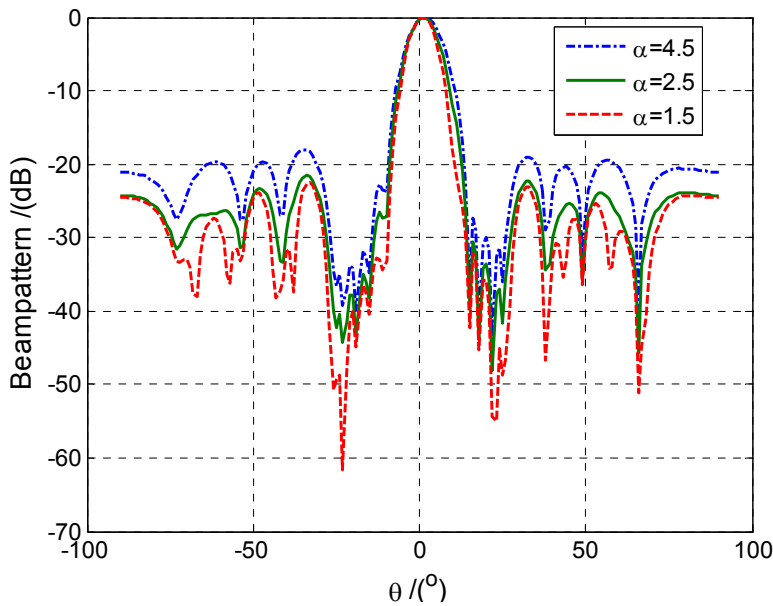


Figure 4.11 Beampattern of VDA with the Poisson window at different α

Next, we take the spatial channel effect into account by assuming that the spatial channel model follows the Von Mises pdf. We measure p_{PU1} and p_{PU2} which have been defined in equation (4-41) by adopting different l_θ in the Von Mises pdf of equation (4-1). All the simulation conditions are the same with that in Figure 4.8. From Table 4-1, we can see that when l_θ is relatively small, more signal power, which should be only received by the CR user, will leak to the PUs. This can be explained by the characteristics of the Von Mises distribution, which resembles a Gaussian distribution for larger l_θ , and is approximately a cardioid distribution for small l_θ . It is noticed that the VDA method with filtering achieves a better performance in suppressing the power of the CR signals received by PUs than without filtering.

Table 4-1 Normalized received power of CR signal by PUs

p_{PU} with different spatial channels		<i>VDA without filtering</i>	<i>VDA with filtering by the Poisson Window function</i> ($\alpha=1.5, N_w=16$)
$l_\theta = 9$	p_{PU1}	6.10%	5.18%
	p_{PU2}	5.97%	5.15%
$l_\theta = 12$	p_{PU1}	4.86%	4.05%
	p_{PU2}	5.12%	4.09%
$l_\theta = 18$	p_{PU1}	3.91%	2.43%
	p_{PU2}	3.76%	2.42%

4.4 Summary

The angular deviation models of spatial wireless channels are characterized as a Von Mises distribution. Consequently adaptive downlink beamformers for the CR BS should limit and control its transmission power in a range of angles around PUs' directions rather than directing point nulls towards PUs. We have presented a new NB method in this chapter, which is called VDA. It is based on the approximation of the CMT method but is capable of generating deeper broadened null patterns around directions of PUs. The VDA method can be calculated iteratively and it implies the implicit principle of the CMT method. What is more, it gives a closed form relationship of the weights of adaptive beamformers with and without the NB technique.

In order to generate deeper broadened nulls, we further suggest a filtering method, which employs window functions as filter for the adaptive beamformer weights. By employing different kinds of window functions or by adjusting parameters of the same window function, we can chose different depth of the broadened null patterns.

By utilizing the VDA method and filtering method together, the adaptive downlink beamformer of CR BS is able to display deep and broadened nulls in the patterns. This guarantees that the CR BS will cause less interference to PUs even when the CR system is using the same spectrum band as PUs. For OFDM CR systems, the VDA method can be used iteratively, which ensures that the system model for the uplink adaptive OFDM beamformers, that we have proposed in chapter 3, can also be adopted at downlink.

Chapter 5 Distributed Beamforming (DB) Techniques for CR

5.1 Introduction

As we have discussed in chapter 4, by applying ABF techniques, in the downlink CR BS can direct its main beam pattern towards CR users while putting null patterns towards directions of PUs in order to cause no harmful interferences to PUs while sharing the same spectrum with PUs. As mentioned in chapter 2, the CR BS can be substituted by CR networks to forward signals to DCR users by adopting the DB method. In this chapter, we introduce, discuss, and analyze the DB method for CR networks.

Instead of requesting the CR BS to be deployed with antenna arrays, we consider in this chapter a decentralized CR network, as shown in Figure 2.6b. The CR network is formed by CR users that are geographically distributed in a certain area. Those CR users are therefore regarded as CR nodes in the CR network. We propose to employ DB at CR networks in order to form beams towards DCR users so that the CR network is able to forward the signals to DCR users cooperatively. Via adopting the DB method, the CR networks increases its coverage range without causing harmful interferences to PUs.

DB is also referred to as collaborative beamforming in WSN, and it has originally been employed as an energy-efficient scheme to solve long distance transmission, in order to reduce the amount of required energy and consequently to extend the utilization time of the sensors [57]. The basic idea of DB is that a set of nodes in wireless networks acts as a virtual antenna array and then forms a beam towards a certain direction to collaboratively transmit a signal. DB has been proposed in [57] and it is shown that by employing K collaborative nodes, the collaborative beamforming can result in up to K -fold gain in the received power at a distant access point.

Recently a cross-layer approach for DB in wireless ad-hoc networks was presented in [58] applying two communication steps in the communication schedule. The improved beam pattern and connectivity properties have been shown in [59], and its reasonable beamforming performance affected by nodes synchronization errors has been discussed in [60]. DB has also been introduced in relay communication systems [61-65]. The authors in [61-64] have developed several DB techniques for relay networks with flat fading channels. In [65], frequency selective fading has been considered.

DB requires accurate synchronization; in other words, the nodes must start transmitting at the same time, synchronize their carrier frequencies, and control their carrier phases so that their signals can be combined constructively at the destination.

Several synchronization techniques for DB can be found in [66], and a review has been given in [67]. In this chapter, we adopt the master-slave architecture proposed in [60], where a designated master transmitter (one of CR nodes in the network) coordinates the synchronization of other (slave) transmitters for DB. Since it has also been proved in [60] that a large fraction of the DB gain can still be realized even with imperfect synchronization corresponding to phase errors with moderately large variance, we focus more on introducing DB methods rather than discussing the synchronization algorithms.

CR has been intensively researched as an enabling technology for secondary access to TV White Space (TVWS) [68]. The TVWS comprises large portions of the UHF spectrum in U.K. and VHF in the United States. These parts of the spectrum are becoming available on a geographical basis for sharing as a result of the switch-over from analog to digital TV. This is where CR users can, using unlicensed equipment, share the spectrum with digital TV transmitters and other radio-supported equipment such as wireless microphones. The authors of [68] have shown that there are 256MHz of spectrum (32 channels) which are the so-called interleaved spectrum, and can be used for CR.

In this chapter, we first introduce the DB method to CR networks in section 5.2. Here we consider the case that all the nodes are uniformly distributed over a circular area in which the CR network is located. As shown in [57], the width of the main beam of the beampattern is decided by two parameters: the physical size of the network R , and the wavelength λ of the signal that the network is transmitting or receiving. It has been calculated in [57] that the main beam of the beampattern will become narrower when the normalized radius \tilde{R} increases, where $\tilde{R} = R / \lambda$. If we consider a CR network with $R=100\text{m}$ and utilizing the spectrum of one of the 32 channels in the UHF of TVWS [68], which is, for instance, 786MHz. We can obtain that $\tilde{R}=262$. In [57], the authors have shown that the width of the main beam can be approximated by $35^\circ / \tilde{R}$. Thus in our example, the width of the main beam will become 0.1° . This is considered to be too narrow, implying that once the DOA estimation of the DCR users is not accuracy enough the main beam in the pattern may miss its direction. Meanwhile it also reveals that the width of the main beam in the beampattern mostly relies on the center frequency at which the CR is able to access.

To solve this problem of the extremely narrow main beam, we propose a novel NS method in section 5.3. The presented NS method is based on the differences in beam width of a broadside array and an end-fire array. A broadside array has been defined in [69] as an array which radiation maximum (or main beam) occurs perpendicular to the axis of the array. An end-fire array has also been defined in [69] as an array that radiation maximum is along the axis of the array. The beampatterns of these two types of arrays allow us to find out that the main beam of the end-fire array is much wider than that of the broadside array. We thus conclude that the “broadside” size of the CR network should be small so that a beampattern with a wider main beam can be maintained. As a

result, we suggest selecting CR nodes, which are able to form a full size end-fire array and a reduced size broadside array. In other words, we choose those CR nodes which are located in the “belt” area along the direction of the DCR user. Simulations will be given afterwards, showing that our NS method is effective in generating a wider main beam in the beam pattern.

In section 5.2 and 5.3, we will demonstrate that, considering the possible working frequency of the CR networks, the main beam of the average beampattern can be designed narrow enough and the sidelobe level in the beampattern will approach $1/K$, where K is the total number of nodes in the network. Thus as long as PUs are not located in the same direction as the beampattern for the DCR user, the transmit power arriving at PUs direction will always be $K-1$ times less than that towards the DCR user. As a result, at one hand unlike the use of ABF techniques, which direct specific nulls towards directions of PUs, the DB method by its nature is capable of guaranteeing $K-1$ times less power towards PUs compared with that towards DCR users. Nulls generating is therefore no longer a problem for the DB method when applied to CR networks. On the other hand, how to generate a main beam with proper width and accurate direction is a challenge for the DB method. In this chapter, we will focus on addressing this issue.

5.2 DB of CR networks

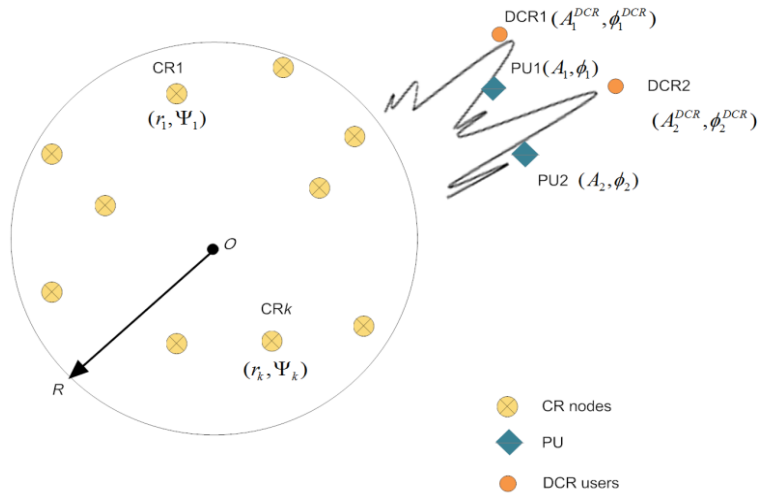


Figure 5.1 CR networks with DCR and PUs

The geometrical structure of the first model together with distant receiver terminals including PUs and DCR users is illustrated in Figure 5.1. K CR nodes are uniformly distributed over a disc centered at O with radius R . We denote the polar coordinates of the k th CR node by (r_k, Ψ_k) . The number of DCR users is L_{DCR} . These DCR users are considered as access points, and located in the same plane at $(A_i^{DCR}, \phi_i^{DCR})$, $i = 1, 2, \dots, L_{DCR}$. Meanwhile the number of PUs is L_{PU} , and these users coexist with DCR users. Their locations are (A_i, ϕ_i) , $i = 1, 2, \dots, L_{PU}$. The CR nodes in

the CR network are requested to form a virtual antenna array and collaboratively transmit a common message $s(t)$.

5.2.1 Necessary assumptions

Without loss of generality, we adopt the following assumptions:

1) The number of CR nodes are larger than that of DCR users, i.e., $K > L_{DCR}$.

This is required to solve the multi beam generating problem in paragraph 5.2.3.

2) All DCR users and PUs are located in the far field of the CR network, such that $A_i^{DCR} \gg R, i = 1, 2, \dots, L_{DCR}$ and $A_i \gg R, i = 1, 2, \dots, L_{PU}$.

3) The bandwidth of $s(t)$ is narrow, so that $s(t)$ is considered to be constant during the time interval R/c , where c is the speed of light.

It has been discussed in chapter 2 that the OFDM scheme is the first recommended candidate for use in the CR network. Since the OFDM signal can be regarded as a combination of narrow band modulated signals, the proposed method in this thesis can also be implemented in wide band CR OFDM systems.

5.2.2 DB for CR networks

Let $x_k(t)$ denote the transmitted signal from the k th node,

$$x_k(t) = s(t)e^{j2\pi ft} \quad (5-1)$$

where f is the carrier frequency. The received signal at an arbitrary point (A, ϕ) in the far field due to the k th node transmission is [70]

$$r_k(t) = \beta_k x_k(t - \frac{d_k}{c}) = \beta_k s(t - \frac{d_k}{c}) e^{j2\pi ft} e^{-j\frac{2\pi}{\lambda} d_k} \quad (5-2)$$

where d_k is the distance between the k th node and the access point (A, ϕ) , and $\beta_k = (d_k)^{-\frac{\gamma}{2}}$ is the signal path loss with γ denoting the path loss exponent. Making use of assumption 2 in the previous paragraph [70], β_k and d_k are approximated by

$$d_k = \sqrt{A^2 + r_k^2 - 2Ar_k \cos(\phi - \Psi_k)} \approx A - r_k \cos(\phi - \Psi_k) \quad (5-3)$$

$$\beta_k = (d_k)^{-\frac{\gamma}{2}} \approx [A - r_k \cos(\phi - \Psi_k)]^{-\frac{\gamma}{2}} \approx A^{-\frac{\gamma}{2}} \left(1 + \frac{\gamma r_k \cos(\phi - \Psi_k)}{2A} \right) \quad (5-4)$$

It is also ensured that $\frac{\gamma r_k \cos(\phi - \Psi_k)}{2A} \ll 1$. Thus β_k can then be approximated by

$A^{-\frac{\gamma}{2}}$. Substituting equation (5-3) and (5-4) into equation (5-2), it follows that [70],

$$r_k(t) \approx A^{-\frac{\gamma}{2}} e^{-j\frac{2\pi}{\lambda} A} s(t - \frac{A}{c}) e^{j2\pi ft} e^{j\frac{2\pi}{\lambda} r_k \cos(\phi - \Psi_k)} \quad (5-5)$$

Figure 5.2 shows the geometry relationships of parameters in equation (5-3).

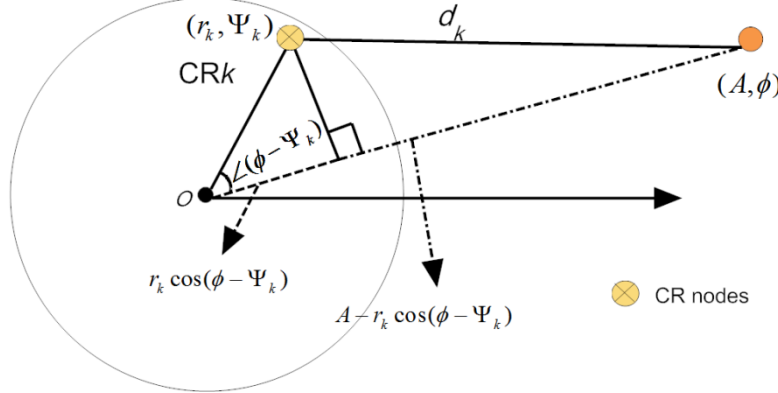


Figure 5.2 Distance between the k th node and an access point (A, ϕ)

We assume there is only one DCR, i.e., $L_{DCR} = 1$, and simplify $(A_1^{DCR}, \phi_1^{DCR})$ by (A_0, ϕ_0) . The case with more than one DCR user will be discussed in paragraph 5.2.3. As proposed in [57], we adopt for the initial phase of each node

$$\varphi_k = -\frac{2\pi}{\lambda} r_k \cos(\phi_0 - \Psi_k) \quad (5-6)$$

The received signal $r_k(t)$ at (A, ϕ) becomes

$$r_k(t) \approx \beta e^{-j\frac{2\pi}{\lambda} A} s(t - \frac{A}{c}) e^{j2\pi f t} e^{j\frac{2\pi}{\lambda} r_k \cos(\phi - \Psi_k)} e^{-j\frac{2\pi}{\lambda} r_k \cos(\phi_0 - \Psi_k)} \quad (5-7)$$

The array factor $F(\phi | r_k, \Psi_k)$ yields:

$$F(\phi | r_k, \Psi_k) \approx \frac{1}{K} \sum_{k=1}^K e^{j\frac{2\pi}{\lambda} r_k [\cos(\phi - \Psi_k) - \cos(\phi_0 - \Psi_k)]} = \frac{1}{K} \sum_{k=1}^K e^{-j\frac{4\pi}{\lambda} r_k \sin(\frac{\phi - \phi_0}{2}) \sin(\frac{\phi + \phi_0 - 2\Psi_k}{2})} \quad (5-8)$$

We assume there are many CR nodes and the locations of CR nodes follow a uniform distribution over the disk of radius R , leading to the pdf

$$\begin{cases} f_{r_k}(r) = \frac{2r}{R^2}, & 0 \leq r < R \\ f_{\Psi_k}(\Psi) = \frac{1}{2\pi}, & -\pi \leq \Psi_k < \pi \end{cases} \quad (5-9)$$

If the CR nodes are distributed according a two-dimensional Gaussian process, the corresponding DB techniques and its beampattern characteristics can be found in [71].

By defining $z_k \triangleq \frac{r_k}{R} \sin\left(\Psi_k - \frac{\phi_1 + \phi_0}{2}\right)$, the compound random variable z_k has a pdf [57]

$$f_{z_k}(z_k) = \frac{2}{\pi} \sqrt{1 - z_k^2}, \quad -1 \leq z_k < 1 \quad (5-10)$$

The array factor in equation (5-8) can now be written as

$$F(\phi | z_k) = \frac{1}{K} \sum_{k=1}^K \exp\left(-j4\pi \tilde{R} \sin\left(\frac{\phi - \phi_0}{2}\right) z_k\right) \quad (5-11)$$

where $\tilde{R} \triangleq R/\lambda$ is the radius of the disk normalized by the wavelength. The far field beampattern is defined by

$$P(\phi|z_k) \triangleq |F(\phi|z_k)|^2 \quad (5-12)$$

and the average array beam pattern of the CR networks becomes [57]

$$P_{av}(\phi) \triangleq E[P(\phi|z_k)] = \frac{1}{K} + \left(1 - \frac{1}{K}\right) \mu^2(\phi) \quad (5-13)$$

where

$$\mu(\phi) = E[F(\phi)] = \left| \frac{2J_1(\alpha(\phi))}{\alpha(\phi)} \right| \quad (5-14)$$

$$\alpha(\phi) \triangleq 4\pi\tilde{R} \sin\left(\frac{\phi - \phi_0}{2}\right) \quad (5-15)$$

$J_n(\cdot)$ stands for the n th order Bessel function of the first kind, which is defined by

$$J_n(x) = \sum_{k=0}^{\infty} \frac{(-1)^k x^{n+2k}}{k!(n+k)! 2^{n+2k}} \quad \text{and} \quad E[\cdot] \text{ stands for the statistical expectation. Above}$$

equations learn us that if each CR node adopts the initial phase as given in equation (5-6), the average pattern generated by the whole CR network can be obtained from equation (5-13).

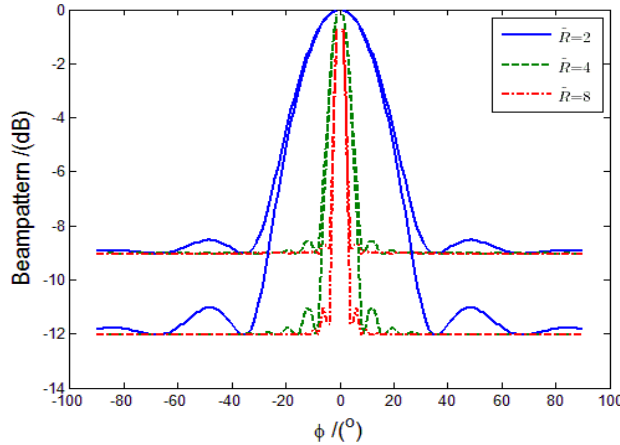


Figure 5.3 Average beampattern of the DB method

Figure 5.3 shows the average beampattern of the DB method for different K ($K = 8, 16$) and \tilde{R} ($\tilde{R} = 2, 4, 8$). We assume that the direction of DCR is $\phi_0 = 0^\circ$. It can be seen that when the beam angle moves away from the direction of DCR, the sidelobe approaches $\frac{1}{K}$, i.e., $10 \log_{10} \left(\frac{1}{8} \right) \approx -9 \text{dB}$ and $10 \log_{10} \left(\frac{1}{16} \right) \approx -12 \text{dB}$, respectively. This leads to the logic conclusions that the sidelobe level decreases when K increases, and that the larger \tilde{R} becomes, the narrower the main beam will be, and consequently the better directivity in the beampattern will be achieved. Figure 5.3 is only for demonstration, because the value of the parameters that we consider ($K = 8, 16$; $\tilde{R} = 2, 4, 8$) are not

realistic in practice. In practical applications, \tilde{R} should be large enough so that CR networks can have enough CR nodes.

5.2.3 DB with multi main beams

So far we have discussed the DB method with only one DCR user. In this paragraph we propose two novel DB methods which are both capable of generating multi main beams towards different DCR users. This work has been published in [72]. The first method geographically groups CR nodes into several ring ranges and a circle in the Centre. Thus by allocating different initial phases to these CR nodes, which are in different areas, this DB method displays different main beams towards different DCR users. Another method entitles each CR node to select its destination access nodes randomly. Consequently, it can be interpreted as several CR networks with the same geographical structure, but with a fewer number of nodes, which separately perform DB towards different DCR users.

A. Geographical grouping method

We first discuss the case when nodes of networks are distributed in a ring range, rather than a circle. Figure 5.4 shows the geographical structure and parameters of the defined ring range.

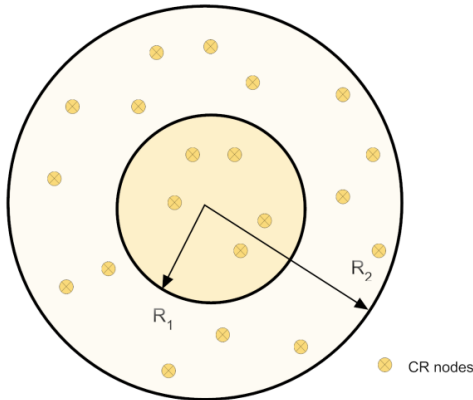


Figure 5.4 Separation of CR nodes into a ring range and a circle range

We assume the locations of those CR nodes in the CR network, which are in the ring range, follow the uniform distribution over the ring of radius $R_1 - R_2$. Thus, the two pdf's are

$$\begin{cases} f_{r_k}(r) = \frac{2r}{R_2^2 - R_1^2}, & R_1 < r_k < R_2 \\ f_{\Psi_k}(\Psi) = \frac{1}{2\pi}, & -\pi \leq \Psi_k < \pi \end{cases} \quad (5-16)$$

If there are K CR nodes in a ring range, as shown in Figure 5.4, we can derive for the average far field beampattern of the DB method

$$P_{av}^{ring}(\phi) = \frac{1}{K} + \left(1 - \frac{1}{K}\right) \left(\frac{\mu^2(\phi) - \xi^2 \mu_{ring}^2(\phi)}{1 - \xi^2} \right)^2 \quad (5-17)$$

where

$$\xi = \frac{R_1}{R_2} \quad (5-18)$$

$$\mu_{ring}(\phi) = \frac{2J_1(\xi\alpha(\phi))}{\xi\alpha(\phi)} \quad (5-19)$$

The proof of equation (5-17) can be found in Appendix D.

By separating CR nodes into different groups, we can synchronize them with different initial phases as given in equation (5-6). For example, CR nodes located in the inner circle will have the initial phases of $\varphi_k^{circle} = -\frac{2\pi}{\lambda} r_k \cos(\phi_1^{DCR} - \Psi_k)$, while for others, which are in the ring range, we adopt another initial phase given by $\varphi_k^{ring} = -\frac{2\pi}{\lambda} r_k \cos(\phi_2^{DCR} - \Psi_k)$. In this way we create two beams towards both $(A_1^{DCR}, \phi_1^{DCR})$ and $(A_2^{DCR}, \phi_2^{DCR})$. If we need to direct main beams towards more than two directions, we can keep grouping CR nodes into several different rings ranges with different radii.

B. Randomly selecting initial phase

Another method to display more than one beam is to let CR nodes randomly choose the DCR to serve. If the k th CR node chooses the i th DCR to transmit signals to, it will adopt the initial phase $\varphi_k = -\frac{2\pi}{\lambda} r_k \cos(\phi_i^{DCR} - \Psi_k)$, $i = 1, 2, \dots, L_{DCR}$. The probability that a CR node chooses a selected DCR is equal to $1/L_{DCR}$. Thus, the far field array factor of the DB method with randomly choosing initial phase equals

$$F(\phi|\eta, r_k, \Psi_k) = \frac{1}{K} \sum_{k=1}^K \exp \left[-j4\pi \tilde{R} \sin\left(\frac{\phi-\eta}{2}\right) \sin\left(\frac{2\Psi_k - \phi - \eta}{2}\right) \right] \quad (5-20)$$

where η is defined as a discrete random variable, which has a pdf

$$Prob(\eta = \phi_i^{DCR}) = \frac{1}{L_{DCR}}, \quad i = 1, 2, \dots, L_{DCR} \quad (5-21)$$

Then the average array beampattern of the random distributed DCR with random selected initial phase becomes

$$\begin{aligned} P_{av}^{rs}(\phi) &\triangleq E \left[|F(\phi|\eta, r_k, \Psi_k)|^2 \right] \\ &= E \left[\left| \frac{1}{L_{DCR}} \sum_{i=1}^{L_{DCR}} F(\phi|\eta = \phi_i^{DCR}, r_k, \Psi_k) \right|^2 \right] = \frac{1}{K} + \left(1 - \frac{1}{K}\right) \left(\frac{1}{L_{DCR}} \sum_{i=1}^{L_{DCR}} \mu_i(\phi) \right)^2 \end{aligned} \quad (5-22)$$

where

$$\mu_i(\phi) = \frac{2J_1(\alpha_i(\phi))}{\alpha_i(\phi)}, \quad \alpha_i(\phi) = 4\pi \tilde{R} \sin\left(\frac{\phi - \phi_i^{DCR}}{2}\right), \quad i = 1, 2, \dots, L_{DCR}.$$

C. Simulation Results of the two DB methods with multi main beams

First we study the average beampatterns of the DB method for both CR networks which contain CR nodes in a circle and in a ring range, respectively. We assume that there is one DCR with $\phi_0 = 0^\circ$. We consider $K = 32$ for both networks. The radius of the bigger circle, which is shown by R_2 in Figure 5.4, satisfies that $\tilde{R}_2 = 32$. The geometry parameter ξ , which is defined in equation (5-18), assumes two ring ranges and equals $\xi = \frac{1}{4}, \frac{1}{2}$.

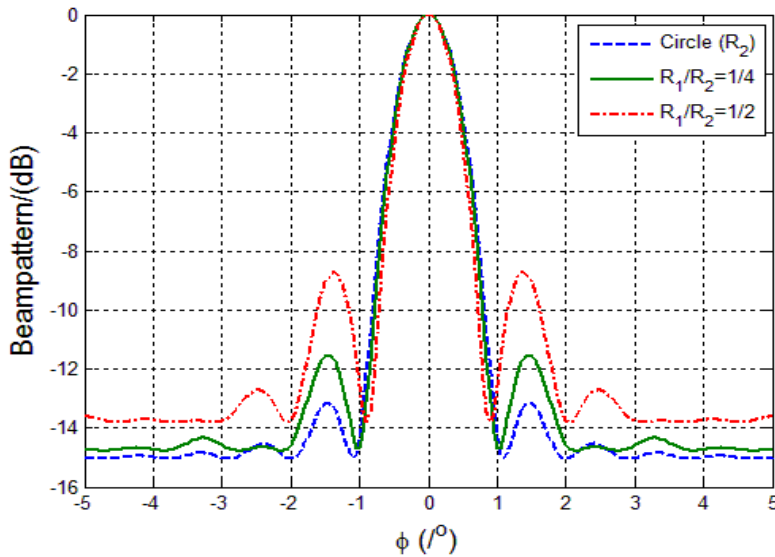


Figure 5.5 Average Beampattern of DB with circle and ring ranges

The average beampattern of the DB method with two geographically different networks are shown in Figure 5.5. The beam pattern of CR nodes distributed in a ring range has higher sidelobes, and a slightly narrower main beam than the pattern of the array in a circle area. We can also see from Figure 5.5 that when the ring range becomes wider (ξ is smaller), the level of sidelobe decreases. The extreme case occurs when $\xi = 0$; a ring evolves into a circle and thus they have the same low level of sidelobes.

The results of the two proposed multi beam generating methods are shown in Figure 5.6. In Figure 5.6, we consider $K = 32$ and $\tilde{R}_2 = 32$. We also assume that there are two DCR, at directions $\phi_1^{DCR} = 0^\circ$ and $\phi_2^{DCR} = 60^\circ$, respectively. For the geographical grouping method we adopt $\xi = \frac{1}{2}$ and $\xi = \frac{1}{\sqrt{2}}$, respectively. We chose the DCR in the inner circle to form the beam towards $\phi_1^{DCR} = 0^\circ$, while the rest direct the

beam at the direction $\phi_2^{DCR} = 60^\circ$. We can see that both methods successfully direct two beams towards the two required directions. According to Figure 5.3, the sidelobe approaches $\frac{1}{K}$ as the beam angle moves away from the target direction, which explains the -15dB asymptotic sidelobe levels of both methods.

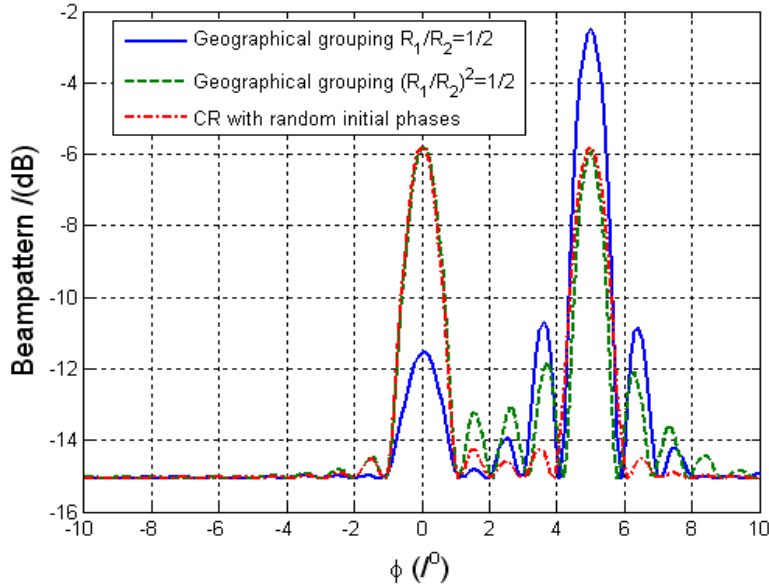


Figure 5.6 Average beampatterns of DB methods with multi main beams

Since we have assumed that the nodes are uniformly distributed on a disc, the number of the CR nodes in a ring range case equals $K(1-\xi^2)$, while this number in the circle is $K\xi^2$. With $\xi = \frac{1}{2}$, the geographical method has a higher main beam at ϕ_2^{DCR} .

This is due to the fact that more CR nodes are assigned in the ring range to direct the main beam towards ϕ_2^{DCR} . When $\xi = \frac{1}{\sqrt{2}}$, it can be seen from Figure 5.6 that both main

beams are almost equal, due to the number of nodes in both areas is equal, i.e., $K(1-\xi^2) = K\xi^2$. When CR nodes are capable of choosing their initial phases, the beampattern tends to have two beams towards ϕ_1^{DCR} , ϕ_2^{DCR} with a split to half of the power. This is a result of the equally probability of selecting different initial phases.

5.3 Nodes Selection (NS) for CR networks with enlarged main beam

We have mentioned in the introduction that if we consider the accessible UHF bands in TVWS for CR networks, \tilde{R} increases rapidly when the working frequency of the CR networks goes higher. In this section we propose a new NS method for CR

networks to select proper nodes to achieve wider main beam in the beampattern of the DB method.

We first consider two extreme cases of the CR network, which are two types of array antennas: broadside array and end-fire array by projecting the location of each CR node along an X and Y axis, and study the properties of these two array antennas. After this we propose a NS method.

5.3.1 A NS method for CR networks

We assume one DCR user is located along the X axis ($\phi_0 = 0^\circ$). We then consider the location of a CR node by projecting it into the Cartesian coordinate system (X and Y directions) as shown in Figure 5.7. In this way we create two virtual arrays: broadside array and end-fire array. We now discuss the performance of the two separate arrays (broadside array and end-fire array) instead of the full CR network.

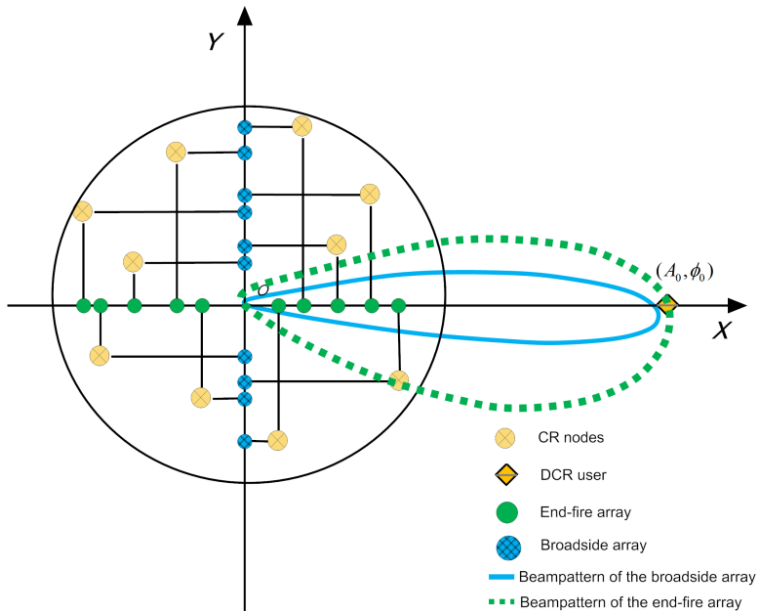


Figure 5.7 Converting locations of CR nodes into broadside and end-fire arrays

The average beampatterns of these two arrays are summarized in the following equations

$$\bar{P}_{\text{broadside}}(\phi) = \frac{1}{K} + \left(1 - \frac{1}{K}\right) \mu_b^2(\phi) \quad (5-23)$$

where

$$\mu_b(\phi) = \left| \frac{2J_1(\alpha_b(\phi))}{\alpha_b(\phi)} \right| \quad (5-24)$$

$$\alpha_b(\phi) = 2\pi\tilde{R}(\sin\phi - \sin\phi_0) \quad (5-25)$$

and

$$\bar{P}_{end-fire}(\phi) = \frac{1}{K} + \left(1 - \frac{1}{K}\right) \mu_e^2(\phi) \quad (5-26)$$

where

$$\mu_e(\phi) = \left| \frac{2J_1(\alpha_e(\phi))}{\alpha_e(\phi)} \right| \quad (5-27)$$

$$\alpha_e(\phi) = 2\pi\tilde{R}(\cos\phi - \cos\phi_0) \quad (5-28)$$

Proofs of equations (5-23) to (5-28) can be found in Appendix E.

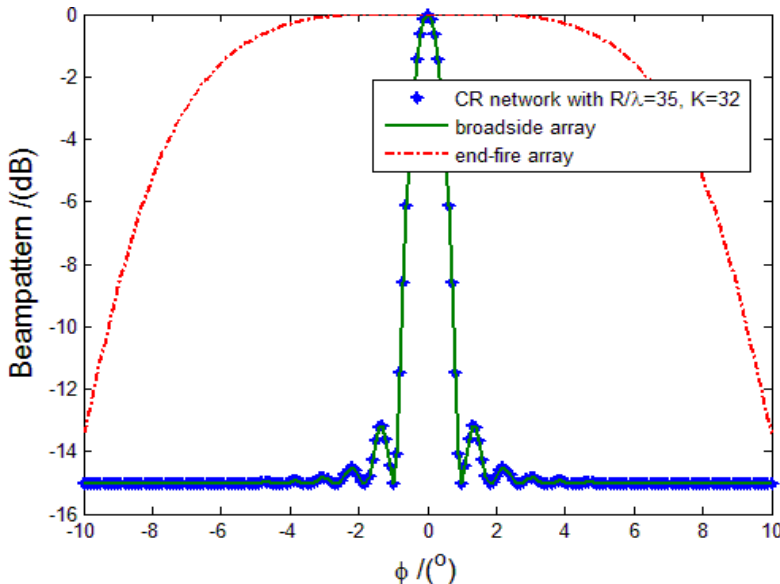


Figure 5.8 Beampattern of CR network, broadside array and end-fire array

The results of equation (5-23) and (5-26) are shown in Figure 5.8. We assume there are 32 nodes in the CR network and the normalized radius is 35, i.e., $K = 32$ and $\tilde{R} = 35$. We also assume there is only one DCR user, and its DOA is $\phi_0 = 0^\circ$. We can conclude from Figure 5.8 that the broadside array has the same average beampattern as the previous CR network. This is due to the result shown in equation (5-23). The $\alpha_b(\phi)$ in equation (5-25) can be approximated to $\alpha(\phi)$ defined in equation (5-15), when ϕ is close to ϕ_0 . As a result, in the angle area close to $\phi_0 = 0^\circ$, the performances of the beampattern of the broadside array and the DB method are very similar to each other. In general, the broadside array has a much narrower main beam than the end-fire array. In addition, a similar conclusion has also been drawn in [69], the author has discovered that the width of the main beam is in a reverse relationship of the size of the broadside array. Thus we are inspired by these two facts that if we want to enlarge the width of the main beam, we have to decrease the length (size) of the broadside array and we can adopt the end-fire array instead.

Based on this idea, we propose a NS method and select those nodes, which are able to form a full size end-fire array and a reduced size broadside array. Thus we choose the nodes in a relatively narrower belt along the DOA of the DCR user, as shown in Figure 5.9. In Figure 5.9, the CR nodes are selected in a way that the size of the “broadside” is limited to D , where $\frac{D}{\lambda} < \tilde{R}$.

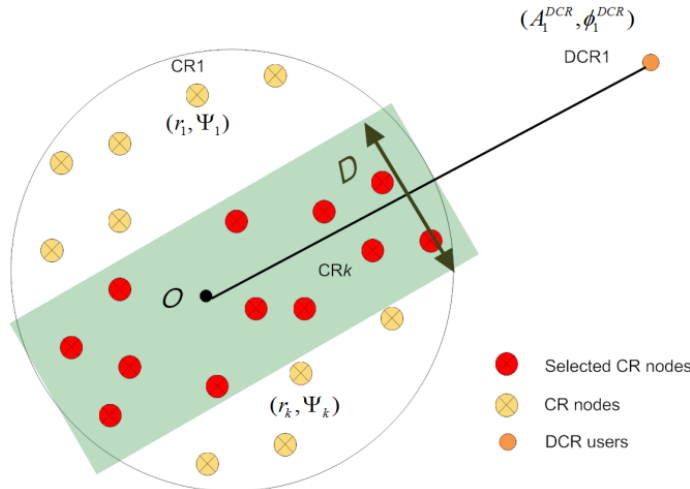


Figure 5.9 NS for CR networks

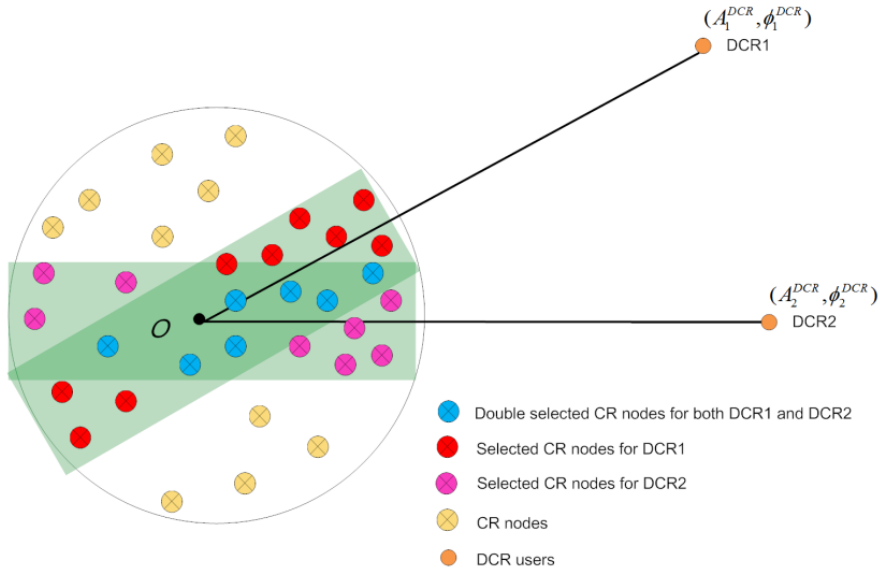


Figure 5.10 NS for CR networks with two DCR users

When we consider the case with more than one DCR user coexisting with the CR network, e.g. two DCR users, the NS method is demonstrated in Figure 5.10. We choose those CR nodes which are in the two “belts” area as shown in Figure 5.10. In addition, for those double selected CR nodes, which are in the cross area, we adopt the method which let them randomly choose one of the two DCR users to serve. The method has already been proposed and discussed in paragraph 5.2.3.

5.3.2 Simulation results of the NS method

Figure 5.11 and 5.12 demonstrate the selected nodes in the CR networks with different values of D by adopting the proposed NS method. Considering the randomness in the distribution of the nodes, the total number of selected nodes varies from each simulation. In order to show a general result of the beampattern, we sum up all the results and divide this sum result by the number of simulations that we run. As a result, the beampattern of the NS method shown in Figure 5.13 is the average beampattern. In Figures 5.11-5.13, we assume there is only one DCR user and its DOA is $\phi_0 = 0^\circ$. We choose the nodes within the width of the belt $D = 15\lambda$ and $D = 35\lambda$, as shown in Figure 5.11 and 5.12, respectively. We assume there are 60 nodes in the network and the normalized radius of the network is 50, i.e., $K = 60$, and $\tilde{R} = 50$. The result of the beampattern shown in Figure 5.13 is the average of 1000 runs.

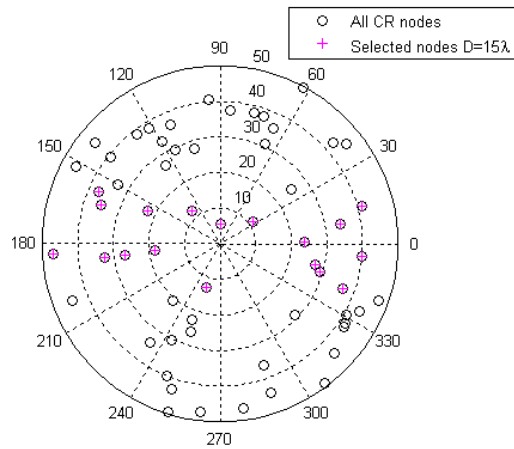


Figure 5.11 Selected CR nodes in the CR networks $D = 15\lambda$ ($\phi_0 = 0^\circ$)

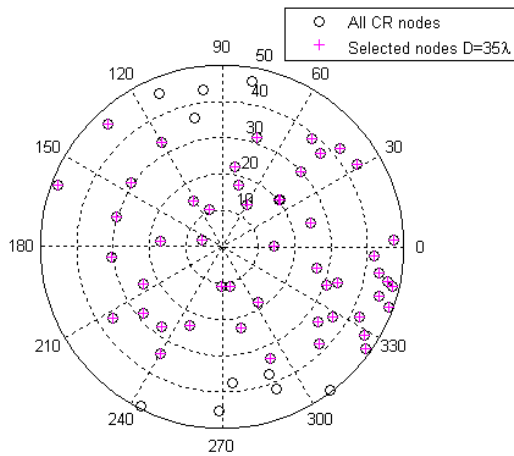


Figure 5.12 Selected CR nodes in the CR networks $D = 35\lambda$ ($\phi_0 = 0^\circ$)

Figure 5.11 and 5.12 show that those CR nodes, which are located in the belt area, as defined in Figure 5.9, are successfully selected for transmission. We can also see from

these two figures that when D is smaller, less number of CR nodes will be selected for transmission.

Figure 5.13 shows that after adopting the proposed NS method, the main beam in the beampattern of the DB method is enlarged. Employing the NS method with defined $D = 15\lambda$ and $D = 35\lambda$, the main beam is about four times and two times wider than that without adopting the NS method. However, with smaller D , less CR nodes will be selected, as shown in Figure 5.10 and 5.11. Therefore the beampattern has a higher sidelobe level than that with a larger D , since the asymptotic sidelobe level of the beampattern is proportional to the reverse of the number of the CR network, as explained in Figure 5.3.

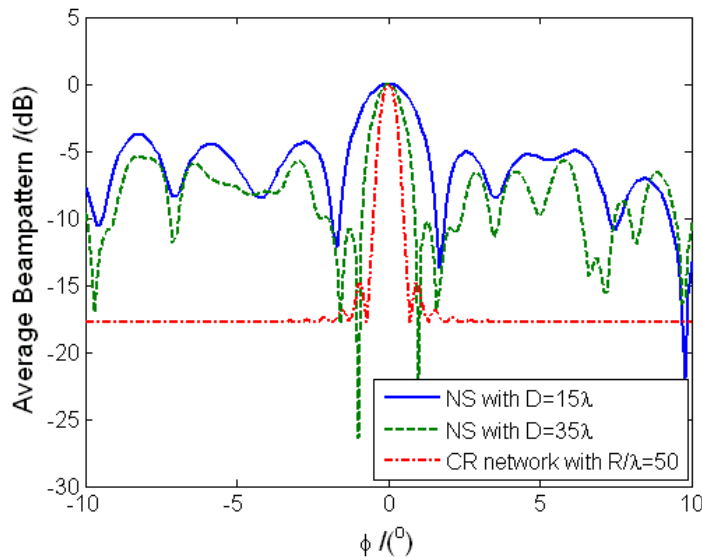


Figure 5.13 Average beampattern of the selected CR nodes ($\phi_0 = 0^\circ$)

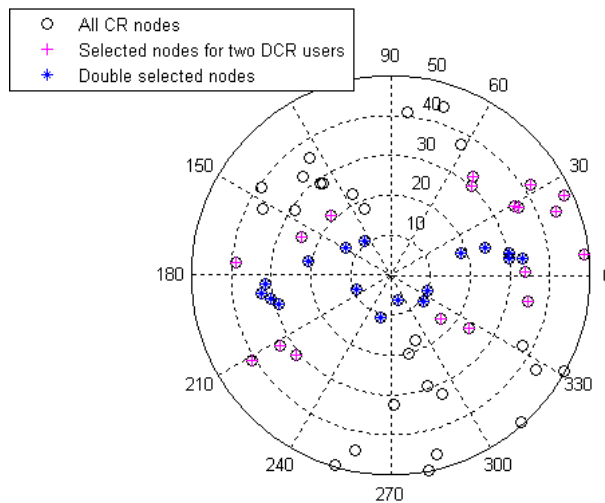


Figure 5.14 Selected CR nodes in the CR networks $D = 15\lambda$ ($\phi_1 = 0^\circ$ and $\phi_2 = 15^\circ$)

Figure 5.14 and 5.15 consider the case with two DCR users, which are located at $\phi_1 = 0^\circ$ and $\phi_2 = 15^\circ$ when $D = 15\lambda$. Figure 5.14 show the selected nodes in the CR

networks to participate in CR transmission towards two DCR users. We can see in Figure 5.14 that there are a few CR nodes which are double selected for participating in transmission towards both DCR users.

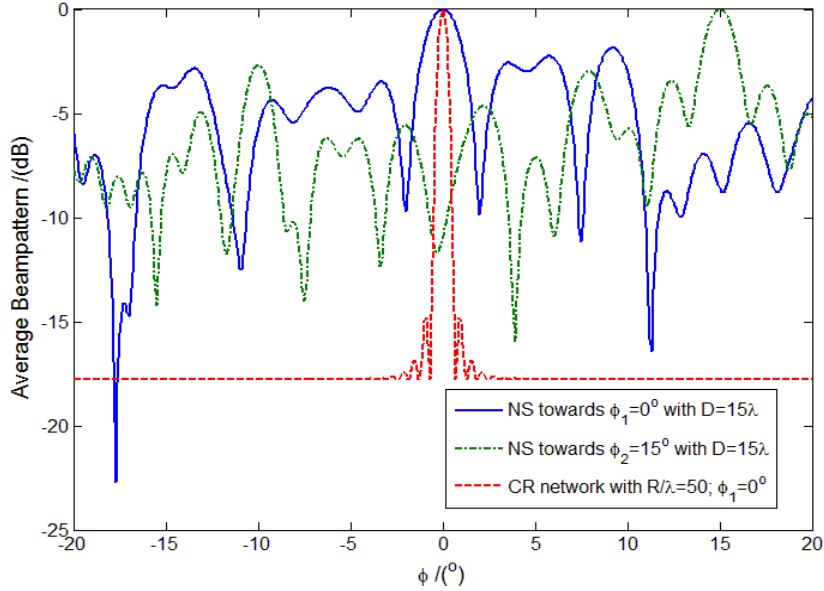


Figure 5.15 Average beampattern of the selected CR nodes for two DCR users

Figure 5.15 shows the average beampattern of the NS method for two DCR users. As can be seen from this figure, the two main beams in the beampattern are directed towards $\phi_1 = 0^\circ$ and $\phi_2 = 15^\circ$, respectively. The main beams are both widened via adopting our NS method. When we employ NS method with $D = 15\lambda$, we can see from Figure 5.15 that both two main beams are broadened to 3° .

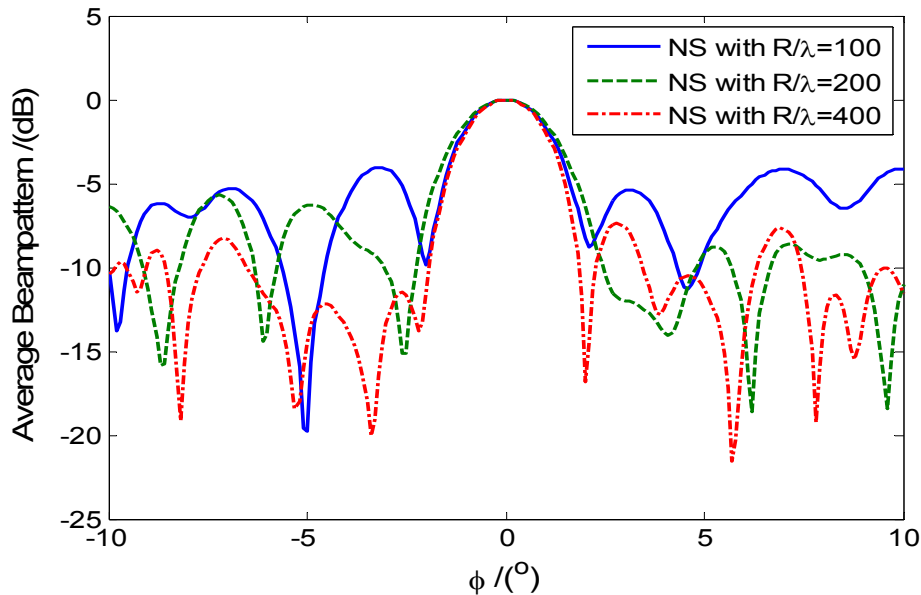


Figure 5.16 Average beampattern of the selected CR nodes with $R/\lambda = 100, 200, 400$

Figure 5.16 shows the result of the average beampattern of our proposed NS method when applied to large CR networks ($\tilde{R} = 100, 200, 400$). We consider that the distribution density of the CR nodes remains the same as that of Figure 5.11-5.15 ($K = 60$, $\tilde{R} = 500$). Only the size of the networks is increased. Consequently the number of CR nodes of the considered CR networks in Figure 5.16 is $K = \frac{60 \times 100^2}{50^2} = 240$, $K = 960$ and $K = 3840$. We adopt $D = 15\lambda$ for all the three CR networks. It can be seen from this figure that the main beams are much wider than those of the DB method without NS method. When the size of the CR network is enlarged, more nodes will be selected to participate in CR transmission. As a result sufficiently lower sidelobes can be achieved. For the case of $\tilde{R} = 400$, far sidelobe levels become approximately $-15dB$, where near sidelobes are higher.

5.4 Summary

We have introduced the DB technique to the CR network, which is constituted of distributed CR nodes. The goal of the DB method is to forward the CR signal to the DCR user, while causing no harmful interferences to coexisting PUs by limiting its transmission power towards directions PUs. This is the same as ABF techniques employed by CR BS.

We have presented two multi main beams generating methods of DB for a CR network. They are the geographical grouping method and the random initial phase choosing method. The first allocates CR nodes into several ring ranges and an inner circle area. By assigning different initial phases to different group of nodes, it achieves several main beams towards different directions. If we define all the initial phases toward different DCR users as a whole set, the second method let CR nodes choose the initial phases from the set randomly. Both methods can achieve multi main beams towards required directions of DCR users.

When introducing the DB method with the same original model of the CR network as shown in Figure 5.1, which assumes that CR nodes are uniformly distributed in a circle area where the CR network is located, we notice that it is unavoidable that the original model will lead to the extremely narrow main beam of the beampattern. To find a new network structure which has less impact of the working frequency, we have proposed a NS method. After studying the average beampattern of the broadside and end-fire arrays, we choose those CR nodes, which are closely located to an end-fire array considering the direction of the DCR user. Our NS method can also be applied to cases with more than one DCR users. The average beampattern of our NS method show that the main beams are successfully directed towards the DCR users and are enlarged for practical applications in CR networks. What is more, for a CR network with large

physical size, our NS method can widen the main beam while maintaining sufficiently low sidelobe levels for CR transmission.

Chapter 6 Adaptive and Distributed Beamforming Techniques for Intelligent WiMAX (I-WiMAX)

6.1 Introductions and background information

In this chapter, we will introduce ABF and DB as two efficient techniques for Intelligent WiMAX (I-WiMAX). I-WiMAX is a green maritime communication system, consisting of SR principles and mobile WiMAX based on the IEEE 802.16e standard.

The present broadband technology has fundamentally changed the way to distribute and access information, and consequently it is envisioned to have tremendous market potentials, if it is introduced in a maritime communication environment. In this chapter, we present the Intelligent WiMAX (I-WiMAX) concept as a new communication architecture, which is dedicatedly designed for green maritime coastal/lake communications and locationing. I-WiMAX is built upon Mobile WiMAX, which is based on the IEEE802.16e standard. The intelligence of I-WiMAX is realized by Adaptive OFDM (AOFDM) and SA concepts.

With the development of the IEEE 802.16e standard, which is an amendment to the 802.16-2004 standards, mobile WiMAX appears to provide high speed data telecommunication services for moving users comparable to the emerging 4G technique. The deployment of Wireless Fidelity (WiFi) on a maritime platform has been presented in [73], where it is demonstrated that in order to meet the requirement of green radio, achieve large range extension and efficient power management, the modification of the MAC layer is quite necessary. Furthermore, supplements of the physical layer were also needed, such as a power amplifier for the transmit path. The advantage of WiMAX is that it has a longer distance range and can provide much better performance than WiFi, in terms of coverage, QoS management and spectrum usage efficiency. Thus WiMAX satisfies the basic requirements to become a proper candidate for green radio access networks with high-potential energy efficiency and it can be predicated that WiMAX, unlike WiFi, can offer large communication coverage requirements without extra physical layer supplements.

SR is capable of sensing the communication environment, and consequently can make the radio system adaptive by adjusting its SR parameters. AOFDM adaptively allocates the radio resources, such as the power, the sub-channels and the module coding scheme according to Channel State Information (CSI). The flexible modulation scheme

of AOFDM, as a developing green technique, will significantly reduce the radiated power requirement. SA recently has been introduced in WiMAX as a “big thing”. OFDM is a proper technology and suits well for SA, much more than the existing 3G technology. The IEEE 802.16e standard provides optional features and a signaling structure that enables the usage of SA [74]. A separate point-to-multipoint frame structure can be defined that enables the transmission of downlink and uplink bursts to use directional beams. With specific signal processing techniques allowing for optimizing the adaptive array performance, the DOA estimation of ships can be executed accurately. Therefore with an advanced ranging technique and DOA information, the ability for locationing can be provided as an important service by I-WiMAX usage in maritime communications.

I-WiMAX, as a novel communication system, is aimed to provide a metropolitan access network, and offers higher bandwidth, larger coverage maritime wireless communication networks than the VHF broadcasting system which is currently adopted as Automatic Identification System (AIS) by ships [75, 76]. Since the ships are capable of enjoying a large amount of information anywhere and anytime, the transportation efficiency will be significantly improved by the abundant and versatile information obtained from the new maritime communication system based on broadband wireless networks. Furthermore the locationing ability of the broadband communication system offering position services via RF localization.

6.2 Concept of I-WiMAX

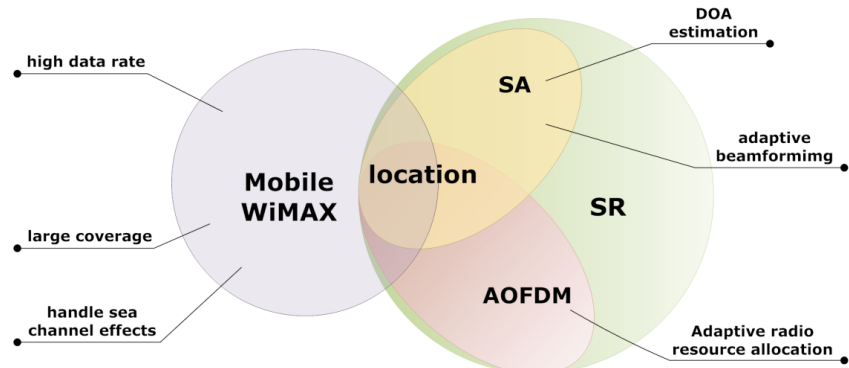


Figure 6.1 I-WiMAX concept of maritime coastal/lake communications

I-WiMAX is built upon SR and mobile WiMAX, as shown in Figure 6.1. SR is a crucial part embedded in I-WiMAX for maritime communication. With SR, the new communication system gains knowledge on the severe sea communication environment, full of echoes and reflections, adapts to it, and therefore increases its cognition and flexibility. The SR technique, which is adopted on top of WiMAX, basically contains two techniques, AOFDM and SA. AOFDM adaptively allocates the radio resource and consequently guarantees the reliable link in the sea channel full of fading and reflection

caused by the rough sea surface. SA ensures a higher SNR which consequently results in larger coverage areas by performing ABF.

Moreover, with SR, the BS can also achieve locationing abilities. SA for I-WiMAX estimates the DOA of each Subscriber Station (in our case, most SS are ships) via employing super resolution array signal processing techniques.

It is the first time that the I-WiMAX concept is introduced delivering maritime communications services over large areas above water surfaces, although the WiMAX performance in port transportation management was investigated in [77]. WiFi, as a Wireless Local Area Network (WLAN) technique, was presented in [73] to be a Line of Sight (LOS), long range communication solution for marine platforms. Mobile WiMAX, based on IEEE 802.16e, is expected to achieve higher data rates and larger coverage, and is a more promising wireless technology for maritime systems. IEEE 802.16-2004 is very useful in replacing a set of documents all describing different parts of the same technology, with different modification directions. However, after its publication, it still needs an upgrade, mainly for the addition of mobility features. This gave way to the 802.16e amendment approved on December 7, 2005 and published in February 2006, which is also known nowadays as mobile WiMAX [78]. The main differences of the IEEE 802.16e standard with regard to the IEEE 802.16-2004 standard are the appearances of mobile stations, the MAC layer handover procedures, Scalable OFDMA (SOFDMA), Multiple Input Multiple Output (MIMO), data security and others [78]. It is obvious that the IEEE 802.16e standard is dedicated to mobile SS for WiMAX. The coverage and throughput of WiMAX have been subjects of considerable debates, with a throughput of 70Mb/s and a coverage area of 50km being claimed as maximum. However, more realistic simulations and trials were run by AT&T in USA and Wireless Broadband (WiBro) in Korea, indicating that the range of mobile WiMAX was about 15km at a data rate of 20Mb/s [79].

Another important reason for introducing WiMAX is the adoption of OFDM as its physical layer, which is more suitable for data transmission in sea communications, compared to Single Carrier (SC) Code Division Multiple Access (CDMA), which has been adopted by both UMTS and High Speed Downlink Packet Access (HSDPA). The use of OFDM increases the data capacity and consequently the bandwidth efficiency with regard to 3G and CDMA. By having carriers very close to each other but still avoiding interferences, due to the orthogonal nature of those carriers, WiMAX presents high spectrum efficiency. In addition, it is also effective against narrow band jamming and interference, as the data are interleaved over multiple carriers. As a result, WiMAX is robust to multipath encountered from the water's reflected surface. However, there are plans to upgrade 3G by introducing OFDM and MIMO in it. The evolution is called, at this moment, LTE.

Locationing ability is a service that can be provided by a maritime wireless communication system for ship navigation and safe transportation. WiMAX adopts

OFDM as its physical layer, and consequently it will outperform other systems, which employ narrowband signals, with regard to the resolution of estimation. The super resolution methods for narrow bands will work very well for OFDM signals, taking advantage of the fact that the OFDM signal is able to be divided into several narrowband signals. As a result, DOA estimation for positioning can be performed after the FFT block in the receiver, together with signal decoding, which is less time consuming and needs only a small computational load.

The working procedure of the novel maritime communication approach is illustrated in Figure 6.2. The CSI is fed back to I-WiMAX, and then SR, which belongs to the physical layer of WiMAX, adjusts its operating parameters, including power management, subcarrier selecting, spatial beam directing and so on. SR makes efficient use of all the radio resource according to the changing communication environment, and thus improves the energy efficiency of green radio. However, in cooperating with SR, WiMAX terminals on ships call for extensions to MAC protocols as described in [73]. For the MAC layer, the required QoS and system throughput should both be satisfied. To maintain high performance of both layers, a MAC-Physics cross layer optimized resource allocation scheme is absolutely required. At the end, the optimized operating parameters are fed back to SR.

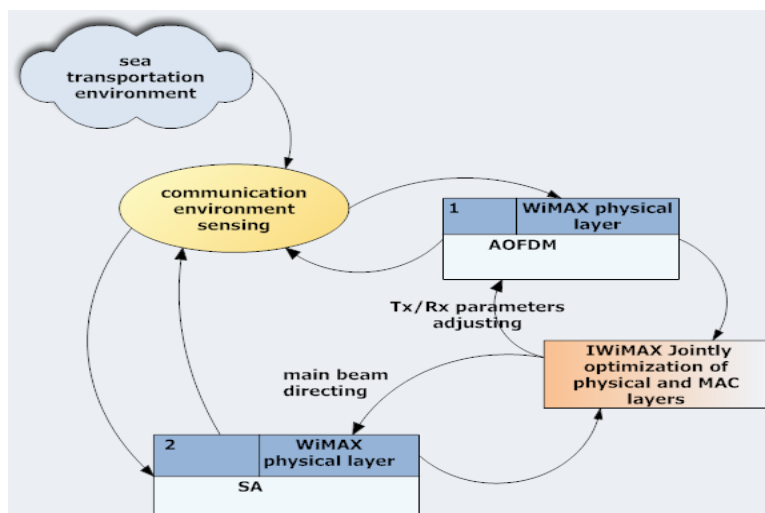


Figure 6.2 Working flow chart of I-WiMAX

6.3 AOFDM for I-WiMAX

AOFDM is different from conventional OFDM in the sense that it improves the system performance by adaptive radio resource allocation, where the allocation scheme is based on the understanding of the channel. The resource request and allocation between the BS and each SS is defined in the IEEE 802.16e standard, but the algorithm for allocation the burst to SS is not specified but open for alternative implementations.

The sea channel is an extremely harsh environment for propagating electromagnetic waveforms. RF communications at the sea surface are difficult due to wave blockage, scattering and reflection of RF signals by the surface causing multipath

propagation; all result in signal fading and loss. In a severe RF environment, the AOFDM for I-WiMAX automatically reduces the data rate and modulation complexity in order to degrade gracefully instead of ceasing to operate. The modulation scheme can be adjusted based on the CSI estimation to guarantee the overall throughput simultaneously supporting good coverage, high data rate and mobility.

Adaptive modulation takes the advantage of the frequency selectivity and time variation by adapting the transmitted signal to match the multipath channel, which is sometimes called “adaptive loading” [80, 81]. AOFDM is able to choose its sub-carriers, which suffer less from fading and face better sub-channels than others. Both the power and data rate in each sub-channel can be adapted. An illustration of how AOFDM adjusts data rate and modulation scheme of I-WiMAX for green radio application is shown in Figure 6.3. From this figure, it can be concluded that the sub-carriers experiencing a good channel with high SNR will be used for higher data rate transmission such as 16 Quadrature Amplitude Modulation (QAM) and QPSK. Meanwhile, to those OFDM sub-carriers which encounter lower SNR, BPSK or even no transmission task are assigned to them. An adaptive radio resource allocation method is suggested to be necessary for green communication and therefore is adopted by SR for I-WiMAX, aiming to maintain the estimated BER and its achievable channel capacity of AOFDM for transmission over a Rayleigh channel [82].

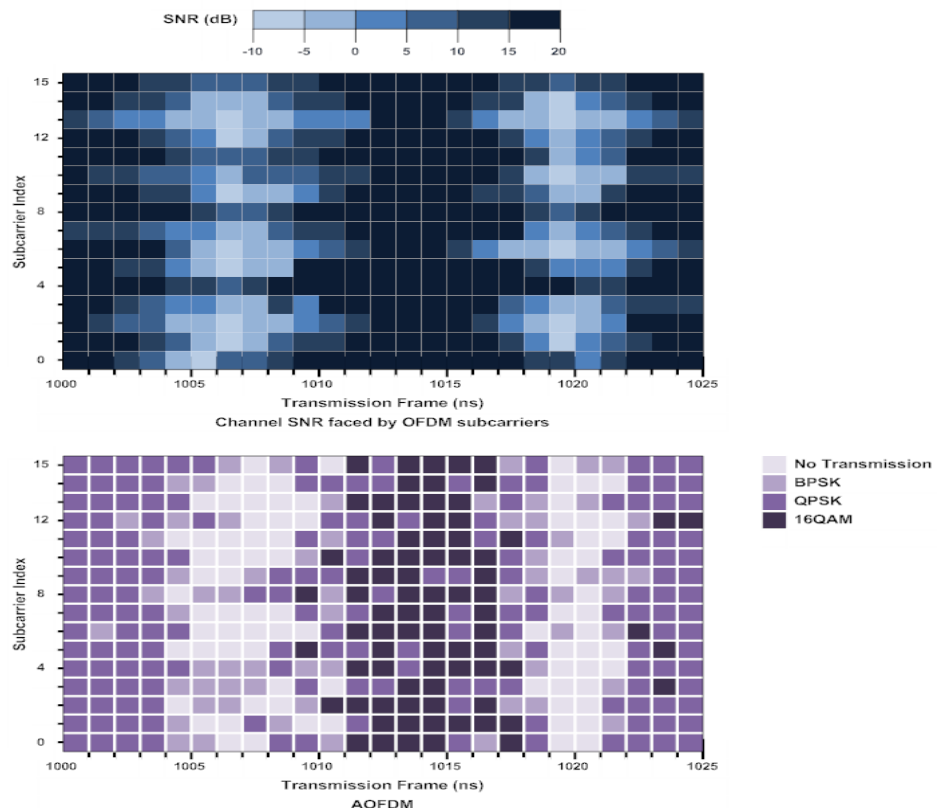


Figure 6.3 Adaptive modulation of I-WiMAX for green radio application

The other radio resources, that can be adaptively allocated, are the power and the selection of sub-carriers. Figure 6.4 illustrates a simple power and subcarriers allocation scheme of I-WiMAX for green radio application. When the Power Spectrum Density (PSD) of the channel is below the defined threshold, those OFDM subcarriers, which locate the actual fading frequency bands, will be assigned to less power. On the other hand, more power will be given to those sub-carriers experiencing good channels. AOFDM assigns the power efficiently to each sub-carrier and saves a large amount of energy for transmitting while maintaining the required QoS. Therefore, it is a most energy efficient scheme for green radio.

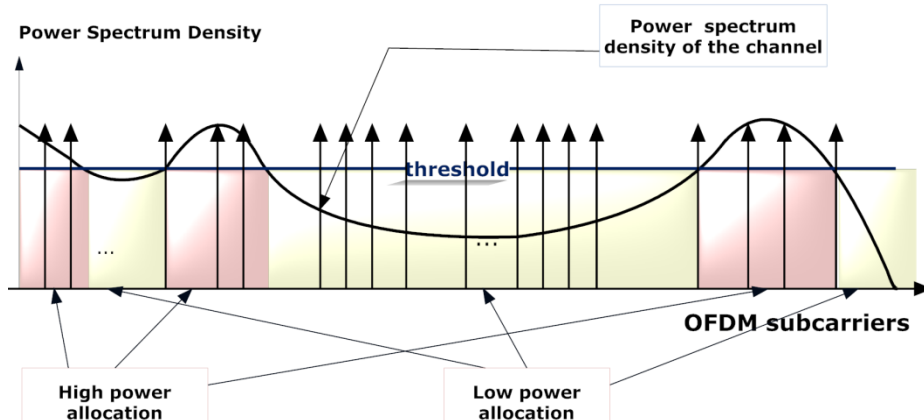


Figure 6.4 Power and subcarriers allocation of I-WiMAX for green radio application

Recently several algorithms were proposed for downlink resource allocation in a WiMAX system in order to reduce the power for transmission in a green radio concept. An optimal and sub-optimal allocation in terms of maximizing the total downlink throughput was investigated in [83], while the study in [84] proposed a Best Sub-carrier Allocation (BSA) algorithm which uses the feedback of the radio channel quality, and sorts the users to choose subcarriers based on their own channel feedback. When perfect CSI is not available at the transmitter side, a jointly estimation of the channel and allocation of the resource in OFDMA networks is proposed in [85]. In the case of uplink, based on minimizing the transmitting power, an efficient solution of suboptimal utilization of modulation and coding schemes, defined in an IEEE 802.16 system, is discussed in [86].

6.4 A technique for I-WiMAX

In this section we demonstrate that the adaptive beamformers for I-WiMAX allow for efficient spectrum reusing. Both uplink and downlink adaptive beamformers are discussed. Particularly the NB method presented in chapter 4 is implemented.

An uplink ABF technique can direct its main beam towards the interested signal source, while displaying nulls to the unwanted directions. This ensures that the transmitted signal from one of the SS can be detected and selected by the BS via beamforming. Therefore, for those re-used OFDM subcarriers, the weights should

guarantee the main beam directed towards the desired SS, while at the same time “null” beams are created towards other SS. The uplink adaptive OFDM beamformer of I-WiMAX can be designed similarly as shown in Figure 3.1.

For the downlink, since SS does not have SA, appropriate beamforming techniques must be provided by the BS to satisfy the link quality for all co-channel SS. If we only use the estimated weights of the uplink for the downlink, the nulls in the patterns towards those co-channel SS may become too narrow. Therefore, NB methods for beamforming, which have been presented in chapter 4, should be considered. Employing the NB technique, the adaptive downlink beamformer of I-WiMAX for green radio is shown in Figure 6.5. I-WiMAX performs downlink beamforming with suppressed power in a certain angular range to guarantee that the co-channel interference caused by spectrum reusing is reduced for SS.

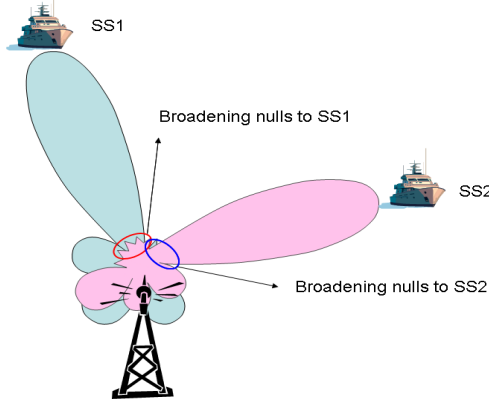


Figure 6.5 NB technique for I-WiMAX (SS1 and SS2 share the same OFDM subcarriers)

6.5 DB for I-WiMAX

We introduce DB to I-WiMAX for long distance communications beyond the coverage range of one BS. As shown in Figure 6.6, accessible SS are regarded as wireless relays, and consequently they form a relay network with flexible and uncertain locations of each node. We show the feasibility of DB for I-WiMAX as well as some simulation results of the method based on OFDM signals.

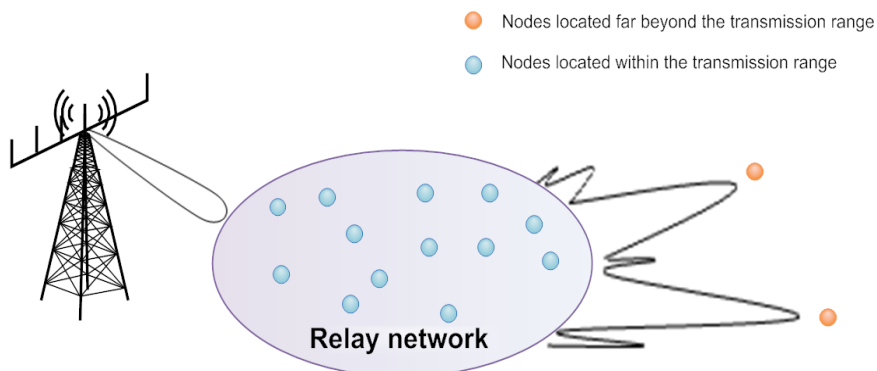


Figure 6.6 DB for I-WiMAX in long distance communications

WiMAX supports two duplexing schemes: Time Division Duplex (TDD) and Frequency Division Duplex (FDD). However, most WiMAX implementations will likely use TDD, because it allows the system operator to receive the most from their investment in spectrum and telecom equipment, while meeting the needs of each individual user. We demonstrate here that TDD is also more suitable for the application of DB to I-WiMAX than FDD.

Figure 6.7 and Figure 6.8 show DB for I-WiMAX in both TDD and FDD schemes. We mark those SS, which are beyond the transmission range as Distant SS (DSS). The uplink defines the link from DSS to BS, while downlink represents the reverse. In TDD mode, as shown in Figure 6.7, DSS, SS and BS require only one channel for uplink and downlink transmission in two distinct time slots. For DSS, the whole Tx and Rx procedure requires double time related to the communication session within the coverage range. In Figure 6.8, it is worth noticing that for DSS and SS, the portions of the spectrum used for Tx and Rx are different; for example, DSS must transmit signals to SS via adopting a spectrum band of the downlink. This is a hard task for such hardware modification. Therefore, TDD scheme is more flexible and more suitable for introducing DB into I-WiMAX.

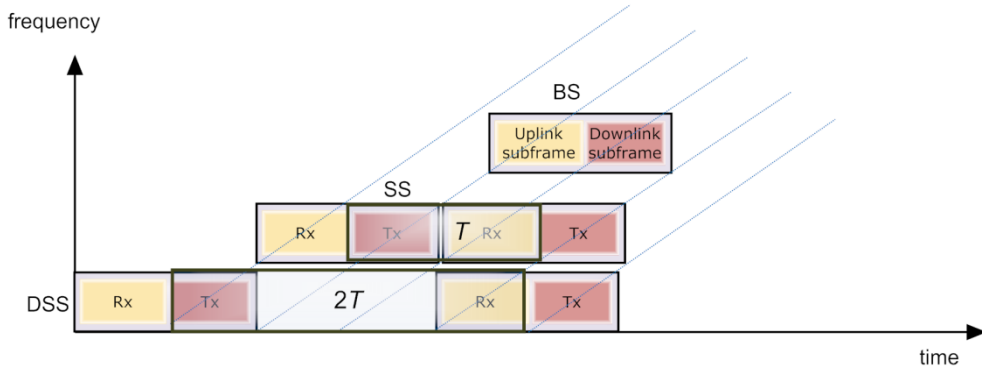


Figure 6.7 DB for I-WiMAX in TDD scheme

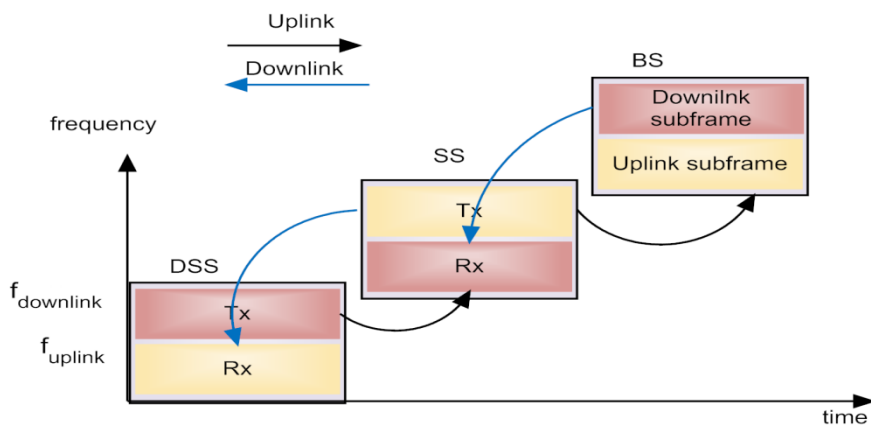


Figure 6.8 DB for I-WiMAX in FDD scheme

There are two most relevant relay strategies: Amplify-and-forward (AF) and decode-and forward (DF) [87]. In the AF, the relay simply transmits the scaled and

phase-shifted version of their received signals, while in the DF scheme, the relay starts with decoding and then re-encodes the received signals prior to retransmitting them. We can see from Figure 6.7 that in the TDD mode, since Tx and Rx are performed in different time slots, both AF and DF can be adopted. In this study, we consider the AF strategy because of its low complexity.

Applying the DB method to the OFDM signal, different subcarriers are required to adopt different initial phases, because they operate at different frequency bands. For WiMAX, there are three frequency bands defined in the standard, 2.5 GHz and 3.5 GHz licensed spectrum, and the unlicensed 5 GHz spectrum. The subcarrier spacing of WiMAX is always 10.94 kHz, which means when the available bandwidth increases, the number of subcarriers will also increase. WiMAX supports the channel bandwidth of 1.25MHz, 5MHz, 10MHz, and 20MHz. We assume that $f_0 = 3.5\text{GHz}$, and the channel band is 1.25MHz. Therefore, 128 subcarriers will be used. Then we can write that

$$\max_i \left(\frac{\widetilde{R}_0}{\widetilde{R}_i} \right) = \max_i \left(\frac{f_0}{f_i} \right) = \frac{3.5\text{GHz}}{3.5\text{GHz} + 10.94\text{kHz} \times 127} \approx 1, \quad 0 \leq i \leq 127 \quad (6-1)$$

Therefore, $\widetilde{R}_0 \approx \widetilde{R}_i$, $0 \leq i \leq 127$, which means that in this case the average beampatterns of the all subcarriers are approximately the same.

Meanwhile, since $f_0 = 3.5\text{GHz}$, the 3dB bandwidth of the average beampattern will become very narrow. It is desirable for I-WiMAX to achieve a narrow main beam. However, when the DSS is moving or the location of the DSS is not accurate enough, too narrow beams may cause problems, as the DSS may not be covered by the main beam. We have provided the NS method as a solution to this problem in section 5.3, which achieves much wider main beam via selecting proper CR nodes for transmission.

6.6 Application of I-WiMAX

Based on the design of WiMAX, the new maritime communication system is capable of high data rate communication with a larger coverage area. As mentioned in the beginning, the coverage range of WiMAX is expected to be at least 15km. However, for maritime communication, due to the variable sea channel conditions, the real coverage may probably shrink somewhat.

The skippers, after introducing the new maritime communication system, are tended to be broadband users, finding dramatic changes about how to share information, conduct business, and seek entertainment on ships. The new maritime communication system not only provides faster web surfing and quicker file downloads on the ship, but also enables several multimedia applications, such as real-time audio and video streaming, multimedia conferencing, High Definition TV (HDTV), Video on Demand (VoD) and interactive gaming, as shown in Figure 6.9. When ships enter the area covered by the BS on shore, abundant information and new additive services will be offered to skippers and people on board. With the broadband technology, it is possible to offer ships

guaranteed quality of service as well as specific service types, such as Voice Over IP (VOIP), video images, Internet access, and so on. Meanwhile, considering its large coverage, the new maritime communication system needs fewer infrastructure and consequently costs less. The ships are capable of enjoying a large amount of information anywhere and anytime. Furthermore, the locationing ability of the broadband communication system offering position services via RF localization is of great value, as also visualized in Figure 6.9.

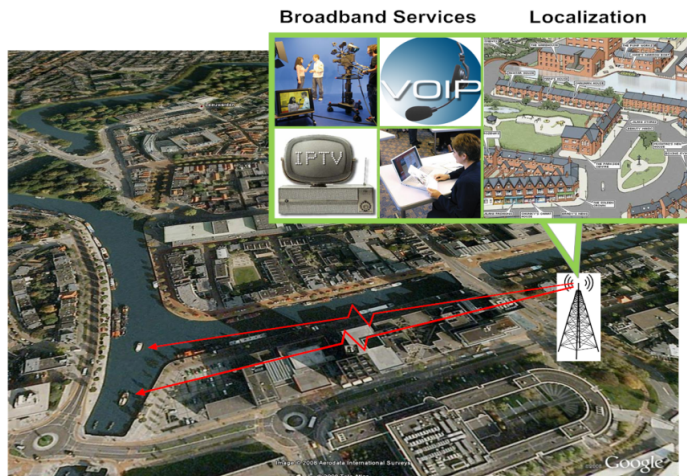


Figure 6.9 Application of I-WiMAX for maritime coastal/lake environment communication

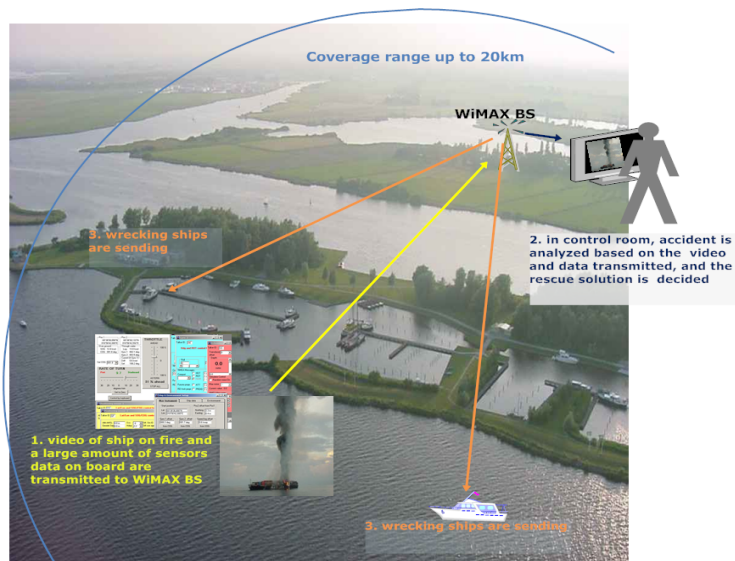


Figure 6.10 Emergency services provided by I-WiMAX.

Particularly when an accident happened on the water, the I-WiMAX shows a potential rescue capability as shown in Figure 6.10. Any ship that encounters disasters is required to send the SOS signal, the live video and all the sensors data to the BS. Then on shore in the control room, the experts are able to analyze the cause of the tragedy, decide the best rescuing operation, and monitor the accident scene. At last, several wrecking ships are assigned to the live spot with the determined rescuing operation to help the ship in trouble. The high speed data rate of I-WiMAX ensures the streaming video and a large

amount of sensor data to arrive the BS in time, which is valuable in providing emergency services.

6.7 Summary

I-WiMAX, as a new maritime wireless communication system, promises a large coverage range, high data rates, efficient spectrum usage, and reliable communications in sea/lake scenarios. It consists of SR and mobile WiMAX. SR introduces two beamforming techniques, ABF and DB, for ultimate efficient spectrum utilization and large coverage.

ABF for uplink can spatially select the receiving signals of interested SS and alleviate co-channel interferences by directing the main beam towards the interested SS and nulls towards others. For downlink ABF, the NB method, which has been discussed in chapter 4, is introduced in I-WiMAX to display spread nulls in a certain range of directions. When taking into account a spatial channel model, it proves that NB is an essential part of I-WiMAX when serving reliable links to more than one SS within the same spectrum band.

For SS (far) beyond the possible communication coverage range, we propose a relay network formed by those accessible SS to transmit the signals further to distant SS, rather than involving another BS. Due to the uncertainty of the location of the relay nodes, DB, which has been investigated in chapter 5 is employed for the SS relay network to transmit signals collaboratively after adopting different initial phases. We showed that the TDD mode of WiMAX is more suitable than FDD.

Chapter 7 Conclusions and Recommendations

CR is an intelligent radio system, which senses the communication environment and then adapts to it automatically. One of the CR objectives is to obtain efficient spectrum utilization. We have proposed an integrating beamforming technique into the CR system, which fully exploits spatial diversity and thus greatly leverages spatial cognition capability to achieve a most efficient spectrum utilization and full spectrum sharing with PUs. The main concerns about applying beamforming techniques to CR are the spatial interferences to PUs due to CR transmission as well as the interferences from PUs at CR receiving. Both problems are well investigated and studied in this thesis. What's more, the concept of exploring spatial diversity for CR can also be applied to CR networks. Similar challenges exist but we have tackled them differently via introducing DB techniques.

7.1 ABF techniques for CR

At the uplink for CR, the main problem is to detect and receive signals from CR users even when their SNR is low in the presence of PUs. For the ABF technique, if the signal of interest has a low SNR and its DOA is uncertain or unknown, the performance of directing main beams towards the direction of interest will be significantly degraded. We therefore have introduced the adaptive Bayesian beamformer and extended it for OFDM CR uplink systems. However the adaptive Bayesian beamformer does not take the presence of interferences into consideration. For this reason we have modified it by employing the proposed PM method. The PM method has successfully eliminated the presence of PUs signals in the covariance matrix and in this way the adaptive Bayesian beamformer can be applied to the CR uplink as a robust beamforming technique.

Since OFDM is recommended to be the best modulation scheme for CR system, we have presented two types of adaptive OFDM beamformers for the CR system at the uplink to successfully receive signals from CR users while rejecting signals from PUs. They are the adaptive OFDM MMSE beamformer and the adaptive Bayesian beamformer. We have investigated and employed the latter for CR BS in order to perform beamforming when signals of CR users have a low SNR and their DOAs are unknown or uncertain. We have designed and calculated all the weights of adaptive OFDM beamformers for different OFDM subcarriers iteratively, which has less complex multiplication computations than an independent weights calculation for each OFDM subcarrier. Simulation results show that the computation loads (the number of complex multiplications) can be decreased by 90%, compared with calculating the weights for

each OFDM subcarrier independently. Thus the CR BS will save computation time for weights calculation in the adaptive OFDM beamformer.

Based on different spectrum access schemes that CR adopts, we have proposed weights-masking and weights-constraint methods to modify the beamforming weights for those OFDM subcarriers which are in the same frequency band as PUs. The weights-masking method is adopted for the “interwave” spectrum access mode and it simply deactivates those OFDM subcarriers which are in the PUs frequency bands. The weights-constraint method benefits from higher spectrum efficiency by forcing the weights of those OFDM subcarriers to direct nulls patterns towards PUs. Though the weights-masking method has a slightly better BER performance than that of the weights-constraint method, the latter can achieve higher bit rate for the CR OFDM system via using maximally the available spectrum.

It is important for CR downlink beamformers to ensure that the power of the transmitted CR signals, which are received by PUs, is less than the interference level determined by PUs. We found out that even in case CR limits its transmission power via employing the ABF technique, due to scatterers and multipath effects, the power of the CR signal may also leak to directions of PUs. Thus the spatial channels are worth studying for further controlling the CR transmission at different directions. Since the angular deviation models of spatial wireless channels are characterized as a Von Mises distribution, adaptive downlink beamformers for the CR BS should limit and control its transmission power in a range of angles around PUs directions rather than directing null patterns towards PUs. We have presented a new NB method to achieve this goal, which is called VDA. It is based on the approximation of the CMT method but it is capable of generating deeper broadened nulls around directions of PUs. The VDA method gives a closed form expression for the relationship of the weights of adaptive beamformers with and without the NB technique. It is also capable of generating deeper null patterns than the CMT method. In order to generate deeper broadened nulls, we have further suggested a filtering method, which employs window functions as filter of the adaptive beamformer. By adopting different kinds of window functions or adjusting parameters of the same window function, we can chose different depths of the broadened null patterns.

By utilizing the VDA method and filtering method together, the adaptive downlink beamformer of the CR BS is able to display deep and broadened nulls. This guarantees that the CR BS will cause less interferences to PUs even when the CR system is using the same spectrum band as PUs. For an OFDM CR system, the VDA method is able to perform in an iterative way too, which ensures that the system model of the uplink adaptive OFDM beamformers can also be adopted at downlink.

7.2 DB for CR networks

We have introduced the DB technique into CR networks, which is constituted of distributed CR nodes. The goal of the DB method is to forward the CR signal to the DCR

users, while causing no harmful interferences to coexisting PUs by limiting its transmission power towards PUs. This is the same as when ABF is employed by the CR BS.

We have first studied the DB methods, which enforces initial phases to CR nodes. In this way CR nodes can form a main beam towards DCR users to collaboratively forward signals. The average beampattern generated by the DB method shows that the asymptotic sidelobe level approaches a level which is the inverse proportion to the total number of nodes which are participating in the transmission. Consequently considering the possible working frequency of the CR networks (256MHz of 32 channels in the TVWS), the main beam of the average beampattern can be designed narrow enough and the sidelobe level in the beampattern will approach $\frac{1}{K}$, where K is the total number of CR nodes in the CR network. Thus unlike the use of ABF techniques, which direct specific nulls towards directions of PUs, the DB method by its nature is capable of guaranteeing $K-1$ times less power towards PUs compared with that towards DCR users. Nulls generating is therefore no longer a problem for the DB method when applied to CR networks.

However, since the width of the main beam can be approximated by $\frac{35^\circ}{\tilde{R}}$, and \tilde{R} should be large enough to have enough number of CR nodes to perform DB, the width of the main beam will then become extremely narrow, e.g., for a possible frequency band for CR application at 786MHz, to collect possible 30 CR nodes, \tilde{R} should be around 250, which results in a width of main beam of 0.1° in the pattern. This is considered to be too narrow, implying that the width of the main beam in the beampattern mostly relies on the center frequency at which CR is able to access. To solve the problem of the extreme narrow main beam, we have proposed a NS method based on the study that the “broadside” size of the CR network should be small so that a beampattern with a wider main beam can be maintained. By selecting CR nodes, which are able to form a full size end-fire array and a reduced size broadside array, our NS method is effective in generating a much wider main beam in the beam pattern. It can also be applied to cases with more than one DR users. The average beampattern of our NS method show that the main beams are successfully directed towards the DCR users and are enlarged for practical applications in CR networks. What is more, for a CR network with large physical size (large \tilde{R}), our NS method can widen the main beam while achieve sufficiently low sidelobe level for CR transmission.

So far no DB method has the possibility of generating more than one main beam in CR. In the presence of more than more DCR users, CR networks are practically obliged to direct main beams towards those DCR users. We have presented two multi main beams generating methods of DB in a CR network. They are the geographical

grouping method and random initial phase choosing method. The first allocates CR nodes into several ring ranges and an inner circular area. By assigning different initial phases to different groups of nodes, it achieves several main beams towards different directions. If we define all the initial phases for optimizing the transmission towards different DCR users as a complete set, the second method lets the CR nodes choose the initial phases from the set randomly.

7.3 ABF and DB for I-WiMAX

I-WiMAX, as a new maritime wireless communication system, promises a large coverage range, high data rates, efficient spectrum usage, and reliable communications in sea/lake scenarios. ABF for uplink can spatially select the receiving signals of interested SS and alleviate co-channel interferences by directing the main beam towards the interested SS and nulls towards others. For downlink adaptive beamforming, the NB method has been introduced in I-WiMAX to display spread nulls in a certain range of directions. When taking into account a spatial channel model, as is seen at the SS, it proves that NB is an essential part of I-WiMAX when serving reliable links to more than one SS within the same spectrum bands.

For SS (far) beyond the possible communication coverage range, we have proposed a relay network formed by those accessible SS to transmit the signals further to distant SS via employing the DB method. Taking into account the working frequency bands of WiMAX, NS is absolute needed for practical usage due to its capability of enlarging the main beam while providing sufficient lower sidelobes in the pattern.

7.4 Recommendations for future work

In this thesis, we have only considered one case describing a more or less realistic wireless channel, i.e., the Rayleigh channel in simulations as discussed in chapter 3. More studies on the time variances in the channel can be carried out and the results can be applied in ABF for CR in future work. The investigations of wireless communication channels can help CR systems to modify and adjust beamformers to adapt to different communication environments. All the methods presented in this thesis can be applied together with channel estimations and equalizations. For both ABF and DB techniques, if we consider dynamic wireless channels, the weight calculations are requested to be performed at each time slot, each frequency interval, and each direction due to the variation of the channels. In chapter 3, we have presented an AOFDM beamformer, which requires less computation time. This is very suitable for real time weights update. On the other hand, understanding multi path, time delay and other properties of the channel can definitely improve and further simplify the ABF and DB methods presented in the thesis. For example, if the multipath effect of the spatial channel from the CR BS to PUs is more severe; deeper nulls should then be generated by

the NB method proposed in chapter 4 so that less power can be scattered to PUs. In addition, if the spatial channel has a significant fading, the NB method may not be needed in the CR downlink beamformer, due to the fact that the signal power towards directions of PUs is already alleviated.

In the study on CR networks, the channel effects between DCR users and each CR node in the CR network are not taken into account. It is possible that the channel between a DCR user and different CR nodes is similar to each other, considering the distances between DCR users and the CR network, and the size of the CR network. As a result, it is suggested for new studies on the channels in a distributed fashion, like the DB method that we have introduced into CR networks. The channel may be characterized statistically and consequently we may derive the average channel properties. We propose therefore that the channels between a network and sink should be considered and studied in a different manner than channels characterized from point to point.

By studying CR networks, we have derived several interesting results based on the distribution of CR users (nodes) in the CR network. We have assumed they are following a uniform distribution, because we treat each area in the CR network equally and assume that each node has equal chance to be located in that area. In real applications, due to the geographical requirements, nodes may not be uniformly distributed anymore. For example, in applications of environment monitoring, if some area is of great interest, more data should be collected to further observe more locally the environment, and therefore more sensors are spread in that area. For some parts, which have less possible environment changes, less number of sensors are placed there. Consequently, the distribution that we have assumed is hard to be achieved anymore. Thus the combined distribution or a sparse distribution should be introduced to describe the sensor networks. Studying different distributions of sensors can also benefit the NS method in a way that we may find out the best distribution of the networks. With the knowledge on an optimal distribution of the networks, we may choose proper nodes which are following optimal distributions. If a Gaussian distribution is the best for a certain type of network, we can choose several nodes, which are following Gaussian distributions, out of the complete network in order to form an optimal network. It is therefore proposed to investigate in future NS methods based on distributions rather than considering the transmitting signal of each node.

Given the worldwide growth in the move to higher data rate mobile broadband, and the increasing contribution of information technology to the overall energy consumption of the world, there is need on environmental grounds to reduce the energy requirements on radio access networks. The green radio program aims to achieve significant reductions in CO₂ emissions [88]. It is pursuing energy reduction from two different perspectives. The first is to examine alternatives to the existing cellular network structures to reduce energy consumption and the second is to study novel techniques to reduce energy consumption in the network. In chapter 5, we have covered the first

perspectives by presenting a new NS schemes to choose proper CR nodes for transmission in order to build a new structure of the network. The second perspective aims at developing a new DB technique. Thus a new green DB method should be studied on top of the DB method discussed in chapter 5, which means it not only is capable of generating the proper and practical main beams towards required directions, but also is able to consume less energy of the whole network. The fact is that for wireless sensor networks, there exists a minimum in the number of nodes, which is decided by the transmission power being able to reach the distant node. Therefore, a possible solution is to control the DB weights of all nodes in a way that all nodes are consuming the same amount of energy at the same time. Compared to the DB method which results in the unbalance of the energy consumption (some nodes are dying out while others are full of energy), it prolongs the life time of the network, since all the nodes will be power off in the end instead of having less amount of nodes which still have power.

List of Abbreviations

ABF	Adaptive beamforming
AOFDM	Adaptive OFDM
AWGN	Additive Gaussian White Noise
AS	Angular Spread
AF	Amplify-and-forward
AIS	Automatic Identification System
BER	Bit Error Rate
BPSK	Binary Phase Shift Keying
BS	Base Station
BSA	Best Sub-carrier Allocation
CDF	Cumulative Distribution Functions
CDMA	Code Division Multiple Access
CMT	Covariance Matrix Taper
CR	Cognitive Radio
CP	Cyclic Prefix
CSI	Channel State Information
DB	Distributed beamforming
DCR	Distant CR
DF	Decode-and Forward
DFT	Discrete Fourier Transform
DOA	Direction Of Arrival
DSS	Distant SS
FCC	Federal Communication Commission
FFT	Fast Fourier Transform
FDD	Frequency Division Duplex
HDTV	High Definition TV
HSDPA	High Speed Downlink Packet Access
IC	Interference Cancelation
IFFT	Inverse Fast Fourier Transform
I-WiMAX	Intelligent WiMAX
LMS	Least Mean Square
LCMV	Linear Constrained Minimum Variance beamformer
LOS	Line of Sight
LTE	Long Term Evolution
MVDR	Minimum Variance Distortionless Response
MSE	Mean Square Error
MMSE	Minimum MSE
MAC	Medium Access Control

List of Abbreviations

MIMO	Multiple Input Multiple Output
NB	Null Broadening
NS	Nodes Selection
OFDM	Orthogonal Frequency Division Multiplexing
PM	Projection Method
PMSE	Program Making and Special Events
PSD	Power Spectrum Density
PU/PUs	Primary User/Primary Users
QAM	Quadrature Amplitude Modulation
QPSK	Quadrature Phase Shift Keying
QoS	Quality of Service
RF	Radio Frequency
RLS	Recursive Least Squares
SA	Smart Antenna
SC	Single Carrier
SDMA	Space Division Multiple Access
SINR	Signal to Interference plus Noise Ratio
SIR	Signal-to-Interference Ratio
SNR	signal-to-noise
SOFDMA	Scalable OFDMA
SR	Smart Radio
SS	Subscriber Station
s .t.	subject to
TDD	Time Division Duplex
TOA	Time Of Arrival
TVWS	TV white space
ULA	Uniform Linear Array
UMTS	Universal Mobile Telecommunication System
UWB	Ultra wideband
VDA	Virtual Direction Adding
VoD	Video on Demand
VOIP	Voice Over IP
WiBro	Wireless Broadband
WiMAX	Worldwide Interoperability for Microwave Access
WLAN	Wireless Local Area Network
WSN	Wireless Sensors Networks

List of Symbols

\mathbf{A}	steering matrix of array antenna
\mathbf{A}_m	steering matrix of the m th OFDM subcarrier
\mathbf{A}_L	steering matrix of the array in the directions of all PUs
$(A_i^{DCR}, \phi_i^{DCR})$	polar coordinates of the i th DCR node
$\mathbf{a}(\theta_{PUL})$	steering vector of the l th PU
$\mathbf{a}_m(\theta_{PUL})$	direction vector of the m th OFDM subcarrier for the l th PU signal
$\mathbf{a}(\theta_i)$	steering vector of the i th narrow band far-field signal
a_x	a normalization factor for Bayesian beamformer
\mathbf{B}_L	orthogonal complement space of \mathbf{A}_L
b_m	symbol modulated on the m th OFDM subcarrier
D	size of the belt area defined by the NS method
$d(t)$	reference or training symbol sequence
d_k	distance between the k th node and point (A, ϕ) in the far field
$F(\phi r_k, \Psi_k)$	array factor of CR networks
f_L	lowest frequencies of the OFDM signal
f_H	highest frequencies of the OFDM signal
$f_{r_k}(r)$	pdf of r_k
$f_{\Psi_k}(\Psi)$	pdf of Ψ_k
$h(n)$	window function utilized as a kind filter
$I_0(\bullet)$	zero-order modified Bessel function
$J_n(\cdot)$	n th order Bessel function of the first kind
K	total number of CR nodes in the network
L	total number of PUs
L_{DCR}	number of DCR users
M	number of OFDM subcarriers

List of Symbols

N	number of array antennas
N_t	number of time samples
$\mathbf{n}(t)$	AWGN
$\mathbf{n}_m(t)$	AWGN for the m th OFDM subcarrier
$P(\phi z_k)$	far field beampattern of CR networks
$P_{av}(\phi)$	average array beam pattern of CR networks
$p_\Theta(\theta)$	Von Mises pdf
$p(\bar{\theta}_i \mathbf{X})$	posterior distribution of $\bar{\theta}_i$ for the Bayesian beamformer
P_{av}^{ring}	average far field beampattern of the ring range
$\bar{P}_{broadside}(\phi)$	average far field beampattern of a broadside array
$\bar{P}_{end-fire}(\phi)$	average far field beampattern of an broadside array
\mathbf{R}_x	autocorrelation matrix of the received signal
\mathbf{R}_N	autocorrelation matrix of the interference and noise
$\hat{\mathbf{R}}_x$	estimation of \mathbf{R}_x
$\mathbf{R}_{x,m}$	autocorrelation matrix of the received signal on the m th subcarrier
\mathbf{R}_{uplink}	uplink covariance matrix
\mathbf{R}_{CMT}	modified \mathbf{R}_x using CMT method
\mathbf{R}_{VDA}	modified \mathbf{R}_x using VDA method
\tilde{R}	normalized radius for CR networks
(r_k, Ψ_k)	polar coordinates of the k th CR node
$r_k(t)$	received signal at an arbitrary point (A, ϕ) in the far field
$s_i(t)$	the i th narrow band far-field signal impinging on the array antennas
$s_{PUl}(t)$	the transmitted signals from the l th PU
T_s	OFDM symbol duration
\mathbf{T}	transposition matrix
$\mathbf{T}_{m \rightarrow m+i}$	transposition matrix mapping the m th to $(m+i)$ th OFDM subcarriers
W	trough width between the outermost nulls
\mathbf{w}	complex weights of array antenna
\mathbf{w}_{MMSE}	weights of MMSE beamformer

\mathbf{w}_{MVDR}	weights of MVDR beamformer
\mathbf{w}_m	weight vector for the m th OFDM subcarrier
$\mathbf{w}_{MMSE,m}$	MMSE weights of the m th OFDM subcarrier
\mathbf{W}_{WM}	weights of the weights-masking method
\mathbf{W}_{CW}	weights of the weights-constraint method
$\mathbf{W}_{B,CW}$	constrained weights of for the adaptive OFDM Bayesian beamformer.
\mathbf{W}_{CMT}	weights of the CMT method
$\tilde{\mathbf{w}}$	new weights with deeper and broadened nulls
\mathbf{X}	a collection of array observations for Bayesian beamformer
$x_k(t)$	transmitted signal from the k th node in the CR network
$\mathbf{x}(t)$	received signal of array antenna
$y(t)$	beamformer output
λ	wavelength of the signal
$\varepsilon(t)$	error signal
θ_{PUl}	DOA of the l th PU
σ_n^2	the variance of the noise
$\overline{\sigma_l}^2$	power of the l th signal
β_k	signal path loss
φ_k	initial phase of each node
ξ	radii ratio of different circles
$(\mathbf{A})^+$	pseudo-inverse of \mathbf{A}
$(\mathbf{A})_{m,n}$	an element of matrix \mathbf{A} at the m th row and the n th column
$(\mathbf{A})_{m,1:N}$	the vector of the m th row of matrix \mathbf{A}
$(\mathbf{A})_{1:N,m}$	the m th column of matrix \mathbf{A}
$O(\bullet)$	asymptotic notation, the order of
\odot	Hadamard product (element by element multiplication of matrix)
$*$	convolution
$diag(\mathbf{a})$	a diagonal matrix with each element of vector \mathbf{a} on the diagonal

Appendix A

Proof of Equation (4-11)

We define $x_m, x_n, m, n = 1, 2, \dots, N$ are the element locations of the array antenna. $x_m = (m-1)d$, and $x_n = (n-1)d$, where d is the distance between two successive array elements. We also define

$$(\mathbf{R}_{VDA}^V)_{m,n} \triangleq (\mathbf{R}_N)_{m,n} \prod_{k=1}^V \left(1 - \frac{4}{3} \sin^2 \left(\frac{\pi}{3^k} \frac{(m-n)W}{2} \right) \right) \quad (\text{A-1})$$

and write for $V = 0$

$$\mathbf{R}_{VDA}^0 = \mathbf{R}_N \quad (\text{A-2})$$

The following iterative result is now formed

$$(\mathbf{R}_{VDA}^V)_{m,n} = (\mathbf{R}_{VDA}^{V-1})_{m,n} \cdot \left(1 - \frac{4}{3} \sin^2 \left(\frac{\pi}{3^V} \frac{(m-n)W}{2} \right) \right) \quad (\text{A-3})$$

For $V = 1$,

$$\begin{aligned} (\mathbf{R}_{VDA}^1)_{m,n} &= (\mathbf{R}_N)_{m,n} \left(1 - \frac{4}{3} \sin^2 \left(\frac{\pi(m-n)W}{2 \times 3} \right) \right) \\ &= \frac{1}{3} (\mathbf{R}_N)_{m,n} + \frac{2}{3} \cos \left(\frac{\pi m W}{3} \right) \cos \left(\frac{\pi n W}{3} \right) (\mathbf{R}_N)_{m,n} \\ &\quad + \frac{2}{3} \sin \left(\frac{\pi m W}{3} \right) \sin \left(\frac{\pi n W}{3} \right) (\mathbf{R}_N)_{m,n} \end{aligned} \quad (\text{A-4})$$

If we adopt the definitions of $\mathbf{D}_{m,k}$ in equations (4-13), \mathbf{R}_{VDA}^1 can be written as

$$\mathbf{R}_{VDA}^1 = \frac{1}{3} \mathbf{R}_N + \frac{2}{3} \mathbf{D}_{1,1} \mathbf{R}_N \mathbf{D}_{1,1} + \frac{2}{3} \mathbf{D}_{2,1} \mathbf{R}_N \mathbf{D}_{2,1} \quad (\text{A-5})$$

Using equations (A-3) and (A-5), we derive

$$\mathbf{R}_{VDA}^2 = \frac{1}{3} \mathbf{R}_{VDA}^1 + \frac{2}{3} \mathbf{D}_{1,2} \mathbf{R}_{VDA}^1 \mathbf{D}_{1,2} + \frac{2}{3} \mathbf{D}_{2,2} \mathbf{R}_{VDA}^1 \mathbf{D}_{2,2} \quad (\text{A-6})$$

Generally, the iterative equation of \mathbf{R}_{VDA}^V becomes

$$\mathbf{R}_{VDA}^V = \frac{1}{3} \mathbf{R}_{VDA}^{V-1} + \frac{2}{3} \mathbf{D}_{1,V} \mathbf{R}_{VDA}^{V-1} \mathbf{D}_{1,V} + \frac{2}{3} \mathbf{D}_{2,V} \mathbf{R}_{VDA}^{V-1} \mathbf{D}_{2,V} \quad (\text{A-7})$$

as shown in equation (4-11)

Appendix B

Proof of Equation (4-22)

By adopting \mathbf{R}_{VDA}^V instead of \mathbf{R}_N in equation (4-4), we know

$$\mathbf{w}_{VDA}^V = \frac{1}{\hat{\mathbf{a}}^H(\theta_1) (\mathbf{R}_{VDA}^V)^{-1} \hat{\mathbf{a}}(\theta_1)} (\mathbf{R}_{VDA}^V)^{-1} \hat{\mathbf{a}}(\theta_1) \quad (B-1)$$

Using the result of the matrix inversion,

$$(\mathbf{A} + \mathbf{B})^{-1} = \mathbf{A}^{-1} - \mathbf{A}^{-1} \mathbf{B} (\mathbf{I} + \mathbf{A}^{-1} \mathbf{B})^{-1} \mathbf{A}^{-1} \quad (B-2)$$

We derive

$$\begin{aligned} (\mathbf{R}_{VDA}^{V+1})^{-1} &= 3 \left(\mathbf{R}_{VDA}^V + \tilde{\mathbf{R}}_{VDA}^{V+1} \right)^{-1} \\ &= 3 \left(\mathbf{R}_{VDA}^V \right)^{-1} - 3 \left(\mathbf{R}_{VDA}^V \right)^{-1} \tilde{\mathbf{R}}_{VDA}^{V+1} \left[\mathbf{I} + \left(\mathbf{R}_{VDA}^V \right)^{-1} \tilde{\mathbf{R}}_{VDA}^{V+1} \right]^{-1} \left(\mathbf{R}_{VDA}^V \right)^{-1} \\ &= 3 \left\{ \mathbf{I} - \left(\mathbf{R}_{VDA}^V \right)^{-1} \tilde{\mathbf{R}}_{VDA}^{V+1} \left[\mathbf{I} + \left(\mathbf{R}_{VDA}^V \right)^{-1} \tilde{\mathbf{R}}_{VDA}^{V+1} \right]^{-1} \right\} \left(\mathbf{R}_{VDA}^V \right)^{-1} \\ &= 3 \left[\mathbf{I} + \left(\mathbf{R}_{VDA}^V \right)^{-1} \tilde{\mathbf{R}}_{VDA}^{V+1} \right]^{-1} \left(\mathbf{R}_{VDA}^V \right)^{-1} \end{aligned} \quad (B-3)$$

where

$$\tilde{\mathbf{R}}_{VDA}^{V+1} = 2\mathbf{D}_{1,V+1}\mathbf{R}_{VDA}^V\mathbf{D}_{1,V+1} + 2\mathbf{D}_{2,V+1}\mathbf{R}_{VDA}^V\mathbf{D}_{2,V+1} \quad (B-4)$$

Substituting equation (B-3) into equation (B-1) yields

$$\begin{aligned} \mathbf{w}_{VDA}^{V+1} &= \frac{1}{\hat{\mathbf{a}}^H(\theta_1) (\mathbf{R}_{VDA}^{V+1})^{-1} \hat{\mathbf{a}}(\theta_1)} (\mathbf{R}_{VDA}^{V+1})^{-1} \hat{\mathbf{a}}(\theta_1) \\ &= \frac{3 \left[\mathbf{I} + \left(\mathbf{R}_{VDA}^V \right)^{-1} \tilde{\mathbf{R}}_{VDA}^{V+1} \right]^{-1}}{3 \hat{\mathbf{a}}^H(\theta_1) \left(\mathbf{R}_{VDA}^V + \tilde{\mathbf{R}}_{VDA}^{V+1} \right)^{-1} \hat{\mathbf{a}}(\theta_1)} (\mathbf{R}_{VDA}^V)^{-1} \hat{\mathbf{a}}(\theta_1) \\ &= \frac{\left[\mathbf{I} + \left(\mathbf{R}_{VDA}^V \right)^{-1} \tilde{\mathbf{R}}_{VDA}^{V+1} \right]^{-1}}{\hat{\mathbf{a}}^H(\theta_1) \left(\mathbf{R}_{VDA}^V + \tilde{\mathbf{R}}_{VDA}^{V+1} \right)^{-1} \hat{\mathbf{a}}(\theta_1)} \hat{\mathbf{a}}^H(\theta_1) (\mathbf{R}_{VDA}^V)^{-1} \hat{\mathbf{a}}(\theta_1) \mathbf{w}_{VDA}^V \\ &= \frac{\hat{\mathbf{a}}^H(\theta_1) (\mathbf{R}_{VDA}^V)^{-1} \hat{\mathbf{a}}(\theta_1)}{\hat{\mathbf{a}}^H(\theta_1) \left(\mathbf{R}_{VDA}^V + \tilde{\mathbf{R}}_{VDA}^{V+1} \right)^{-1} \hat{\mathbf{a}}(\theta_1)} \left[\mathbf{I} + \left(\mathbf{R}_{VDA}^V \right)^{-1} \tilde{\mathbf{R}}_{VDA}^{V+1} \right]^{-1} \mathbf{w}_{VDA}^V \end{aligned} \quad (B-5)$$

which shows the result in equation (4-22).

Appendix C

Proof of Equation (4-29)

Using the result of equation (4-22) we know

$$\mathbf{w}_{VDA,m}^{V+1} = \mathbf{U}_m^V \mathbf{w}_{VDA,m}^V \quad (\text{C-1})$$

Using the result of equation (C-1) and equation (3-38), we obtain

$$\begin{aligned} \mathbf{w}_{VDA,m+i}^V &= \left(\mathbf{T}_{VDA,m \rightarrow m+i}^V \right)^H \mathbf{w}_{VDA,m}^V = \left[\left(\prod_{k=1}^{V-1} \left(\mathbf{U}_m^k \right)^H \right)^{-1} \mathbf{T}_{m \rightarrow m+i} \prod_{k=1}^{V-1} \left(\mathbf{U}_{m+i}^k \right)^H \right]^H \mathbf{w}_{VDA,m}^V \\ &= \mathbf{U}_{m+i}^{V-1} \mathbf{U}_{m+i}^{V-2} \cdots \mathbf{U}_{m+i}^1 \left(\mathbf{T}_{m \rightarrow m+i} \right)^H \left(\mathbf{U}_m^1 \right)^{-1} \left(\mathbf{U}_m^2 \right)^{-1} \cdots \left(\mathbf{U}_m^{V-1} \right)^{-1} \mathbf{w}_{VDA,m}^V \quad (\text{C-2}) \\ &= \mathbf{U}_{m+i}^{V-1} \mathbf{U}_{m+i}^{V-2} \cdots \mathbf{U}_{m+i}^1 \left(\mathbf{T}_{m \rightarrow m+i} \right)^H \mathbf{w}_{VDA,m}^1 \\ &= \mathbf{U}_{m+i}^{V-1} \mathbf{U}_{m+i}^{V-2} \cdots \mathbf{U}_{m+i}^1 \mathbf{w}_{VDA,m+i}^1 \end{aligned}$$

Appendix D

Proof of Equation (5-17)

We define

$$u_k \triangleq \frac{r_k}{R_2} \sin \frac{\phi + \phi_0 - 2\Psi_k}{2} \quad (\text{D-1})$$

We can calculate the pdf of random variable u_k by

$$f_U(u_k) = \begin{cases} \frac{1}{\pi(1-\xi^2)} \sqrt{1-u_k^2}, & \xi < u_k \leq 1 \\ \frac{1}{\pi(1-\xi^2)} (\sqrt{1-u_k^2} - \sqrt{\xi^2 - u_k^2}), & |u_k| \leq |\xi| \\ \frac{1}{\pi(1-\xi^2)} \sqrt{1-u_k^2}, & -1 \leq u_k < -\xi \end{cases} \quad (\text{D-2})$$

Then we can obtain the expectation of $\exp(-j\alpha(\phi)u_k)$ by

$$\begin{aligned} & E[\exp(-j\alpha(\phi)u_k)] \\ &= \frac{1}{\pi(1-\xi^2)} \left[\int_{-1}^1 \sqrt{1-u_k^2} \exp(-j\alpha(\phi)u_k) du_k - \int_{-\xi}^{\xi} \sqrt{\xi^2 - u_k^2} \exp(-j\alpha(\phi)u_k) du_k \right] \quad (\text{D-3}) \\ &= \frac{1}{1-\xi^2} \left[\mu(\phi) - \xi^2 \frac{2J_1(\alpha(\phi)\xi)}{(\alpha(\phi)\xi)} \right] = \frac{1}{1-\xi^2} \left[\mu(\phi) - \xi^2 \mu_{ring}(\phi) \right] \end{aligned}$$

Using the result of equation (D-3), we further derive

$$\begin{aligned} P_{av}^{ring}(\phi) &= E \left[\left| \sum_{k=1}^K \exp(-j\alpha(\phi)u_k) \right|^2 \right] \\ &= \frac{1}{K} + \frac{1}{K^2} E \left[\sum_{k=1}^K \exp(-j\alpha(\phi)u_k) \sum_{l=1, l \neq k}^K \exp(j\alpha(\phi)u_l) \right] \quad (\text{D-4}) \\ &= \frac{1}{K} + \frac{K-1}{K} E[\exp(-j\alpha(\phi)u_k)]^2 = \frac{1}{K} + \frac{K-1}{K} \left(\frac{\mu(\phi) - \xi^2 \mu_{ring}(\phi)}{1-\xi^2} \right)^2 \end{aligned}$$

which shows the result in equation (5-17).

Appendix E

Proofs of Equations (5-23)-(5-28)

We assume the Cartesian Coordinates of the k th CR node to be $(r_{k,x}, r_{k,y})$, where

$$r_{k,x} = r_k \cos \Psi_k \quad (\text{E-1})$$

$$r_{k,y} = r_k \sin \Psi_k \quad (\text{E-2})$$

Using equation (5-23), we can further separate the initial phase of the k th CR node into two parts, which are dedicated to the broadside array $\varphi_{k,b}$ and to the end-fire array $\varphi_{k,e}$. It means

$$\varphi_k = \varphi_{k,b} + \varphi_{k,e} \quad (\text{E-3})$$

where

$$\varphi_{k,b} = -\frac{2\pi}{\lambda} r_k \sin \phi_0 \sin \Psi_k \quad (\text{E-4})$$

$$\varphi_{k,e} = -\frac{2\pi}{\lambda} r_k \cos \phi_0 \cos \Psi_k \quad (\text{E-5})$$

The array factor for the broadside array can be written as

$$\begin{aligned} F_{\text{broadside}}(\phi) &= \frac{1}{K} \sum_{k=1}^K \exp \left(j \frac{2\pi}{\lambda} r_k \sin \Psi_k \sin \phi + \varphi_{k,b} \right) \\ &= \frac{1}{K} \sum_{k=1}^K \exp \left[j \frac{2\pi}{\lambda} r_k (\sin \Psi_k \sin \phi - \sin \phi_0 \sin \Psi_k) \right] \\ &= \frac{1}{K} \sum_{k=1}^K \exp \left[j 2\pi \tilde{R} (\sin \phi - \sin \phi_0) \frac{r_k}{R} \sin \Psi_k \right] \end{aligned} \quad (\text{E-6})$$

Using the pdf of z_k in equation (5-10), and the results in equations (5-10)-(5-13), we can derive in a similar way that

$$\overline{P}_{\text{broadside}}(\phi) = E \left[|F(\phi)|^2 \right] = \frac{1}{K} + \left(1 - \frac{1}{K} \right) \mu_b(\phi) \quad (\text{E-7})$$

where

$$\mu_b(\phi) = \left| \frac{2J_1(\alpha_b(\phi))}{\alpha_b(\phi)} \right| \quad (\text{E-8})$$

$$\alpha_b(\phi) = 2\pi \tilde{R} (\sin \phi - \sin \phi_0) \quad (\text{E-9})$$

Similarly we can also obtain the average beampattern for the end-fire array, which can be written as

$$\bar{P}_{end-fire}(\phi) = \frac{1}{K} + \left(1 - \frac{1}{K}\right) \mu_e^2(\phi) \quad (E-10)$$

where

$$\mu_e(\phi) = \left| \frac{2J_1(\alpha_e(\phi))}{\alpha_e(\phi)} \right| \quad (E-11)$$

$$\alpha_e(\phi) = 2\pi \tilde{R} (\cos \phi - \cos \phi_0) \quad (E-12)$$

The above equations (E-7)-(E-12) show the result of equation (5-23)-(5-28).

References

- [1] J. Mitola, III, "Cognitive radio: an integrated agent architecture for software defined radio," Ph.D., Royal institute of technology Stockholm, Sweden, 2000.
- [2] S. Srinivasa and S. A. Jafar, "The throughput potential of cognitive radio: a theoretical perspective," in *Signals, Systems and Computers, 2006. ACSSC '06. Fortieth Asilomar Conference on*, 2006, pp. 221-225.
- [3] W. Cheng-xiang, C. Hsiao-hwa, H. Xuemin, and M. Guizani, "Cognitive radio network management," *Vehicular Technology Magazine, IEEE*, vol. 3, pp. 28-35, 2008.
- [4] O. Akan, O. Karli, and O. Ergul, "Cognitive radio sensor networks," *Network, IEEE*, vol. 23, pp. 34-40, 2009.
- [5] J. Mitola, III, "Cognitive radio for flexible mobile multimedia communications," in *Mobile Multimedia Communications, 1999. (MoMuC '99) 1999 IEEE International Workshop on*, 1999, pp. 3-10.
- [6] S. Haykin, "Cognitive radio: brain-empowered wireless communications," *Selected Areas in Communications, IEEE Journal on*, vol. 23, pp. 201-220, 2005.
- [7] FCC, "Cognitive Radio Technologies Proceeding (CRTP)," in *ET Docket No. 03-108*, ed, 2003.
- [8] IEEE USA Position: Improving spectrum usage through cognitive radio technology [Online]. Available: <http://www.ieeeusa.org/policy/positions/cognitiveradio.asp>
- [9] IEEE1900, "Standard definitions and concepts for spectrum management and advanced radio system technologies," ed, 2006.
- [10] D. Cabric, S. M. Mishra, D. Willkomm, R. Brodersen, and A. Wolisz, "A cognitive radio approach for usage of virtual unlicensed spectrum," presented at the 14th IST Mobile and Wireless Communications Summit, 2004.
- [11] J. O. D. Neel, "Analysis and design of cognitive radio networks and distributed radio resource management algorithms," Doctore of Philosophy, Virginia Polytechnic Institute and State University, 2006.
- [12] M. Jun, G. Y. Li, and J. Biing Hwang, "Signal processing in cognitive radio," *Proceedings of the IEEE*, vol. 97, pp. 805-823, 2009.
- [13] T. A. Weiss and F. K. Jondral, "Spectrum pooling: an innovative strategy for the enhancement of spectrum efficiency," *Communications Magazine, IEEE*, vol. 42, pp. 8-14, 2004.
- [14] I. Budiarjo, M. Lakshmanan, and H. Nikookar, "Cognitive radio dynamic access techniques," *Wireless Personal Communications*, vol. 45, pp. 293-324, 2008.
- [15] B. D. Van Veen and K. M. Buckley, "Beamforming: a versatile approach to spatial filtering," *ASSP Magazine, IEEE*, vol. 5, pp. 4-24, 1988.
- [16] H. Krim and M. Viberg, "Two decades of array signal processing research: the parametric approach," *Signal Processing Magazine, IEEE*, vol. 13, pp. 67-94, 1996.

References

- [17] A. O. Boukalov and S. G. Haggman, "System aspects of smart-antenna technology in cellular wireless communications-an overview," *Microwave Theory and Techniques, IEEE Transactions on*, vol. 48, pp. 919-929, 2000.
- [18] J. Capon, "High-resolution frequency-wavenumber spectrum analysis," *Proceedings of the IEEE*, vol. 57, pp. 1408-1418, 1969.
- [19] B. Widrow and S. D. Stearns, *Adaptive signal processing*. Englewood Cliffs, N.J: Prentice Hall, 1985.
- [20] P. Balaban and J. Salz, "Optimum diversity combining and equalization in digital data transmission with applications to cellular mobile radio. I. Theoretical considerations," *Communications, IEEE Transactions on*, vol. 40, pp. 885-894, 1992.
- [21] J. H. Winters, "The diversity gain of transmit diversity in wireless systems with Rayleigh fading," *Vehicular Technology, IEEE Transactions on*, vol. 47, pp. 119-123, 1998.
- [22] B. Suard, A. F. Naguib, G. Xu, and A. Paulraj, "Performance of CDMA mobile communication systems using antenna arrays," in *Acoustics, Speech, and Signal Processing, 1993. ICASSP-93., 1993 IEEE International Conference on*, 1993, pp. 153-156 vol.4.
- [23] A. F. Naguib, A. Paulraj, and T. Kailath, "Capacity improvement with base-station antenna arrays in cellular CDMA," *Vehicular Technology, IEEE Transactions on*, vol. 43, pp. 691-698, 1994.
- [24] P. Popovski, H. Yomo, K. Nishimori, R. Di Taranto, and R. Prasad, "Opportunistic interference cancellation in cognitive radio systems," in *New Frontiers in Dynamic Spectrum Access Networks, 2007. DySPAN 2007. 2nd IEEE International Symposium on*, 2007, pp. 472-475.
- [25] H. Xuemin, C. Zengmao, W. Cheng-Xiang, S. A. Vorobyov, and J. S. Thompson, "Cognitive radio networks," *Vehicular Technology Magazine, IEEE*, vol. 4, pp. 76-84, 2009.
- [26] H. Xuemin, W. Chengxiang, and J. Thompson, "Interference modeling of cognitive radio networks," in *Vehicular Technology Conference, 2008. VTC Spring 2008. IEEE*, 2008, pp. 1851-1855.
- [27] T. X. Brown, "An analysis of unlicensed device operation in licensed broadcast service bands," in *New Frontiers in Dynamic Spectrum Access Networks, 2005. DySPAN 2005. 2005 First IEEE International Symposium on*, 2005, pp. 11-29.
- [28] M. Wax and Y. Anu, "Performance analysis of the minimum variance beamformer in the presence of steering vector errors," *Signal Processing, IEEE Transactions on*, vol. 44, pp. 938-947, 1996.
- [29] Y. Anu and M. Wax, "Performance analysis of the minimum variance beamformer," in *Acoustics, Speech, and Signal Processing, 1995. ICASSP-95., 1995 International Conference on*, 1995, pp. 1661-1664 vol.3.
- [30] M. Viberg and A. L. Swindlehurst, "Analysis of the combined effects of finite samples and model errors on array processing performance," *Signal Processing, IEEE Transactions on*, vol. 42, pp. 3073-3083, 1994.
- [31] H. Cox, R. Zeskind, and M. Owen, "Robust adaptive beamforming," *Acoustics, Speech and Signal Processing, IEEE Transactions on*, vol. 35, pp. 1365-1376, 1987.

- [32] C. Y. Tseng and L. J. Griffiths, "A unified approach to the design of linear constraints in minimum variance adaptive beamformers," *Antennas and Propagation, IEEE Transactions on*, vol. 40, pp. 1533-1542, 1992.
- [33] D. D. Feldman and L. J. Griffiths, "A projection approach for robust adaptive beamforming," *Signal Processing, IEEE Transactions on*, vol. 42, pp. 867-876, 1994.
- [34] S. A. Vorobyov, A. B. Gershman, and L. Zhi-Quan, "Robust adaptive beamforming using worst-case performance optimization: a solution to the signal mismatch problem," *Signal Processing, IEEE Transactions on*, vol. 51, pp. 313-324, 2003.
- [35] C. J. Lam and A. C. Singer, "Bayesian beamforming for DOA uncertainty: theory and implementation," *Signal Processing, IEEE Transactions on*, vol. 54, pp. 4435-4445, 2006.
- [36] K. L. Bell, Y. Ephraim, and H. L. Van Trees, "A Bayesian approach to robust adaptive beamforming," *Signal Processing, IEEE Transactions on*, vol. 48, pp. 386-398, 2000.
- [37] M. Budsabathon, Y. Hara, and S. Hara, "Optimum beamforming for pre-FFT OFDM adaptive antenna array," *Vehicular Technology, IEEE Transactions on*, vol. 53, pp. 945-955, 2004.
- [38] S. Kapoor, D. J. Marchok, and H. Yih-Fang, "Adaptive interference suppression in multiuser wireless OFDM systems using antenna arrays," *Signal Processing, IEEE Transactions on*, vol. 47, pp. 3381-3391, 1999.
- [39] S. Liu, S. Feng, and W. Ye, "A beamspace-based pre-FFT beamforming algorithm for OFDM systems with antenna array," in *Microwave, Antenna, Propagation and EMC Technologies for Wireless Communications, 2007 International Symposium on*, 2007, pp. 490-495.
- [40] N. Ma and P. a. Li, "A simple and effective post-FFT beamforming technique for QAM-OFDM systems," in *Microwave, Antenna, Propagation and EMC Technologies for Wireless Communications, 2007 International Symposium on*, 2007, pp. 70-73.
- [41] L. Zhongding and F. P. S. Chin, "Post and pre-FFT beamforming in an OFDM system," in *Vehicular Technology Conference, 2004. VTC 2004-Spring. 2004 IEEE 59th*, 2004, pp. 39-43 Vol.1.
- [42] D. Z. Filho, C. M. Panazio, F. R. P. Cavalcanti, and J. M. T. Romano, "On downlink beamforming techniques for TDMA/FDD systems," presented at the XIXSimpósio Brasileiro de Telecomunicações, Fortaleza, Brazil, 2001.
- [43] M. H. Islam and L. Ying-Chang, "Beam synthesis method for beamforming adaptation in cognitive radio based wireless communications systems," in *Radio and Wireless Symposium, 2007 IEEE*, 2007, pp. 555-558.
- [44] S. Xin, W. Jinkuan, H. Yinghua, and M. Yan, "Robust adaptive beamforming using a Bayesian approach," in *TENCON 2006. 2006 IEEE Region 10 Conference*, 2006, pp. 1-4.
- [45] G.L.Stuber, *Principles of mobile communication*. Boston: MA: Kluwer, 1996.
- [46] J. S. Sadowsky and V. Kafedziski, "On the correlation and scattering functions of the WSSUS channel for mobile communications," *Vehicular Technology, IEEE Transactions on*, vol. 47, pp. 270-282, 1998.
- [47] A. Abdi, J. A. Barger, and M. Kaveh, "A parametric model for the distribution of the angle of arrival and the associated correlation function and power spectrum at

References

- the mobile station," *IEEE Transactions on Vehicular Technology*, vol. 51, pp. 425-434, 2002.
- [48] R. J. Mailloux, "Covariance matrix augmentation to produce adaptive array pattern troughs," in *Antennas and Propagation Society International Symposium, 1995. AP-S. Digest*, 1995, pp. 102-105 vol.1.
- [49] M. Zatman, "Production of adaptive array troughs by dispersion synthesis," *Electronics Letters*, vol. 31, pp. 2141-2142, 1995.
- [50] J. R. Guerci, "Theory and application of covariance matrix tapers for robust adaptive beamforming," *Signal Processing, IEEE Transactions on*, vol. 47, pp. 977-985, 1999.
- [51] H. C. Song, W. A. Kuperman, W. S. Hodgkiss, P. Gerstoft, and J. S. Kim, "Robustness of broadening against source motion," in *Sensor Array and Multichannel Signal Processing Workshop Proceedings, 2002*, 2002, pp. 470-474.
- [52] H. Song, W. A. Kuperman, W. S. Hodgkiss, P. Gerstoft, and K. Jea Soo, "Null broadening with snapshot-deficient covariance matrices in passive sonar," *Oceanic Engineering, IEEE Journal of*, vol. 28, pp. 250-261, 2003.
- [53] J. Riba, J. Goldberg, and G. Vazquez, "Robust beamforming for interference rejection in mobile communications," *Signal Processing, IEEE Transactions on*, vol. 45, pp. 271-275, 1997.
- [54] K. Hugl, J. Laurila, and E. Bonek, "Downlink performance of adaptive antennas with null broadening," in *Vehicular Technology Conference, 1999 IEEE 49th*, 1999, pp. 872-876 vol.1.
- [55] Y. Yixin and W. Chunru, "Adaptive beampattern synthesis based on broadening," in *Antennas and Propagation Society International Symposium, 2004. IEEE*, 2004, pp. 3996-3999 Vol.4.
- [56] Y. A. Brychkov and A. P. Prudnikov, "Integral transforms of generalized functions" *Journal of Mathematical Sciences*, vol. 34, pp. 1630-1655, 1986.
- [57] H. Ochiai, P. Mitran, H. V. Poor, and V. Tarokh, "Collaborative beamforming for distributed wireless ad hoc sensor networks," *Signal Processing, IEEE Transactions on*, vol. 53, pp. 4110-4124, 2005.
- [58] D. Lun, A. P. Petropulu, and H. V. Poor, "A cross-layer approach to collaborative beamforming for wireless Ad Hoc networks," *Signal Processing, IEEE Transactions on*, vol. 56, pp. 2981-2993, 2008.
- [59] K. Zarifi, S. Affes, and A. Ghayeb, "Distributed beamforming for wireless sensor networks with random node location," in *Acoustics, Speech and Signal Processing, 2009. ICASSP 2009. IEEE International Conference on*, 2009, pp. 2261-2264.
- [60] R. Mudumbai, G. Barriac, and U. Madhow, "On the feasibility of distributed beamforming in wireless networks," *Wireless Communications, IEEE Transactions on*, vol. 6, pp. 1754-1763, 2007.
- [61] J. Yindi and H. Jafarkhani, "Network beamforming using relays with perfect channel information," *Information Theory, IEEE Transactions on*, vol. 55, pp. 2499-2517, 2009.
- [62] Z. Gan, W. Kai-Kit, A. Paulraj, and B. Ottersten, "Collaborative-relay beamforming with perfect CSI: optimum and distributed implementation," *Signal Processing Letters, IEEE*, vol. 16, pp. 257-260, 2009.

- [63] V. Havary-Nassab, S. Shahbazpanahi, A. Grami, and L. Zhi-Quan, "Distributed beamforming for relay networks based on second-order statistics of the channel state information," *Signal Processing, IEEE Transactions on*, vol. 56, pp. 4306-4316, 2008.
- [64] S. Fazeli-Dehkordy, S. Shahbazpanahi, and S. Gazor, "Multiple peer-to-peer communications using a network of relays," *Signal Processing, IEEE Transactions on*, vol. 57, pp. 3053-3062, 2009.
- [65] C. Haihua, A. B. Gershman, and S. Shahbazpanahi, "Filter-and-Forward distributed beamforming in relay networks with frequency selective fading," *Signal Processing, IEEE Transactions on*, vol. 58, pp. 1251-1262, 2010.
- [66] D. R. Brown and H. V. Poor, "Time-Slotted round-trip carrier synchronization for distributed beamforming," *Signal Processing, IEEE Transactions on*, vol. 56, pp. 5630-5643, 2008.
- [67] R. Mudumbai, D. R. Brown, U. Madhow, and H. V. Poor, "Distributed transmit beamforming: challenges and recent progress," *Communications Magazine, IEEE*, vol. 47, pp. 102-110, 2009.
- [68] M. Fitch, M. Nekovee, S. Kawade, K. Briggs, and R. MacKenzie, "Wireless service provision in TV white space with cognitive radio technology: A telecom operator's perspective and experience," *Communications Magazine, IEEE*, vol. 49, pp. 64-73, 2011.
- [69] C. A. Balanis, *Antenna Theory: Analysis and Design, 3rd Edition*: Wiley-Interscience, 2005.
- [70] K. Zarifi, S. Affes, and A. Ghayeb, "Collaborative null-steering beamforming for uniformly distributed wireless sensor networks," *Signal Processing, IEEE Transactions on*, vol. 58, pp. 1889-1903, 2010.
- [71] M. F. A. Ahmed and S. A. Vorobyov, "Collaborative beamforming for wireless sensor networks with Gaussian distributed sensor nodes," *Wireless Communications, IEEE Transactions on*, vol. 8, pp. 638-643, 2009.
- [72] X. Lian, H. Nikookar, and L. P. Lighthart, "Efficient radio transmission with adaptive and ristributed beamforming for Intelligent WiMAX," *Wirel. Pers. Commun.*, vol. 59, pp. 405-431, 2011.
- [73] C. D. Moffatt, "High-Data-Rate, Line-of-Site network radio for mobile maritime communications," in *OCEANS, 2005. Proceedings of MTS/IEEE*, 2005, pp. 1-8.
- [74] A. Hottinen, M. Kuusela, K. Hugl, Z. Jianzhong, and B. Raghothaman, "Industrial embrace of smart antennas and MIMO," *Wireless Communications, IEEE*, vol. 13, pp. 8-16, 2006.
- [75] S. J. Chang, "Development and analysis of AIS applications as an efficient tool for vessel traffic service," in *OCEANS '04. MTTS/IEEE TECHNO-OCEAN '04*, 2004, pp. 2249-2253 Vol.4.
- [76] P. A. Lessing, L. J. Bernard, C. B. J. Tetreault, and J. N. Chaffin, "Use of the Automatic Identification System (AIS) on autonomous weather buoys for maritime domain awareness applications," in *OCEANS 2006*, 2006, pp. 1-6.
- [77] J. Joe, S. K. Hazra, S. H. Toh, W. M. Tan, and J. Shankar, "5.8 GHz fixed WiMAX performance in a sea port environment," in *Vehicular Technology Conference, 2007. VTC-2007 Fall. 2007 IEEE 66th*, 2007, pp. 879-883.
- [78] IEEE 802.16 working group. Available: <http://www.IEEE802.16.org/16>
- [79] WiMAX Telecom. Available: <http://www.wimax-telecom.net/en/index.php>

References

- [80] T. Keller and L. Hanzo, "Adaptive multicarrier modulation: a convenient framework for time-frequency processing in wireless communications," *Proceedings of the IEEE*, vol. 88, pp. 611-640, 2000.
- [81] A. Czylwik, "Adaptive OFDM for wideband radio channels," in *Global Telecommunications Conference, 1996. GLOBECOM '96. 'Communications: The Key to Global Prosperity*, 1996, pp. 713-718 vol.1.
- [82] R. K. Mallik, M. Z. Win, J. W. Shao, M. S. Alouini, and A. J. Goldsmith, "Channel capacity of adaptive transmission with maximal ratio combining in correlated Rayleigh fading," *Wireless Communications, IEEE Transactions on*, vol. 3, pp. 1124-1133, 2004.
- [83] Z. Ying Jun and K. B. Letaief, "Multiuser adaptive subcarrier-and-bit allocation with adaptive cell selection for OFDM systems," *Wireless Communications, IEEE Transactions on*, vol. 3, pp. 1566-1575, 2004.
- [84] N. Damji and T. Le-Ngoc, "Dynamic downlink OFDM resource allocation with interference mitigation and macro diversity for multimedia services in wireless cellular systems," *Vehicular Technology, IEEE Transactions on*, vol. 55, pp. 1555-1564, 2006.
- [85] L. Curtis and J. Tuqan, "An efficient algorithm for channel estimation and resource allocation in OFDMA downlink networks," in *Acoustics, Speech and Signal Processing, 2008. ICASSP 2008. IEEE International Conference on*, 2008, pp. 3145-3148.
- [86] L. Jorgueski and R. Prasad, "Downlink resource allocation in beyond 3G OFDMA cellular systems," in *Personal, Indoor and Mobile Radio Communications, 2007. PIMRC 2007. IEEE 18th International Symposium on*, 2007, pp. 1-5.
- [87] J. N. Laneman, D. N. C. Tse, and G. W. Wornell, "Cooperative diversity in wireless networks: Efficient protocols and outage behavior," *Information Theory, IEEE Transactions on*, vol. 50, pp. 3062-3080, 2004.
- [88] H. Congzheng, T. Harrold, S. Armour, I. Krikidis, S. Videv, P. M. Grant, H. Haas, J. S. Thompson, I. Ku, W. Cheng-Xiang, L. Tuan Anh, M. R. Nakhai, Z. Jiayi, and L. Hanzo, "Green radio: radio techniques to enable energy-efficient wireless networks," *Communications Magazine, IEEE*, vol. 49, pp. 46-54, 2011.

Publications of the author

Book chapters

1. X. Lian, H. Nikookar, L. Ligthart, book chapter: “Application of green radio to maritime coastal/lake communications and locationing introducing Intelligent WiMAX (I-WiMAX)”, March 2010, River Publisher.
2. X. Lian, H. Nikookar, L. Ligthart, book chapter: “Distributed beamforming techniques for wireless radio network”, accepted for publication as a book chapter of *Communications Navigation Sensing and Services, (CONASENSE)*, 2013.

Journal Papers

3. X. Lian, H. Nikookar, L. P. Ligthart, “Distributed beamforming with nodes selection for cognitive radio networks”, accepted for publication in journal of *Communications Navigation Sensing and Services (CONASENSE)*, 2013.
4. X. Lian, H. Nikookar, L. P. Ligthart, “A nodes selection scheme for collaborative beamforming technique in cognitive radio networks”, under review for *IEEE Wireless Communication Letters*.
5. X. Lian, H. Nikookar, L. P. Ligthart, “Distributed beamforming with Phase-Only control for green cognitive radio network”, *EURASIP Journal on Wireless Communications and Networking*, vol. 56, Feb. 2012.
6. X. Lian, H. Nikookar, L. P. Ligthart, “Efficient radio transmission with adaptive and Distributed Beamforming for Intelligent WiMAX”, *Journal on Wireless Personal Communications*, vol. 53, no. 3, pp. 405-431, 2011.
7. X. Lian and J. Zhou, “Unsymmetrical two L-shape arrays 2-D DOA estimation employed a more generalized propagator method”, *Chinese Journal of Aeronautics*, vol.25, No.5, 2007. (in Chinese, Abstract available in English)
8. X. Lian and J. Zhou, “Compensation for the mutual coupling effect in the application of the ESPRIT algorithm in signal snapshot array processing”, *Chinese Journal of Electronics*, vol.21, No.5, 2007. (in Chinese, Abstract available in English)
9. X. Lian and J. Zhou, “A robust adaptive beamformer for the antenna on the MAV”, *Journal of NUAA*, vol.38, No.3, Jun. 2006. (in Chinese, Abstract available in English)

Conference papers

10. N. M. Tesssema, X. Lian, H. Nikookar, “Distributed beamforming with close to optimal number of nodes for green wireless sensor networks”, *Online Conference on Green Communications (GreenCom), 2012 IEEE*, 25-28 Sept. 2012.

11. N. M. Tesssema, X. Lian, H. Nikookar, "Beamforming with efficient node selection techniques for green cognitive radio networks", *Radar Conference (EuRAD), 2012 9th European*, Oct. 31-Nov. 2, 2012.
12. X. Lian, H. Nikookar, "Downlink beamforming with broadened and deepened nulls for Cognitive Radio", *Microwave Conference (EuMC), 2012 42nd European*, Oct. 29-Nov. 1, 2012.
13. X. Lian, H. Nikookar, L. P. Ligthart, "Null broadening techniques for cognitive radio", *European Wireless Technology Conference (EuWiT)*, Paris, France, Sep. 27-28, 2010.
14. H. Lu, H. Nikookar and X. Lian, "Performance evaluation of hybrid DF-AF OFDM cooperation in Rayleigh Channel," *European Wireless Technology Conference (EuWiT)*, Paris, France, Oct. 2010.
15. X. Lian, H. Nikookar, L. P. Ligthart, "Intelligent WiMAX (I-WiMAX): A green radio technology for wireless communications and locationing", *Joint CTIF Workshop, Green energy with Focus on Cognitive Network & Spectrum Management*, May. 2010, Alborg, Denmark.
16. X. Lian, H. Nikookar, L. P. Ligthart and J. Zhou, "Adaptive OFDM Beamformer with constrained weights for cognitive radio", *IEEE 69th Vehicular Technology Conference (VTC)*, Barcelona, Spain, Apr. 2009.
17. X. Lian, H. Nikookar and J. Zhou, "Adaptive robust beamformer for cognitive radio", *European Wireless Technology Conference (EuWiT)*, Amsterdam, The Netherlands, Oct. 2008.
18. X. Lian and J. Zhou, "2-D DOA estimation for uniform circular arrays with PM", *7th International Symposium on Antennas, Propagation, and EM Theory (ISAPE)*, Guilin, China, Oct. 2006.

Relationship between chapters and publications (a cross reference table)

Publications \ Chapters	1	2	3	4	5	6	10	11	12	13	14	15	16	17
1						✓	✓	✓	✓	✓			✓	✓
2						✓		✓	✓	✓	✓	✓	✓	✓
3	✓					✓			✓	✓		✓		
4	✓					✓			✓	✓		✓		
5	✓	✓	✓	✓	✓	✓	✓	✓			✓	✓		
6	✓					✓						✓		
7						✓		✓	✓					

Summary

CR is capable of achieving efficient radio resource management while providing high data rate and reliable wireless communication services via implementation cognitions in three domains: time, frequency and space. This thesis explores potentials and limitations in CR by focusing on space domain. The purpose of investigating spatial diversity of CR is to achieve full spectrum reuse with PUs via distinguish itself from PUs by different spatial directions. This thesis discusses two system models for CR system. One is a centralized CR network with a CR BS equipped with array antennas, while CR users and PUs have no array antennas and they are located around the CR BS. The other model is a distributed CR network, which regards CR users in the network as CR nodes and a (sub-) set of these nodes forwards required signals to Distant CR (DCR) users in the presence of distant PUs. However, these signals should be suppressed in directions of PUs. Since the thesis emphasizes on exploiting spatial diversity in CR and CR networks, it adopts spatial signal processing techniques, i.e., the beamforming which has been also used in wireless communication systems.

For the centralized CR network (the first model), both uplink and downlink BF techniques for CR BS are considered in this thesis. At uplink (receiving side), the signals received at the CR BS, which are coming from CR users, have low SNR. An adaptive Bayesian beamformer allows for directing CR BS main beams to CR users even when the DOA of each CR user is uncertain or completely unknown. In the thesis the first model is used in combination with the proposed modulation method in order to solve the problem of adjacent interferences with desired signal sources for the adaptive Bayesian beamformers. As OFDM has been proposed as a promising candidate for the physical layer of CR systems, an adaptive OFDM beamformer has been presented for CR BS. It calculates all the weights of adaptive OFDM beamformers for different OFDM subcarriers iteratively to spare complex multiplication computations. Based on different spectrum access schemes that CR adopts, this thesis has suggested weights-masking and weights-constraint methods to modify the beamforming weights for those OFDM subcarriers which are in the same frequency band as needed by PUs. The weights-masking method simply deactivates those OFDM subcarriers which are in the PUs' frequency bands, while the weights-constraint method benefits from higher spectrum efficiency by forcing the weights of those OFDM subcarriers to direct pattern nulls towards the PUs.

At downlink (transmit side), it is assumed that CR users and PUs have no array antenna. Despite there are nulls in the CR BS antenna pattern towards PUs, the PUs may

Summary

still receive CR signals due to scatter and multipath effects from CR BS signals. After studying the angular deviation models of spatial wireless channels, a new NB (null-broadening) method has been presented in this thesis, which is called VDA. The method is capable of generating deeper and broadened null patterns around directions of PUs, and it can be calculated iteratively. Generating deeper and broadened nulls (a kind of filtering method) employs window functions as filter for the adaptive beamformer weights, to be utilized in combination with the VDA method. Thus the adaptive downlink beamformer of CR BS is able to display deep and broadened nulls in the patterns, which guarantees that the CR BS will cause less interference to PUs even when the CR system is using the same spectrum band as PUs.

The second model as discussed in the thesis is a CR network which contains geographically distributed CR users. Each CR user can be regarded as a virtual antenna element of an array. With this approach DB has been introduced in CR networks. Two DB methods have been proposed in this thesis to generate multi beams towards directions of DCR users. To solve the problem of the extreme narrow main beam pattern, a novel NS method has been proposed. The method selects those CR nodes that are able to form an end-fire array maximizing the number of nodes and a broadside array with reduced size by node selection. It has been shown in the beampattern that the main beams are successfully directed towards the DCR users. In practical applications the antenna gain of the main beam can so be increased, while sufficiently low sidelobe levels for CR transmission can be maintained needed for CR networks with large size.

I-WiMAX is shown in this thesis as a beamforming application applied for a new maritime wireless communication system promising a large coverage range, high data rates, efficient spectrum usage, and reliable communications in sea/lake scenarios. It adopts the ABF for uplink, which can spatially select the receiving signals of interested SS and alleviate co-channel interferences by directing the main beam towards the interested SS and nulls towards others. It also adopts the proposed NB method at downlink beamforming to display spread nulls in a certain range of directions. For far SS beyond the possible communication coverage range, a model of a relay network, which is inspired by the CR network, has been introduced. Thus the NS method for the DB technique has been employed for practical usage due to its capability of enlarging the gain of the main beam.

Samenvatting

Cognitieve radio (CR) is in staat om efficiënt radio resource management te bereiken en daarbij hoge data snelheid en betrouwbare draadloze communicatie diensten te bieden dankzij implementatie van kennis in drie domeinen: tijd, frequentie en ruimte. Dit proefschrift verkent het potentieel en de beperkingen van CR met focus op het ruimte domein. Het doel van het onderzoek naar ruimtelijke diversiteit van CR is om volledig spectrum hergebruik met primaire gebruikers (PU's) te bereiken via het onderscheid tussen CR en primaire gebruikers die in andere ruimtelijke richtingen liggen. Dit proefschrift bespreekt twee systeem modellen voor CR. Het eerste is het gecentraliseerde CR netwerk met een cognitieve radio basis station (CR BS); CR BS is uitgerust met een antennestelsel aannemende dat CR gebruikers en primaire gebruikers geen antennestelsel hebben en hun locaties rondom het cognitieve radio basis station liggen. Het andere model is dat van een gedistribueerd CR netwerk, waarbij CR gebruikers in het netwerk beschouwd worden als CR nodes. Een (sub-) set van deze nodes stuurt gewenste signalen door naar verafgelegen (DCR) gebruikers waar ook verafgelegen primaire gebruikers zijn. Deze signalen moeten echter in de richting van PU's worden onderdrukt. Aangezien in dit proefschrift de nadruk ligt op ruimtelijke diversiteit in CR en CR netwerken wordt aandacht gegeven aan signaal verwerkingstechnieken in het ruimtelijk domein, zoals bundelvorming waarvan het nut al is aangetoond in draadloze communicatie systemen.

Voor een gecentraliseerd CR netwerk (het eerste model) worden zowel uplink als downlink bundelvormingstechnieken voor CR BS beschouwd. In de uplink (ontvangende zijde) hebben de signalen ontvangen door het cognitieve radio basis station (afkomstig van cognitieve radio gebruikers) een lage signaal - ruis verhouding. Adaptieve Bayesian bundelvorming is in staat om hoofdbundels van de stralingsdiagrammen van cognitieve basis stations te richten op cognitieve radio gebruikers, zelfs als de richting naar elke cognitieve radio gebruiker onzeker of onbekend is. In het proefschrift wordt het eerste model gebruikt in combinatie met een modulatie methode die interferenties met gewenste bronsignalen in de adaptieve Bayesian bundelvormer voorkomt. OFDM is voorgesteld als een veelbelovende kandidaat voor de fysieke laag van CR systemen; een adaptieve OFDM bundelvormer wordt in dit proefschrift gepresenteerd voor CR BS. Het berekent iteratief de gewichtsfactoren van adaptieve OFDM bundelvormers voor verschillende OFDM sub-carriers zodat het aantal complexe berekeningen/vermenigvuldigingen minder wordt. Op basis van verschillende spectrum toegangsschema's, toelaatbaar in CR, worden gewichtsfactor-markeringen en gewichtsfactor-beperkingen voorgesteld om zodoende gewichtsfactoren te wijzigen voor die OFDM sub-carriers, die ook nodig zijn

Samenvatting

voor primaire gebruikers. De gewichtsfactor-markeermethode deactiveert de OFDM sub-carriers die in de primaire gebruikers' frequentiebanden liggen; de gewichtsfactor-beperkingmethode profiteert van een hogere efficiëntie van het spectrum middels gewichtsfactoren van OFDM sub-carriers waardoor in het stralingsdiagram 'nullen' worden gemaakt in de richting van de primaire gebruikers.

Bij downlink (zend zijde) kunnen ondanks de 'nullen' in het stralingsdiagram (richting PU's) de primaire gebruikers nog steeds cognitieve radio signalen ontvangen door verstrooiing- en multipad effecten op CR BS signalen, aannemende dat CR gebruikers en PU's geen antennestelsel hebben. Na bestudering van hoekafwijkingen in de ruimtelijke modellen van draadloze kanalen, wordt in dit proefschrift een nieuwe NB methode gepresenteerd, welke Virtual Direction Adding (VDA) genoemd wordt. De methode is in staat om iteratief diepere en verbreedde 'nul' stralingsdiagrammen te berekenen rondom richtingen PU's. Om deze diepere en verbreedde 'nul' diagrammen te genereren (een soort filter methode) worden specifieke (zogenoemde window) functies voor gewichtsfactoren in adaptieve bundelvorming toegepast in combinatie met de VDA methode. Adaptieve downlink bundelvorming van het cognitieve radio basis station (CR BS) is zo in staat om diepere en verbreedde 'nul' stralingsdiagrammen te maken, welke garanderen dat de CR BS voor minder storing zorgt naar de primaire gebruiker, zelfs als het cognitieve radio systeem een zelfde spectrum band gebruikt als de primaire gebruiker.

Het tweede model dat wordt besproken in dit proefschrift is het cognitieve radio netwerk, welke geografisch gedistribueerde cognitieve radio gebruikers bevat. Elke cognitieve radio gebruiker kan worden gezien als een virtueel element van een antennestelsel. Met deze aanpak wordt gedistribueerde bundelvorming (DB) geïntroduceerd in cognitieve radio netwerken. Twee gedistribueerde netwerken worden in dit proefschrift voorgesteld om meerdere hoofdbundels in de antenne diagrammen te genereren naar cognitieve radio gebruikers op verre afstand. Om het probleem van een extreem smalle hoofdbundel in het stralingsdiagram op te lossen wordt een nieuwe node selectie (NS) voorgesteld. Hierin selecteert de cognitieve radio die nodes nodig om een zogenoemde endfire antenne stelsel te vormen met maximalisering van het aantal nodes en een zogenoemde broadside antennestelsel met gereduceerde afmeting in broadside (en dus met minder nodes). Het stralingsdiagram toont aan dat de hoofdbundels succesvol worden gestuurd richting de cognitieve radio gebruikers op verre afstand. Op deze wijze worden praktische applicaties van cognitieve radio netwerken realistisch. Ook blijven voldoende lage zijklussen (richting PU's) behouden voor cognitieve radio netwerken met een groot afstands bereik.

I-WiMAX (Intelligent WiMAX) is een nieuw maritiem draadloos communicatie system met grote reikwijdte, hoge data snelheid, efficiënt gebruik van het spectrum en betrouwbare manier van communiceren van en naar locaties op meren en op zee. I-WiMAX beschikt over adaptieve bundelvorming voor de uplink, waardoor ruimtelijk de

ontvangende signalen van geïnteresseerde geabonneerde stations worden geselecteerd en co-channel interventies worden verlaagd dankzij bundelsturing naar abonnees en ‘nul’ diagrammen in overige richtingen. Voor downlink bundelvorming beschikt het ook over de voorgestelde methode van verbreden van ‘nul’ stralingsdiagrammen, te realiseren over een bepaald richtingsinterval. Voor verafgelegen abonnees voorbij de CR BS radio reikwijdte wordt een model van heruitzending geïntroduceerd geïnspireerd op het idee van het cognitieve radio netwerk. Voor praktisch gebruik is een node selectie methode voor gedistribueerde bundelvorming opgezet waardoor de reikwijdte in de richting van verafgelegen abonnees wordt vergroot.

Acknowledgement

It would not have been possible to write this doctoral thesis without the help of kind people around me. Above all, I would like to thank my promoter, Professor L. P. Ligthart. Professor Ligthart is someone you will instantly feel that he is a tough person with a strong mind and will. He has been so far my best role of model for a scientist and engineer; I wish I could be as persistent and enthusiastic as him. He has been supportive and has given me his valuable advices and unsurpassed knowledge. He also shared his wonderful ideas with me and provided me with insightful discussions about the thesis. I appreciate his direction very much.

I am also grateful to my supervisor, Dr. H. Nikookar for his scientific advices and insightful suggestions. Dr. Nikookar is my primary resource for getting my research questions answered and he is instrumental in helping me with research problems.

I am thankful to my former research supervisor in Nanjing University of Aeronautics and Astronautics, Professor Jianjiang Zhou. He has been helpful in providing advices many times during my graduate school career in China. I often think about my time as a master student in his labs. He encouraged me to go abroad and pursue my research career as a PhD student.

I will forever be thankful to my parents, Yongjie Lian and Liying Gao, for their ultimate support and their permanent belief in me. When I was little, everyone complained that my hometown, Urumqi, was so far away from any other city in China. However, my dad pointed to the west and told me that if we flew to this direction, soon we could arrive in Europe. His words deeply rooted in my mind and I decided to go to Europe when I grew up to see, to feel and to broaden my views. My parents always provide me with their unconditional love, and I could not have made it this far without them. Their encouragement and love for me are my “batteries” to stimulate me moving forward in my PhD study in TU Delft. I will also thank my two aunts, Liyun Gao and Liju Gao, they have been treating me like their own daughter and supporting me all the way along. Special thanks to the additional to my family, Jos Wubbeling, my husband, as well as his wonderful family who has been supportive and caring.

The best outcome from these past five years in Delft is finding my best friend, soul-mate, and husband. Jos has been a true and great supporter during my PhD study in good and bad times. He helped me with the Dutch translation of the summary in the thesis. I truly thank him for being there for me even when I am irritable. His ultimate patience and enthusiasm are contagious.

Acknowledgement

I thank all the present members of the MTS-Radar group. Professor Yarovoy has been knowledgeable, helpful and friendly to me during my PhD study. Dr. Galina Babur has been a true and close friend to me since we first met. I wish good luck to her research and the best for her family. I thank Diego Caratelli for his very insightful mathematical guidance and suggestions. Dr. Krasnov's opinion and suggestions have been of great value to me. Yuan He is also kind and nice to me. I wish him all the best in his PhD study. Minke van der Put, our passionate and capable secretary, helped me with administration forms and thesis printing. This list is far from complete; it is a pity that I could not list all the names here, but I will never forget their friendly help.

I would like to thank the past members of the MTS-Radar group. Hao Lu, my office mate, has been so kind and helpful to me. He shared with me his valuable ideas and it has been such a pleasant time working with him. Muge and Firat are wonderful people and now they are my close friends wherever they are. I would also like to thank one of MSc student, Netsanet Merwai. I quite enjoyed working with her and we have had a very delightful experience of working on the topic of nodes selection for wireless sensor networks together. Ying Wang is my best friend. I appreciate her ultimate help and support.

Besides our group, I would like to give my sincere thanks to CICAT stuff members. Franca Post and Cees Timmers were so helpful when I first arrived in the Netherlands. Anna Hoek is a very cheerful person and gave me recommendations for being a facilitator for PhD starter activities. I also thank Derong Kong for his help in proving my hypothesis from statistics point of view.

I am such a lucky person to have such a bunch of wonderful and kind people around me. They brought me joy and support during my study in TUDelft. I give them all my endless thanks and will always be grateful to them.

Curriculum Vitae



Name	Xiaohua Lian
Date of Birth	May 10, 1980
Place of Birth	Urumqi, P. R. China
Email	xiaohualiantud@gmail.com

Oct. 2012-Present
Technical Designer

Nov. 2007-Present
Ph.D. Candidate

Apr. 2005-Nov. 2007
Ph.D. Candidate

Sep. 2002-Apr. 2005
Master of Engineering

Sep. 1998-Jun. 2002
Bachelor of Engineering